Exploring novel methods to achieve systemic delivery of SMN for treatment of spinal muscular atrophy

Emily McFall

Thesis submitted to the
Faculty of Graduate and Postdoctoral Studies
in partial fulfilment of the requirements
for the Masters degree in Microbiology and Immunology

Department of Biochemistry, Microbiology, & Immunology

Faculty of Medicine

University of Ottawa

Abstract

Spinal muscular atrophy (SMA) is an inherited neurodegenerative disease caused by insufficient levels of the survival motor neuron protein (SMN), leading to progressive deterioration of α-motor neurons, onset of muscle atrophy and, in severe disease, death. We investigated whether reducing the size of Adenovirus (Ad) vectors, through use of a short fibre protein, could enhance delivery of a transgene to muscle and motor neurons after systemic delivery *in vivo*. Unfortunately, the biodistribution of the smaller Ad vector was unaltered compared to wildtype Ad, with most of the virus localizing to the liver. However, we determined Ad-derived SMN was efficiently packaged into cellular exosomes, suggesting a novel approach to protein delivery. We showed that exosomes naturally contain SMN both *in vitro* and *in vivo* and that exosomes can be used to deliver SMN to recipient cells. Further testing is required to establish if SMN-containing exosomes can function as an SMA therapeutic.

Acknowledgements

I would like to thank my supervisor, Dr. Robin Parks, for allowing me to work on two interesting projects. For his support and encouragement in times of struggle as everything did end up fine. Lastly, for his trust in allowing me to set my own schedule and experiment designs all the while being available whenever aid was needed. I would also like to thank my TAC members Dr. Rashmi Kothary and Dr. Bernard Jasmin who not only helped guide me on my research projects but my career path. I would like to thank the Ontario government and the Canadian Institutes of Health Research for funding my research.

I would like to thank each member of the Parks lab for making my graduate experience fun and memorable. To Joe Burns for taking me to Disneyland and making me laugh and cringe with his lively comments. To Kalisa Campbell for the stories, giggles and whatever. To Carmen Wong for putting up with my repetitive stats questions but mostly for coming out dancing. To Natacha Provost and André Richard for offering help and always trying to interrupt the best of my results. To Briti Saha for staying positive and to Mélissa Geoffroy for expanding my French vocabulary. Lastly and most importantly to Kathy Poulin as I never would have got this far without your help, amazing knowledge of everything in the Parks lab and our combined math skills. Next I would like to thank members in other labs who helped in my training and provided support Dr. Lyndsay Murray, Dr. Justin Boyer, Chantal Mazerolle, Dr. Erin Bassett, John Lunde, Dr. Dylan Burger, the animal care facility, in particular Kim and Eileen, and lastly my close friend Faduma Jama.

Finally I would like to thank my extensive editing team Joe, Carmen, André, Natacha, Kristen Marcellus, Yue Fainaru and Sruthi Kalyanasundaram. I would like to thank Scott Nichols who stood by me through the good days and the grumpy ones and lastly my parents who listened to the stories and provided all the support in the world.

Contributions

I would like to acknowledge both Dr. Robin Parks and Kathy Poulin who created and purified all the viruses used in this study.

Table of Contents

List of Abbreviations

293	Human embryonic kidney cells
β-gal	β-galactosidase
A549	Adenocarcinomic human alveolar basal epithelial cells
A549::SMN	A549 cells with over expression of Flag-SMN through hygromycin selection
Ad	Adenovirus
Ad5	Adenovirus serotype 5, (Ad5 ΔE1/ΔE3 is considered control Ad for this thesis)
ASO	Antisense oligonucleotides
BSA	Bovine serum albumin
C2C12	Mouse myoblast C2C12 cells
CAR	Coxsackievirus adenovirus receptor
CARM1	Co-activator-associated arginine methyltransferase 1
CMV	Cytomegalovirus
CNS	Central nervous system
DMEM	Dulbecco's modified Eagle's medium
DNA	Deoxyribonucleic acid
E1	Early region 1
EDTA	Ethylenediaminetraacetic acid
ESCRT	Endosomal sorting complex required for transport
FBS	Fetal bovine serum
Flag	Epitope tag DYKDDDDK
HUVEC	Human umbilical vein endothelial cells
Hpi	Hours post infection
ILV	intraluminal vesicles
IP	Intraperitoneal
IV	Intravenous
kb	Kilobases
kDa	Kilodaltons
MDa	Megadaltons
LD	Laemmli loading dye
MEM	Minimum essential medium
MOI	Multiplicity of infection
MN1	Cholinergic motor neuron cells
mRNA	Messenger RNA
MVB	Multivesicular bodies
N3S	293N3S cells
NMJ	Neuromuscular junction
pA	Polyadenylation signal
PBS	Phosphate buffered saline
PFA	Paraformaldehyde
RGD loop	Amino acid sequence Arg-Gly-Asp
RIPA	Radioimmunoprecipitation assay buffer

RNA	Ribonucleic acid
rRNA	Ribosomal RNA
RT	Room temperature
SDS	Sodium dodecyl sulfate
SDS-PAGE	Sodium dodecyl sulfate polyacrylamide gel electrophoresis
shRNA	Short hairpin RNA
siRNA	Short interfering RNA
SMA	Spinal muscular atrophy
SMN	Survival motor neuron
SMNΔ7	Truncated SMN protein produced from *SMN2*
SMN1	Survival motor neuron 1 gene (telomeric)
SMN2	Survival motor neuron 2 gene (centromeric)
snRNP	Small nuclear ribonucleic particle
TA	Tibialis anterior
TBST	Tris buffered saline tween
TCA	Trichloroacetic acid
X-gal	5-bromo-4-chloro-3-indolyl-β-D-galatopyranoside

List of Figures

List of Tables

Chapter 1 - Background

1.1 Spinal Muscular Atrophy

1.1.a What is SMA?

Spinal muscular atrophy (SMA) occurs in approximately 1 in 6,000 live births making it the most common inherited neurodegenerative disease leading to infant mortality [13,37]. SMA is an autosomal recessive disorder with a carrier frequency of approximately 1 in 50 in America [80, 83]. The disease presents as progressive deterioration of skeletal muscle and α-motor neurons in the anterior horn of the spinal cord [37]. SMA results in weakness in the proximal limbs, hypotonia, trunk paralysis and impairment of the ability to breathe leading to suffocation and death [37].

1.1.b SMN genes

SMA is caused by a deficiency in the survival motor neuron (SMN) protein due to the inactivation of the *SMN1* gene [56]. In 95% of cases, inactivation occurs through a homozygous deletion of the *SMN1* gene while the other 5% of cases display non-synonymous point mutations [88]. Thus far, it appears humans are the only species to have undergone a gene duplication event of the 500 kb *SMN1* element resulting in an additional copy of the gene, *SMN2* [56]. Both SMN genes are found on chromosome 5q13.2 with *SMN1* at the telomeric position [56]. Over the 32 kb region of the SMN gene, there is 99% homology between *SMN1* and *SMN2*, with quasi-identical promoter sequences suggesting equal transcription levels [76,27]. *SMN2* differs from *SMN1* in only 5 point mutations: 3 intronic sites (intron 6 position -45, intron 7 position +100, intron 7 position +214) and 2 exonic sites (exon 7 position +6, exon 8 position +245) [64]. All of these mutations are synonymous, resulting in equivalent full length proteins (Figure 1.1) [64]. However,

extensive research has shown, the cytosine to thymidine mutation within exon 7 of *SMN2* results in an alternate splicing event and the loss of exon 7 [64]. This altered splicing produces a truncated protein, SMNΔ7 [63]. SMNΔ7 lacks the normal 16 carboxyl amino acids; however, the junction of exon 6 to exon 8 results in SMNΔ7 acquiring 4 unique terminal amino acids [9]. It is thought that this cytosine to thymidine mutation in *SMN2* may lead to alternate splicing through the disruption of an exon-splicing enhancer site which consequently promotes the exclusion of exon 7 [63]. However, the exact exon-splicing enhancer site affected by the point mutation has not yet been identified. As such, alternate theories exist involving the formation of other *cis* elements or improper mRNA secondary structures to explain this splicing event [75]. Since SMA patients lack *SMN1*, they rely solely on the SMN protein produced from the *SMN2* gene. Unfortunately *SMN2* is correctly spliced, producing functional full length SMN, only 10-15% of the time [63]. This reduced yield of functional SMN is insufficient to compensate for the loss of *SMN1*, resulting in a disease state.

1.1.c Disease pathogenesis

SMA patients can be divided into four different levels of disease severity. Type I, also known as Werdnig-Hoffman disease, is an extremely severe form of SMA and unfortunately the most common [55]. Type I SMA patients are diagnosed shortly after birth, never gain the ability to sit and generally die before the age of two [92]. Type II patients are diagnosed between 6-18 months of age and have a life expectance of 10-40 years [92]. These patients may be able to sit independently but never walk [92]. Type III SMA, also known as Kugelberg-Welander disease, is diagnosed at later stages in childhood [55]. Patients with Type III SMA have normal life expectancy and are physically mobile, but not all symptoms

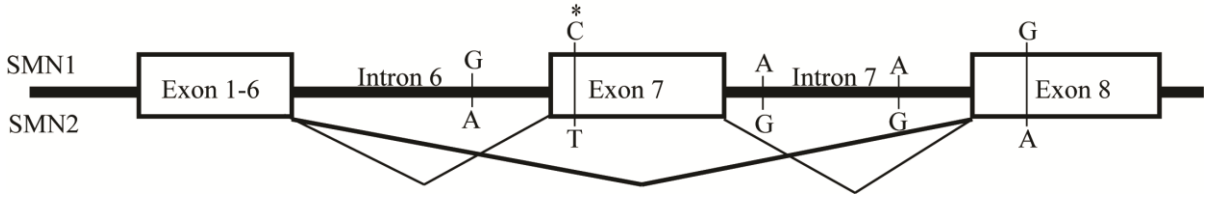
SMN1
SMN2
Exon 1-6
Intron 6
G
A
*
C
T
Exon 7
A
G
Intron 7
A
G
G
A
Exon 8

Figure 1.1 *Schematic of SMN1 and SMN2*. Due to a recent duplication event, humans encode two SMN genes on chromosome 5. *SMN1* (telomeric) and *SMN2* (centromeric) differ in only five synonymous point mutations resulting in equivalent full length proteins. However, the cytosine to thymidine mutation at position 6 within exon 7 (*) results in alternate splicing of *SMN2* through the exclusion of exon 7. Figure modified from Mittal B. [74].

are alleviated [92]. Type IV SMA is the only type with an adult onset; although these patients live with proximal limb muscle atrophies, their symptoms are significantly reduced and they are often never diagnosed as SMA patients [92]. Some researchers and families recognize a fifth level of SMA severity, Type 0. In patients with Type 0 SMA there is an inadequate level of SMN to sustain life and the fetus is lost prior to birth or soon afterwards (Table 1.1) [92].

SMA severity is proportional to the copy number of *SMN2* [56, 29]. Increased copy number of *SMN2* results in an enhanced amount of full-length SMN which in turn alleviates disease pathogenesis [57]. In general, Type I patients have 1-2 copies of *SMN2*, Type II patients have 3 copies, Type III patients have 3-5 copies of *SMN2* and the *SMN2* copy number in Type IV patients is unclear but thought to be 4-6 [29]. The loss of both *SMN1* and *SMN2* is embryonic lethal, indicating the essential need for the SMN protein [80]. Genetic screening for parents of affected children or siblings can be done to determine *SMN2* copy number for a more accurate risk assessment [73].

Research involving SMA mouse models (discussed below) have led to the discovery of SMN thresholds, which are believed to be relevant to humans as well [9]. A protein threshold level implies that more protein is transcribed than needed for proper functioning of the cell. Evidence for a threshold level of SMN was determined through SMN knockdown experiments with shRNAs, where a reduction to 20% wildtype SMN levels resulted in no morphological change in HeLa cells [120]. As such, it is concluded that not all of the SMN transcribed by *SMN1* is needed for proper functioning. In conjunction with this, the amount of SMN required from *SMN2* does not need to be equivalent to that of *SMN1*, but simply over the threshold level for proper functioning. Since Type IV patients have between 4 and 6 copies of *SMN2* the human SMN threshold level must be greater than the

Table 1.1 Clinical classifications of SMA

Type	Age of onset	Physical characteristics	Life Expectancy	SMN2 copy number
0	prenatal	Fetus displays reduced movement	Fatal at birth	unknown
I	< 6 months	Children are never able to sit	2 years	1-2
II	6 - 18 months	Children can sit independently	10-40 years	3
III	>18 months	Children can walk independently	Normal	3-5
IV	Adulthood	Patients display mild muscle weakness	Normal	4-6

Table modified from Russman [92]

amount of full-length SMN yielded by 6 copies of *SMN2*. Assuming equal transcription rates between *SMN1* and *SMN2* due to their quasi-identical promoter sequences and assuming *SMN2* produces full length SMN protein 10% of the time, 6 copies of *SMN2* produces 30% of the total SMN protein found under normal conditions. This would suggest that the human SMN threshold level is higher then 30%.

1.1.d SMN protein and function

SMN is a 38 kDa, 294 amino acid protein which is ubiquitously expressed in multicellular organisms [56, 49]. The protein is found in both the cytoplasm and the nucleus [61]. In the cytoplasm, SMN can be detected within the trans-Golgi network and interacts with various proteins [106]. Within the nucleus SMN is found in gemini of coiled bodies or gems for short [57]. These gems co-localize with coilin in Cajal bodies [118]. SMN self-associates and interacts with Gemin 2-8 to form the SMN complex [37]. This SMN complex is also known to form close associations with UNR-interacting protein [61, 17]. Self-association of SMN and its participation in the SMN complex increases the protein's overall stability. Burnett *et al* showed that exons 2, 6 and 7 are important in self-association and therefore play a role in SMN stability [13]. SMNΔ7 is also able to associate with full length SMN [13]. However, the loss of exon 7 in SMNΔ7 significantly reduces its half-life to only two hours compared to over four hours for full length SMN [13].

The varied functions of SMN are being investigated extensively to determine the causal factor leading to the disease state specifically in motor neurons. SMN is best known for its strict requirement in the formation of the Sm protein ring on small nuclear ribonucleic particles (snRNPs), a necessary component of spliceosomes [61]. Surprisingly, it was found that SMN deficiency does not result in a uniform reduction in snRNPs, but some genes and

some cell types appear preferentially reduced [120]. This finding may suggest a possible reason for why an ubiquitous expressed protein results specifically in a motor-neuron disease. Recent experiments have identified a potential gene, stasimon, which is expressed in neurons and affected by snRNP splicing [66]. Stasimon is required for normal synaptic transmission of motor neurons and its addition in SMA animal models results in significant phenotypic improvement [66] Unfortunately, stasimon deficiency cannot account for all defects observed in SMA animal models. For example Lotti *et al* showed that although the addition of stasimon improved defects in the neuromuscular junctions (NMJ) in SMN-deficient *Drosophila* stasimon was unable to correct for irregular locomotion and rhythmic motor activity, suggesting a more complex mechanism is occurring [66].

SMN is also thought to be involved in gene expression and translation [43]. Sanchez *et al* observed SMN co-fractioned with polyribosomes suggesting a physical association with the translational machinery [43]. They went on to show that SMN is not required for polyribosome assembly and therefore SMN alters translation of only a subset of mRNAs, including CARM1 (co-activator-associated arginine methyltransferase 1) [43]. As observed with SMN's function in splicing, the limited number of mRNA affected may lead to a cell specific effect and explain why deterioration in SMA occurs mainly in the motor neurons.

The NMJ appear to form properly in SMA models but become denervated at early stages of disease development [60], suggesting a role of SMN in maintaining synapse formation [60]. Ling *et al* showed that the NMJs affected depended on a combination of determinants, although head and trunk muscles proved to be key targets for denervation [60]. Additional studies showed that following damage, SMA murine models demonstrated decreased NMJ remodeling [78]. Possibly related to the defects in the NMJ, Ting *et al* showed decreased SMN levels resulted in reduced size of neuronal growth cones [106]. It is

known that SMN functions with hnRNP to localize β-actin mRNA in these growth cones [90] Decreases in growth cone size as a result of low SMN levels may affect proteins which are enriched in growth cones, like β-actin [90].

Although it is thought that SMN has a specific neuronal function or neurons are more highly affected by SMN activity, SMN is necessary for survival of all cell types [49]. As such, some peripheral tissues are also affected in SMA. Peripheral tissues appear to have a lower SMN threshold level than motor neurons and therefore maintain proper functioning in mild cases of SMA [91]. For instance, there is a relationship between Type I SMA and congenital heart failure [91]. Similarly, Martinez-Hernandez *et al* showed that murine muscle tissue in SMA models differs from that of wild-type mice in terms of growth, behaviour and architecture [69]. Overall it remains unclear which, if any, of these functions lead to the disease progression observed in SMA.

1.1.e Animal models

The SMN gene is high conserved across species; however, only humans are known to have undergone a gene duplication event and therefore all other animals have only one gene, *smn* [65]. This *smn* gene functions equivalently to *SMN1* in humans and the lack of *smn* is embryonic lethal [5]. As such, SMA does not occur naturally in animals. In order to study SMA , animal models with altered levels of SMN protein were created to reflect the different levels of disease severity; species include zebrafish, *Drosophila*, cats and murine models, where murine models remain the most common [65, 26]. The creation of murine SMA models involved the introduction of various combinations of both human and murine SMN genes to achieve varying levels of the protein resulting in differing rates of disease progression [5]. Removal of one murine *smn* gene, *smn*+/-, or the addition of four copies of

human *SMN2* in a null *smn* background resulted in a normal life span with the latter presenting peripheral necrosis of the tail and ears [5]. This indicates that the murine threshold level is just over four copies of *SMN2*. Reducing the *SMN2* copy number by half resulted in a severe case of SMA, representative of Type I SMA patients [5]. In this murine model, *smn*-/-;*SMN2*, with only two copies of *SMN2*, mice have a life expectancy of 6-7 days and exhibit decreased muscle movements, decreased size and develop tail and ear necrosis [54]. However, life expectancy can be increased to 14 days with the addition of a gene encoding the truncated SMNΔ7 protein [54]. This mouse model, *smn*-/-;*SMN2*;Δ7, indicates that the miss-spliced protein product from *SMN2* may still contribute to SMN function. Lastly, Bowerman *et al* created a mild murine model, $SMN^{2B/-}$, from a C57BL/6 background to reflect Type III SMA patients [8]. Bowerman and colleagues inserted a three nucleotide substitution in the exon-splicing enhancer site of exon 7 within the *smn* gene [8]. This resulted in alternate splicing of the *smn* gene similar to that of human *SMN2* and as such reflects the splicing defect in SMA [8, 5]. These mice have a longer life expectancy of 28 days with the disease phenotype presenting itself at post-natal day 10 as decreased muscle strength, decreased size and tail necrosis [8].

1.1.f Current treatments

There is no cure for SMA and most treatment options involve alleviating symptoms [80]. Research is ongoing to determine methods to increase SMN levels in SMA patients, thereby preventing disease progression. There are many proposals under investigation including (i) enhancing SMN stability, (ii) correction of *SMN2* splicing and (iii) introduction of corrected SMN genes [80].

The small amount of full length SMN produced in SMA patients can be targeted for stability therapeutics. Stability of SMN can be enhanced through phosphorylation as demonstrated by Burney *et al* who showed forskolin stimulates PKA phosphorylation and in turn increases SMN stability [13]. Enhanced stability of SMNΔ7 is also being explored as findings in murine models suggest that SMNΔ7 may be partially functional [54]. Improved SMNΔ7 stability can be achieved by translational read-through to prevent termination at the initial stop codon, in this way increasing the size of the SMNΔ7 protein and consequently stability [42]. Aminoglycoside antibiotics, some of which are FDA approved, have been shown to bind ribosomes allowing for translational read through [42]. Unfortunately, the compound tested by Heier and Didonato, G418, showed increases in motor function *in vivo* but presented significant toxicity preventing any conclusions involving improvement of weight or survival time [42].

SMN levels can be enhanced through splicing correction using small molecules, antisense oligonucleotides (ASO) or *trans*-splicing mRNA. ASOs block Intronic Splicing Silencers near exon 7 increasing the amount of full length SMN transcribed [80]. Studies have shown ASOs are able to successfully enhance inclusion of exon 7, increase the number of gems and display promising long term results [94, 44]. ASOs can also spread systemically, however maximum inclusion of exon 7 in the spinal cord and brain are observed with direct central nervous system (CNS) injections [44]. Small molecules can be used for splicing correction or to enhance SMN transcription, for example histone decetylase inhibitors (Trichstatin A and Valproic acid) and β-adrenergic agonist (salbutamol) [5, 81]. Some of these small molecules are approved by the FDA for treatment for other disorders and therefore could function as SMA therapeutics in the near future [10]. Unfortunately, double bind clinical trials suggest some of these drugs may be more efficient at increasing

SMN levels in murine models than humans or the observed benefits may be partially due to the placebo effect [19, 81]. Another avenue to correct *SMN2* splicing is through *trans*-splicing mRNA. *Trans*-splicing requires two different mRNAs, the endogenous mutated mRNA and exogenous corrected mRNA [21]. Coady and Lorson have shown that *trans*-splicing is beneficial in the CNS and distal tissues through increases in snRNP assembly and longer life span following intracerebral-ventricular injections [21].

Lastly, introduction of the SMN gene can be achieved through administration of viral vectors or stem cells [80]. Pluripotent stem cells, from Type I SMA patients, were corrected by converting the key point mutation in *SMN2* to reflect the sequence of *SMN1* [22]. These cells were differentiated into motor neurons and experiments have demonstrated both increased size of motor neurons and number of gems [22]. Preliminary results with AAV viral vectors resulted in widespread transduction of the SMN gene, demonstrated enhanced survival times and improvements in physical health [6].

Research remains underway to determine the best treatment to delay disease progression, however all methods are associated with risks and challenges. Also being developed is a biomarker panel for the plasma proteins in SMA patients, the goal being to determine disease severity, predict motor function and evaluate therapeutics through biomarkers [48]. Research continues in labs across the world and conferences are held annually to share new knowledge about SMA.

1.2 **Adenovirus**

1.2.a Adenovirus background

Adenovirus (Ad) is a double stranded DNA virus with a 36 kb genome [110]. Replication occurs within the nucleus and the genome is packaged into a ~950 Å naked icosahedral capsid for a total weight of 150 MDa [68]. Ad has nine capsid proteins, three major: hexon (pII), penton (pIII) and fiber (pIV), and five minor: pVI, pVIII, pIIIa, pIVa2 and pIX [110]. There are over 50 serotypes of Ad which can be divided into six different subtypes [110]. Although all serotypes have similar structural and genomic characteristics they can differ in their interactions with host cells [68].

Ad has been greatly studied over the past 60 years and has helped in the discovery of host-virus interactions and eukaryotic processes such as alternate splicing and apoptosis [68]. Ad is able to infect a variety of species including humans, and can lead to respiratory, gastrointestinal and eye infections [68]. Fortunately, most infections remain subclinical unless in an immunocompromised person [68].

1.2.b Fiber and retargeting

Fiber, one of the major capsid proteins, functions in Ad attachment to host cells [68]. The protein is projected from the capsid surface in trimers from a penton base at each of the 12 vertices [72]. Fiber is composed of a tail, shaft and knob (Figure 1.2) [72]. Ad attachment and uptake into host cells is a two step process: first the fiber knob interacts with the cellular coxsackie-adenovirus receptor (CAR) [68]. CAR is a member of the immunoglobulin family and is expressed on most cell types [115]. CAR functions as the primary receptor for most Ad serotypes including Ad5 [68]. Once the virus is attached to the host cell, fiber's flexible shaft is able to bend, decreasing the distance between the virus and the cell [68]. This allows

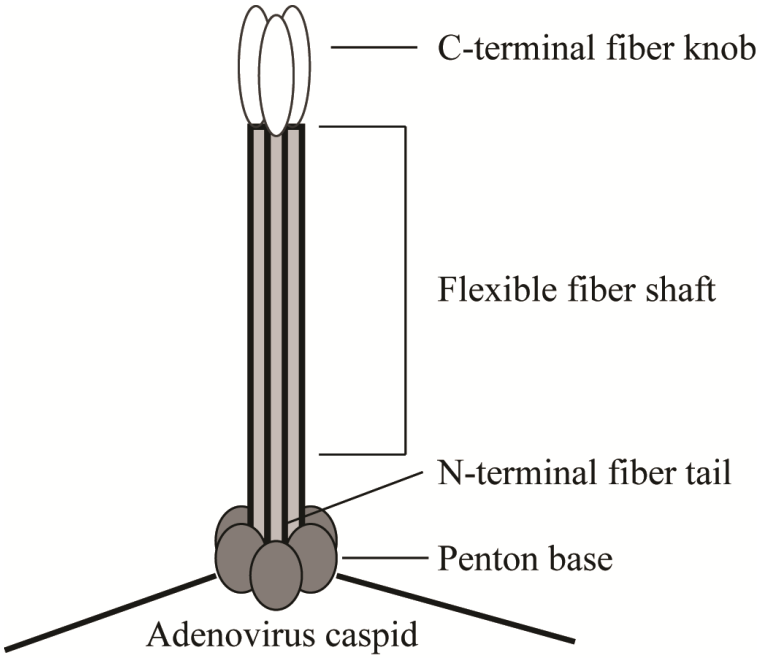
C-terminal fiber knob
Flexible fiber shaft
N-terminal fiber tail
Penton base
Adenovirus caspid

Figure 1.2 *Fiber structure and domains*. Fiber is projected in trimers from a penton base located at each of the adenovirus capsid vertices. The fiber protein has three domains, an N-terminal tail buried within the penton base, a flexible shaft and a C-terminal knob involved in cellular binding. Figure modified from Medina-Kauwe [72].

for the second step of viral entry where the RGD loop (Arg-Gly-Asp) in the penton based interacts with cellular α_v integrins to stimulate endocytosis [68].

It is well established that Ad predominately localizes to the liver after systemic delivery [47]. This event occurs not only due to the physical structure of the liver but the scavenging Kupffer cells which reside there [84]. Due to this high liver tropism there is ongoing research to explore Ad retargeting. A number of capsid proteins including: hexon, pIX, penton and fiber have been manipulated in an attempt to alter Ad targeting [84]. These protein modifications are achieved through the addition of targeting ligands via covalent, non-covalent or genetic modifications [84]. These ligands can increase specificity towards cell specific receptors or decrease specificity for CAR, either way altering Ad tropism. Bramson *et al* showed that the addition of poly-lysine residues to the Ad5 H-I loop within the fiber knob enhanced Ad muscle infection *in vivo* through increasing specificity to heparan sulphate proteoglycans [11]. Heparan sulphate proteoglycans are highly sulphated carbohydrates that can mediate CAR-independent attachment for some Ad serotypes, including Ad5 [119]. It is also possible to alter targeting by combining different Ad serotypes to form chimeric vectors. The small differences in Ad serotypes can result in different host-viral interactions [68]. For instance Ad35 is known to interact mainly with CD46 not CAR, while Ad9 is thought to bind two different primary receptors, one of which is CAR [119, 98]. Shayakhmetov *et al* created a chimeric vector (Ad5/9) to observe differences in receptor binding [98]. Based on Shayakhmetov results, it was concluded that two factors play a major role in Ad internalization i) knob specificity to the primary receptor and ii) the length of the shaft hence the distance between the virus and the cell membrane [98]. Overall, differences in fiber knob and shaft domains as well as additional targeting ligands can affect receptor attachment and therefore alter Ad targeting.

1.2.c Adenovirus vectors in gene therapy

Ad has great potential as a viral vector for gene therapy [68]. Ad-based vectors are created through the removal of essential viral genes, mainly early region 1 (E1), to ensure the virus is no longer replication competent [23]. Desired therapeutic genes can then be inserted into the viral genome. Ad has many advantages, in terms of gene therapy, over other vector systems such as: large cloning capacity, remaining primarily episomal and a relatively good safety profile [116]. In 1993 the first human study was done using a recombinant Ad to treat cystic fibrosis [23]. Since that time clinical trials have been initiated for a variety of other diseases with varying degrees of success [116]. Researchers have been looking into means of improving Ad as a viral vector, mainly through Ad retargeting, discussed above. Presently Ad is the leading platform for human clinical trials, representing approximately 23% of viral vectors in 2012 [32]. There are currently two approved therapeutics bases on Ad viral vectors, both for the treatment of cancer and only approved in China [116].

One drawback to Ad as a viral vector is its ability to activate the immune system as Ad epitopes are easily recognized [23]. Work to address this issue has taken place through two methods, first when the immune response becomes too robust to a given Ad vector, the viral backbone can be replaced with an alternate Ad serotype [23]. Second, reducing the number of genes which encode viral proteins within a vector decreases the immune response. As such, several generations of Ad have been developed with differing degree of attenuation [23]. First generation Ad, the most common, has the removal of only the essential E1 gene allowing for a cloning capacity of 4.7 kb [82]. In comparison helper dependent Ad has all viral genes removed allowing for a 37 kb cloning capacity [82]. The duration of expression from a vector *in vivo* varies depending on the immune response [82]. Current studies have shown that helper dependent Ad can persist for over 7 years in non-human primates with

high levels of gene transduction [12].

1.3 **Exosomes**

1.3.a Exosome discovery

During normal conditions, as well as in states of distress, cells release microvesicles to carry out various cellular functions [112]. Different forms of these free-floating microvesicles are characterized by both size and cellular site of origin; however there is some over-lap [112]. For example, microparticles are 100-1000 nm in size and formed through external budding of the plasma membrane, while apoptotic bodies are over 1 µm and formed during cellular breakdown [101, 99]. In 1983, Johnstone's team studied small vesicles released from reticulocytes during their study of the transferrin receptor [112]. Johnstone defined these vesicles as exosomes based on the term described two years earlier by Trams *et al* [107]. Exosomes represent the third major type of microvesicles released from cells, with a diameter of only 30-100 nm and a cup-shaped morphology [71, 62].

1.3.b Exosome formation and release

Unlike other microvesicles such as apoptotic bodies or microparticles, exosomes do not bud from the plasma membrane [62]. Instead exosomes originate from endosomes [62]. Endosomes can undergo a series of internal budding events to morph into multivesicular bodies (MVB) [111, 38]. The vesicles enclosed within the MVB are intraluminal vesicles (ILV), which contain both membrane and cytosolic proteins [104]. ILV are structured with an interior cytosolyic bilayer, an exposed lumen membrane and an overall negative charge [104, 84]. As the MVB develops it can progress through different paths (Figure 1.3) [62]. The MVB can merge with a lysosome where the MVB and its contents will be degraded, or the MVB can merge with the plasma membrane resulting in release of the ILV [62, 111]. Once these vesicles are released into the extracellular matrix they are termed exosomes [62].

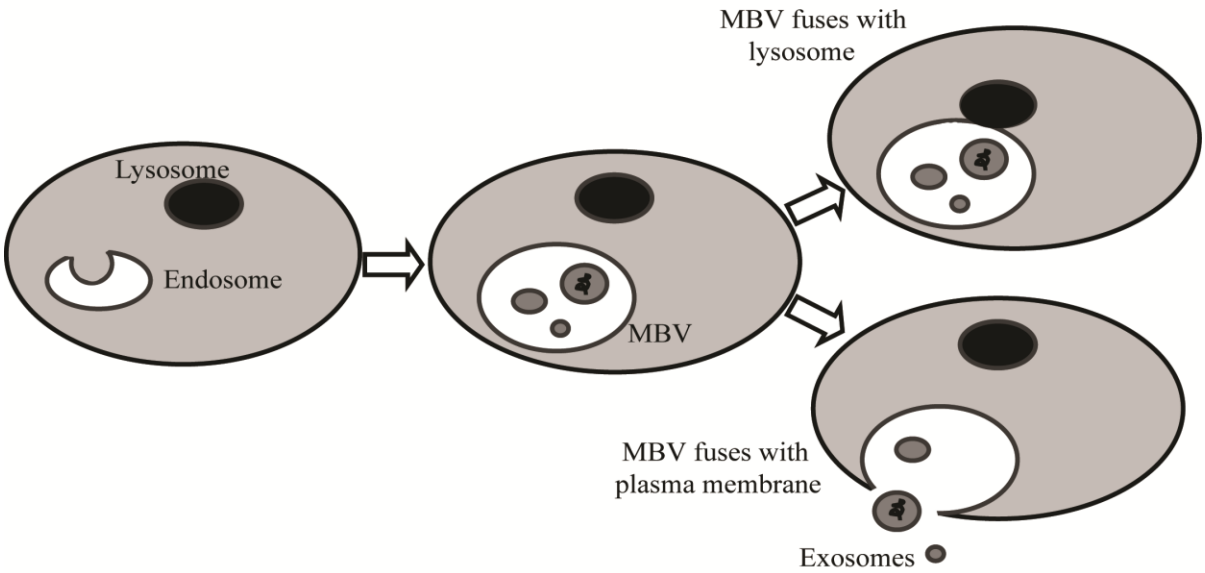
MBV fuses with
lysosome
Lysosome
Endosome
MBV
MBV fuses with
plasma membrane
Exosomes

Figure 1.3 *Exosome formation and release*. Endosomes which undergo a series of internal budding are referred to as multivesiclar bodies (MVB). Membrane proteins and cytosolic proteins can be captured during budding and be contained in these intraluminal vesicles (ILV). The MVB can either merge with a lysosome leading to degradation or fuse with the plasma membrane to release all ILV, now termed exosomes.

Some researchers believe there may be different populations of MVB which progress through specific pathways [62]. Trends have been observed that ILV high in phosphatidylinositol-3-phosphate, Rab7 and ubiquitinated proteins are processed by lysosomes while ILV high in ceramide, Rab11, Rab27 and cholesterol are released as exosomes [62, 99, 109].

Exosomes are estimated to be able to encompass 100 proteins and net 10,000 nucleotides [70]. Cytosolic and membrane proteins can be triggered for exosome packaging through signalling-induced ubiquitination [3]. Surprisingly cytosolic proteins (i.e. tubulin and SOD1), which lack any signal peptides, can also be found within exosomes due to the internal budding process during exosome formation [104, 33]. The method of 'sorting' proteins, mRNAs and microRNAs into exosomes is currently unknown; however studies have shown that some proteins are packaged at a higher rate in different stress conditions [58]. Similarly, the RNA contained in exosomes may represent only a sub-set of the RNAs expressed in the donor cell suggesting, exosomes are loaded with specific RNAs [108]. In fact, some microRNA and mRNA seem to be exclusively packaged into exosomes as they are found at much higher concentrations than that of the donor cell [108].

In the last several years, significant progress has been made in determining the mechanism involved in exosome release. Different cell types and cells at different stages of development are thought to vary in the amount of exosomes produced [2]. Release occurs in both a constitutive and regulated manner, where release can be altered through stress factors and stimulation signals [95, 62]. Studies have shown the importance of endosomal sorting complex required for transport (ESCRT) during exosome formation, particularly ILV formation [62]. ALIX a component of the ESCRT machinery is known to interact with syndecans through the adaptor protein, syntenin, which is required for proper budding and

ILV cleavage [3]. Kosaka *et al* demonstrated that exosome release is not dependent on ESCRT machinery but is dependent on ceramide [52]. Inhibiting ceramide biosynthesis, through down-regulation of neutral sphingomyelinase 2, has been directly shown to decreases exosome budding [52, 51]. Other components such as calcium levels and protein cross-linking or protein clustering also play a role in the rate of exosome release [58, 53, 111]. Carayon *et al* suggest that exosome packaging is a combination of pathways that work simultaneously or vary in dominance depending on cell type and level of cellular maturation [16].

1.3.c Exosome entrance

Much of the exosome field focuses on immune cells and the functions of immune generated exosomes. For this reason information on exosome entrance in immune cells is far better understood than in other cells types [62]. Exosome entrance occurs through fusion or receptor mediated endocytosis [70]. Fusion of exosomes to a cellular membrane appears to be lipid-dependent and results in the immediate transfer of membrane proteins [62, 70]. Endocytosis can occur through receptor/ligand mediated interactions [20] which implies cell specific communication [108]. Receptor mediated endocytosis requires the participation of the recipient cell's cytoskeleton and is affected by both temperature and calcium levels [77]. Some receptors involved in exosome attachment include: PS, CD11a, CD54, CD9, CD81and integrins [77]. Endocytosis by phagocytic cells occurs rapidly with most studies observing exosome internalization in as little as 30 minutes [30]. Exosomes are initially contained in early endosomes, which can then be processed to late endosomes approximately two hours following active up-take [77]. At this point, exosomes can be degraded and their cargo can be processed, such as peptides being presented to T-cells or signals from microRNAs [77].

Alternatively, exosomes can reside in recycling endosomes resulting in enhanced intercellular transport and release through transcytosis [53, 97]. In comparison, non-phagocytic cells display lower levels of exosome uptake mainly due to exosomes remaining bound to the cell surface [30]. Endocytosis appears to be dependent on actin, Annexin2, Annexin6 and dynamin2 but can occur with or without clathrin [58, 30]. Recipient cell internalization has been shown in various cell lines including: dendritic cells, macrophages, cancer cells and liver cells [77, 51, 70].

1.3.d Exosome markers

Exosomes have a unique lipid composition that can be used to distinguish them from apoptotic bodies and microparticles [15]. Exosome characterization is achieved through shape, size and by probing for common exosome markers [71]. Protein content can vary depending on the exosome's cell-of-origin; however, there are some proteins more commonly found within exosomes which can be used for exosome identification [112]. These universal exosome markers may have essential roles in exosome formation [117] as they include proteins involved in the endocytic pathway (tetraspaninis – CD63 and CD81), cell structure (actin and tubulin), membrane proteins (Flotillin-1 and 2), antigen presentation peptides (MHC I and MHC II), cell adhesion proteins (integrins), stress regulators (Hsc70 and Hsp90), apoptosis related proteins (ALIX) and intracellular transport proteins (annexins) [104, 100]. Expression levels of universal markers vary between cell types, as well as between exosomes and their corresponding donor cells [117]. This variation decreases the reliability of some of these markers as loading controls i.e. actin [117]. Proteins rarely found within exosomes, including proteins that localize to the mitochondria and endoplasmic reticulum, i.e. SMAC and calnexin respectively, are used as negative exosome markers [33].

Unfortunately these proteins can sometimes be captured in exosomes during budding. Therefore neither the positive nor negative exosome markers are a perfect system.

1.3.e Exosome functions

Research in exosomes boomed in the late 90's when it was determined that exosomes are released from a number of cell types and are implicated in other roles besides waste removal [52]. These functions include but are not limited to: antigen presentation, antiviral activity, cellular adhesion and cell signalling [70]. Many studies have shown the contribution of exosomes in the immune system. Exosomes produced from B cells express MHC II molecules and are able to participate in antigen presentation to stimulate T-cells [87]. Studies suggest that exosomes are able to activate T-cells both directly and indirectly with the aid of dendritic cells [15]. This may be dependent on the type of T-cells as well as the exosome's ability to transfer MHC molecules to dendritic cell populations [105]. Exosomes aid in immune function through other means including transfer of antiviral molecules induced by IFN-α activation [58]. Second, exosomes aid in cellular adhesion. Exosomes function to enhance adhesion of cells to each other and culture dishes, implying that exosomes themselves are quite successful at cellular attachment [53]. Studies done by Clayton *et al* showed the ability of exosomes to interact with components of the extracellular matrix and other cells through integrin molecules expressed on their surface [20]. Lastly and most importantly, studies have shown that exosomes are able to transfer information in the form of mRNA, microRNA and proteins between cells resulting in phenotypic change in the recipient cell [108, 112]. For instance, normal cells use exosomes as messengers to prevent the growth of tumours by releasing growth-inhibitory signals in the form of microRNAs [51]. Of note, these signals do not prevent the growth of healthy cells, suggesting differences

in cell tolerance [51]. Valadi *et al* found the RNA packaged in exosomes tended to have roles in cell development, protein synthesis and post-translational modifications [108].

Although exosomes have a number of advantageous functions for the host, they can be exploited to aid in tumour growth and the spread of pathogens [40, 86]. Within a tumour microenvironment, exosomes can be used to promote invasiveness and motility [86]. For example, studies have shown that miRNAs, i.e. miR-210 and miR-21, can be transferred through exosomes to enhance cancer metastasis, angiogenesis and apoptosis [49, 41]. In fact, cancer cells are thought to up regulate exosome release and/or secrete exosomes with higher protein concentrations than non-cancerous cells [49]. Similarly, viruses and intercellular pathogens have been shown to be contained within exosomes including: hepatitis C, HIV negative regulatory factors, Epstein-Barr miRNA and prion proteins [85, 97]. Not only does this aid in the pathogenicity and spread to adjacent cells, but this also functions to mask the pathogen from antibody-mediated neutralization [85].

1.3.f Exosome therapeutics

Exosomes are found in various body fluids, including urine and serum, where in the latter exosomes are estimated to have a concentration of three million/μL [112]. The presence of exosomes in body fluids suggesting they are able to circulate throughout the body whilst functioning in intercellular communication [15]. Studies of exosome delivery *in vivo* have shown a very short half-life in serum, approximately two minutes, and localization predominantly to the liver, with some detection in the lungs, kidneys and spleen [102]. Fortunately, studies have shown that exosomes can be genetically modified to alter their targeting for disease treatment [62]. Alvarez *et al* showed that neuronal-targeted exosomes were able to cross the blood brain barrier, be taken up by neurons in the brain and delivered

functional siRNA cargo [2]. Currently, exosome treatments are being tested in Phase 1 and 2 clinical trials for melanoma, non-small cell lung cancer and colorectal cancer [28, 112]. In these studies, exosomes are collected, purified, and the desired protein is attached directly to the exterior of the exosomes, which is referred to as direct loading [112]. The direct-loaded exosomes were then redelivered into the same individual as a vaccine to treat different types of cancers [112]. In this way, the immune system will not reject the exosomes; however this process must be carried out on an individual basis [112]. Other studies have shown that exosomes can also be loaded with cargo through electroporation [2]. Another avenue of investigation is looking at combining exosomes and gene therapy, as AAV caspids can associate with microvesicles and this interaction enhances viral infectivity *in vitro* [67]. Furthermore, exosomes have potential to be useful therapeutics since they appear well tolerated from both toxicological and immunological standpoints and they do not show decreased efficiency with repeated administration [2]. Lastly, since exosomes are not alive they can be easily stored and retain their biological activity [112].

Exocarta is an online database that has been created to assist exosome investigators in sharing data. To date, over 4,500 proteins, 1,600 mRNAs and 750 mircoRNA have been identified within exosomes isolated from different species and cell types [71]. Exocarta also describes different exosome purification methods, for instance differential centrifugation is used by 84% of studies, ultra-centrifugation is used by 30% of studies, and immunoaffinity-based isolation is used in only 9% of studies [71]. Of note most studies are now using a combination of purification techniques including the addition of filtration steps to enhance protocol stringency and homogeneity of the final sample [71]. Commercial fits including Exoquick and Exomir are also available as an alternate exosome collection method.

1.4 **Rationale**

SMA is caused by the deficiency of SMN, which results in α-motor neuron and skeletal muscle deterioration. Systemic addition of SMN could lead to phenotypic, lifelong correction of the defects caused by SMA. As such, two different methods, both involving an SMN expressing Ad vector, were investigated to enhance SMN levels *in vitro* and *in vivo*. First (1) we investigated whether a reduction in the Ad fiber protein, to reduce the overall size of the virus, could enhance gene delivery to muscle and motor neurons. Second (2) we investigated whether the liver could be used as a protein production factory to produce large amounts of a secreted SMN protein for circulation and uptake throughout the body. Surprisingly, our initial studies determined that SMN is naturally released from cells in exosomes which caused us to explore this process as a potential novel therapeutic.

1.5 **Hypothesis**

There are two major hypotheses, one for each approach:

1. Ads fiber protein can be modified to allow for altered infection tropism and decreased overall size of the virion resulting in enhanced dissemination throughout the body.
2. Following liver transduction of an SMN-expressing Ad vector, virally produced SMN can be secreted from cells, spread throughout the body, be taken up by other tissues and function in recipient cells.

1.6 **Objectives**

The specific aims designed to test these hypothesizes are:

1. (i) Generate an Ad virus which infects the desired tissues, i.e. the spinal cord and skeletal muscle, (ii) determine the most effective delivery method and (iii) investigate the optimal viral dose to be used *in vivo*.
2. (i) Determine if SMN can be released from cells (ii) investigate how SMN release can be enhanced (iii) evaluate if released SMN is taken up by recipient cells and (iv) study this process *in vivo*.

Chapter 2 – Materials and Methods

All solutions are described in detail in Appendix 1

2.1 **Cell culture.** All cell culture media and reagents were obtained from Invitrogen (Burlington, ON). Monolayers of human embryonic kidney 293 cells [36], 293N3S [35] and adenocarcinomic human alveolar basal epithelial A549 cells (American Type Culture Collection) were grown in complete minimum essential medium (MEM) (see Appendix 1). Rat cholinergic motor neuron MN1 cells [93] were graciously provided by from Dr. Jocelyn Cote (University of Ottawa) and were maintained in complete Dulbecco's modified Eagle's medium (DMEM). Undifferentiated mouse myoblast C2C12 cells [7] were grown in complete DMEM. Confluent plates were switched to differentiation medium for 4 days in order to induce myotubes differentiation.

2.2 **Cloning and Nucleofection.** A new cell line, A549::SMN, was created from a pCD2-SMN [24] plasmid digested with Xbal, BamH I and BgI II to allow for the insertion of EMCV/IRES and hygromycin resistance. This new plasmid was transfected into A549 cells using the Amaxa Cell Line Nucleofector Kit T (Lonza). Cells were pooled following transfection and positive cells were selected for using 150 µg/mL hygromycin (Invitrogen) in complete MEM.

2.3 **Generation and propagation of viruses.** A plasmid, pRP2014, containing an Ad5 genome excluding Ad5 E1 and E3 region was used as the backbone for all viruses in this study [84]. The viruses are replication defective and were generated using standard techniques [89]. A cytomegalovirus (CMV) immediate early enhancer/promoter-β-galactosidase expression cassette (pCA38) [1] was inserted in place of the E1-deletion, using RecA-mediated recombination [18], as detailed previously [114] to create the control virus Ad5LlacZ. Drs. Dmitry Shayakhmetov and Andre Lieber (University of Washington) kindly

provided a plasmid containing a modified fibre protein with the Ad9 shaft and Ad5 knob [98]. The modified fibre gene was subcloned into pRP2014 along with pCA38 and designated Ad5SlacZ. To introduce the poly-lysine motif into the H-I loop of the knob domain, a BglII/PstI fragment containing this region was first subcloned into pSP72 (Promega). This plasmid was PCR amplified and the linear product recircularized creating a molecule encoding a short fibre knob domain that has been changed from GDTT-PSAY to GDTT-AGKKKKKKKGA-PSAY. The resulting plasmid was recombined with pRP2014 and pCA38 and designated Ad5SpKlacZ (Figure 3.1).

Additional viruses were created from plasmids containing Flag-SMN, Flag-SMN-myc-his or Flag-SP-SMN [14]. Once again, plasmids were subcloned into pRP2014, with the transgene under regulation by the CMV immediate early enhancer/promoter, and designated Ad-SMN, Ad-SMN-myc-his or Ad-SP-SMN respectively (Figure 4.1). All viruses were created and purified by Dr. Robin Parks or Kathy Poulin.

2.4 **Particle counts.** An aliquot of virus was diluted in assay buffer, heated for 20 minutes at 65^{o}C, and the absorbance determined as $1A_{260} = 1.1x10^{12}$ particles.

2.5 ***In vitro*** **infections.** Triplicate 35 mm dishes of A549, MN1, or undifferentiated or differentiated C2C12 cells were seeded at a density of 0.3 x 10^{6} cells per 35 mm dish. The following day cells were infected at an MOI (multiplicity of infection) of 10 with Ad5LlacZ, Ad5SlacZ or Ad5SpKlacZ (or mock infected). All viruses were diluted in PBS to a final volume of 200 µL. Infections were done for 1 hour at 37ºC with periodic rocking to redistribute virus on the monolayer, then 1 mL fresh media was added to the cells. Crude protein extracts were prepared from the infected cells 24 hours post infection (hpi) by lysing the cells with 175 µL of Lysis Solution (Applied Biosystems). The samples were centrifuged at 9400 xg for 2 minutes at room temperature (RT), the supernatant was then collected and

stored at -80^{o}C. Infections with Ad-SMN and Ad-SP-SMN were done on confluent 35 mm or 150 mm dishes of A549 cells at MOI 5, 10, 25, 50 or 100. Twenty-four hpi, media was collected and crude protein extracts were harvested using 200 µL of 2x LD (Laemmli loading dye) per 35 mm dish. Samples were stored at -20ºC until use.

2.6 **Trichloroacetic acid media precipitation.** Duplicate 35 mm dishes of confluent cells were washed with PBS prior to adding complete media. In the case of virally infected cells, washing took place immediately after the 1 hour infection period. After a 24 hour incubation, media was collected and centrifuged at 2,500 xg for 5 minutes. The supernatant was collected. Two hundred and fifty µL of 100% trichloroacetic acid **(**TCA) was added to 1 mL media and incubated on ice for 1 hour. The solution was centrifuged at 16,000 xg for 5 minutes. The supernatant was removed the pellet was washed with 200 µL 100% ethanol and centrifuged at 16,000 xg for 5 minutes. Again the supernatant was removed and the pellet resuspended in 100 µL 2x LD. Samples were stored at -20ºC until use.

2.7 ***In vivo*** **injections.** Five different viruses were tested: Ad5LlacZ, Ad5SlacZ, Ad5SpKlacZ, Ad-SMN and Ad-SMN-myc-his. Three viral concentrations were used $5x10^{11}$ VP/kg (low), $1x10^{12}$ VP/kg (middle) and $5x10^{12}$ VP/kg (high). Six to eight week old C57Bl/6J (Charles River) or CD1 mice were injected intravenously (IV - tail vein) or intraperitoneally (IP) with 100 µL virus (or mock infected) or TA (tibialis anterior) injected. For TA injections, mice were anesthesized with halothane, and injected with virus diluted in PBS or in 16 mg/mL Dextran Texas Red Fixable dye (Life Technologies) to a final volume of 25-30 µL for both the right and left TA muscle. One, two or three days post injection mice were euthanized with 100 µL euthanyl (CDMV Inc., Quebec City, QC) followed by decapitation (CDMV, Quebec City, QC) or sacrificed through cardiac puncture and chest

opening. All procedures were approved by the University of Ottawa Animal Care Facility and Animal Care Committee protocol review group.

2.8 **Tissue Homogenization.** Liver, TA muscle, and spinal cords were removed, immediately frozen in liquid nitrogen and stored at -80^{o}C. Full livers were homogenized in 1 mL of PBS using a Power Gen 125 homogenizer (Fisher Scientific) at speed 5.5 for approximately 10 seconds or until no solid chunks were visible. Samples were incubated on ice, then sonicated using a Vibra Cell (Sonic Materials Inc.) twice for 15 seconds with a 10 second rest period between. Spinal cords were homogenized in 300 μL of PBS using a Power Gen 125 homogenizer at speed 4.5 for approximately 10 seconds or until no solid chunks were visible. Samples were incubated on ice then sonicated once for 15 seconds. Both liver and spinal cord samples were then centrifuged at 850 xg for 10 minutes and the supernatant collected. Sample supernatant was either stored at -20^{o}C until use or if the samples were to be used for β-galactosidase **(**β-gal) determination further processed. TA muscles were homogenized using a liquid nitrogen chilled mortar and pestle. The ground muscle was then resuspended in 400 μL RIPA buffer. Both liver and TA samples from mice injected with a β-gal-expressing virus were further processed by heating in a 55^{o}C water bath for 15 minutes, followed by centrifugation at 16,000 xg for 10 minutes. The supernatant was collected and stored at -20^{o}C.

2.9 **Tissue Sectioning.** TA muscles, spinal cord, and diaphragm were removed and immediately incubated in 2% paraformaldehyde (PFA) fixative for 1 hour, followed by 3 washes in PBS and a final incubation in 30% sucrose for 48-72 hours. Tissues were equilibrated in 50:50 30% sucrose:OCT (Tissues Tek 4583) solution for 1-2 hours on a rocking platform. Samples were embedded in the same 50:50 mixture by flash freezing in

liquid nitrogen and stored at -80^{o}C until sectioning. These tissues were later sectioned in transverse or longitudinal 12µm sections using a Leica CM 1850 and stored at -20^{o}C.

2.10 **β-galactosidase staining.** Sectioned tissues were hydrated in PBS for 1-2 minutes and then fully submerged in X-gal stain for 24 hours at 37^{o}C. Slides were washed in PBS for 1 minute and covered with a 1:1 PBS:30% glycerol solution and a glass cover slip. Quantification of the stained areas was performed using ImageJ (Wayne Rasband, Research Services Branch, National Institute of Mental Health, Bethesda, Maryland, USA). A color intensity threshold was applied to determine the area of the muscle section showing X-gal staining, which is reported as the percentage of the total cross-sectional area of the muscle.

2.11 **Exosomes collection.** Confluent 150 mm plates of A549, A549::SMN or 293 cells were washed twice with PBS and then incubated in unmodified MEM for 24 hours at 37^{o}C. Ad-SMN infected A549 cells, were infected at MOI 50 and washed with PBS immediately following infection to remove unattached virus. Exosomes were harvested using three different methods (i) ultracentrifugation, (ii) ultracentrifugation and filtering or (iii) Exoquick (System Biosciences). To harvest exosomes via ultracentrifugation, the media was collected and centrifuged at 2,000 xg for 20 minutes. This supernatant was transferred to new tubes and centrifuged at 10,000 xg for 30 minutes. The supernatant was transferred to new tubes and centrifuged at 100,000 xg for 1.5 hours. The supernatant was discarded, the pellet was resuspended in PBS and centrifuged at 100,000 xg for 1 hour. The pellet was then collected and resuspended in approximately 100 µL of PBS and stored at -80ºC. To harvest exosomes by ultracentrifugation and filtration the 10,000 xg centrifugation step was replaced with a filtration step using a 0.2µm filter. This latter method was used for all exosome experiments unless stated otherwise. To harvest exosomes using the Exoquick reagent the System Biosciences protocol for Exoquick-media (Catalogue number: SYEXOTC2A1) was

followed and samples resuspended in deionized water. Exosome concentration was determined using a Bradford (Bio-Rad) assay with (addition of 10 µL RIPA to lyse the exosomes) or without exosome lysis. The size of exosome particles was determined through Nanoparticle Tracking Analysis using a Brunel Microscope Ltd Nanosight and NTA 2.3 Analytical Software. The Nanosight was set to a 60 second duration, 15-20 millisecond shutter time, automatic blur with threshold level varying between samples. For comparison, Dr. Dylan Burger (University of Ottawa) kindly supplied us with purified apoptotic bodies, microparticles, exosomes, vesicle free media and cell lysates, all resuspended in RIPA from human umbilical vein endothelial cells (HUVECs).

Serum exosomes were harvested following cardiac puncture, blood was allowed to clot for approximately 2 hours at RT. Blood was centrifuged at 1,000g for 10 minutes and serum was collected and stored at -80ºC. Serum exosomes were harvested using Exoquick-serum (catalogue number: SYEXOQ5A1) as per the manufacturer's instructions.

2.12 **Analysis of exosome-mediated delivery of protein to cells.** A549 cells were incubated with 5 ug exosomes for 4 hours. Following incubation, cells were wash with PBS and harvested for immunoblot using 2x LD.

2.13 **Chemiluminescent β-galactosidase assay.** Homogenized tissues, cells harvested in Lysis Solution (Applied Biosystems) and exosomes were assayed for β-gal activity using a commercial kit Galacto-star (Applied Biosystems) as per the manufacturer's instructions. In all cases, 10 µL of sample was incubated for 1 hour in the reaction solution and analyzed for 1 second using a 20/20n luminometer (Turner BioSystems). Tissue data was normalized to the amount of protein in each sample, as determined by Bradford assay (BioRad).

2.14 **Immunofluorescence analysis.** Tissue slides were blocked in BSA (bovine serum albumin) Blocking Buffer for 1 hour. All incubations were preformed in a dark humidified

chamber. After blocking, 1/400 β-gal (Invitrogen) or 1/800 laminin (Invitrogen) primary antibody diluted in BSA Blocking Buffer was applied and stored at 4°C overnight. Slides were washed 3 times with PBS and incubated with 1/500 anti-rabbit-FITC (Invitrogen) or 1/500 anti-chicken-Alexafluor-488 (Invitrogen) secondary antibody for 1 hour. Slides were washed 3 times with PBS and covered with Dako fluorescent mounting medium (Dako) and a glass cover slip. Slides were stored at 4°C for a minimum of 24 hours before viewing. A549 and A549::SMN cells were grown for 24 hours on 18 mm disks (Fisher) contained in 35 mm dishes. Cells were washed twice with PBS and fixed for 10 minutes with 1 mL 4% PFA per 35 mm plate. The cells were washed twice with PBS then covered with BSA Blocking Buffer for 30 minutes. The BSA Blocking Buffer was removed and the cell covered disks were placed on glass slides. The cells were incubated with 1/500 Flag primary antibody diluted in BSA Blocking Buffer overnight at 4ºC. The primary antibody was removed and the cells washed 3 times for 5 minutes with PBS. The secondary antibody, 1/ 5,000 anti-rabbit-FITC (Invitrogen), was then incubated with the cells for 1 hour at RT in the dark. The secondary antibody was removed and the cells were washed twice for 5 minutes with PBS. Cells were covered with Hoechst diluted in BSA Blocking Buffer, to a final concentration of 0.2 µg/mL, for 20 minutes at RT in the dark. The Hoechst (Life Technologies) was removed and the cells were washed 3 times for 5 minutes with PBS. Dako mounting solution was added and the cells were covered with a glass cover slips. Slides were stored at 4ºC in the dark.

2.15 **Immunoblot analysis.** Western blot was used to determine the presence of various proteins in TCA precipitates, cells lysed in 2x LD, exosomes, serum, homogenized tissues and to examine the accuracy of Ad particle counts. Samples were diluted in 2x LD. Viruses were diluted to 10^9 viral particles in PBS and 2x LD. All samples were boiled for 5 minutes

at 100^{o}C and separated by electrophoresis on a 12 or 15% SDS-polyacrylamide gel. The separated proteins were transferred using a Trans-blot SD Semi-Dry transfer cell (Bio-Rad) for 1.5 hours to a polyvinylidene difluoride membrane (Immobilon-P, Millipore). The membrane was then incubated in Milk Blocking Solution for 1 hour prior to probing with various primary antibodies overnight at 4^{o}C (Table 2.1). Binding of the primary antibody was detected using a goat anti-mouse 1/10,000 or goat anti-rabbit 1/5,000 secondary antibody conjugated to horseradish peroxidase (BioRad) for 1 hour at RT. Washing was done three times for 5 minutes with TBST between each incubation period. Proteins were visualized by chemiluminescence reaction (Thermo Scientific ECL western blotting substrate) and autoradiography.

2.16 **Statistical analysis.** Statistical significance of the data was determined using ANOVA and Sigma Stat software. Groups which contained a significant difference were further processed by Dunn's or Tukey tests as recommended by the Sigma Stat program. All error bars represent standard deviation and the p-value was set to 0.05.

Table 2.1 Primary antibodies

Antibody	Species	Dilution	Company
All Ad	Rabbit	1/10,000	Abcam
Pan-actin	Rabbit	1/10,000	Cell Signaling
Alix	Rabbit	1/1,000	Sigma
β-gal	Rabbit	1/1,000	Life Technologies
Calnexin	Rabbit	1/1,000	Cell Signaling
Flag	Mouse	1/10,000 - cells 1/1,000 - exosomes/media	Sigma
Flotillin-2	Rabbit	1/1,000	Cell Signaling
GAPDH	Mouse	1/20,000	Abcam
His	Mouse	1/1,000	Cell Signaling
Myc	Mouse	1/1,000	Santa Cruz
SMAC	Rabbit	1/1,000	ProSci
SMN	Mouse	1/10,000 - cells 1/1,000 - exosomes/media	BD Transduction
SMN	Rabbit	1/1,000	Santa Cruz
Tubulin	Mouse	1/10,000	Oncogene
Tubulin	Rabbit	1/10,000	Abcam

Chapter 3 – Reduced virion size does not enhance viral distribution *in vivo*

3.1 Introduction

The goal of this project was to enhance virus delivery to muscle and motor neurons, the damaged tissues in SMA, through reducing the overall diameter of the virus by 30%. To achieve this reduction in size the Ad5's fiber protein was modified. Fiber is one of the three major capsid proteins and is composed of a tail, shaft and knob domains [72]. Fiber is projected from the capsid surface and therefore increases the diameter of the total virion [72]. The primary function of fiber is to initiate viral binding with the host cell through interactions with cellular receptors, usually CAR [68]. Fiber proteins from different Ad serotypes can vary in tissue tropism and fiber binding can be further altered through genetic or covalent modifications [84].

A series of fiber modified Ad constructs were created and tested by previous lab members [34]. Ad5 was used as a control to determine the efficiency of infection of the modified viruses. Preliminary results suggested that two of these viruses have potentially altered biodistribution. Both modified viruses contain an Ad9 shaft with an Ad5 knob. This modification decreases the overall size of the virion by 50 nm, possibly improving systemic distribution. Constructs containing the Ad9 shaft are referred to as short (S), whereas control Ad5 constructs are long, (L), Figure 3.1. The second modification is the addition of 7 lysine residues to the H-I loop in the fiber knob of a virus containing the shortened Ad9 shaft designated Ad5SpKlacZ. These additional poly-lysine residues increase specificity to cellular heparan sulphate proteoglycans instead of CAR [11]. Since not all cell types have high CAR expression, i.e. mature muscle, the poly-lysine modification allows for an increase in the number of cellular targets the virus can infect. As well, poly-lysine residues increase the overall charge of the virion, possibly improving interactions with the negatively charged

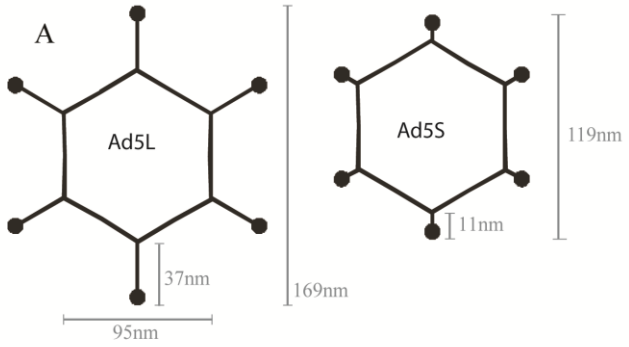

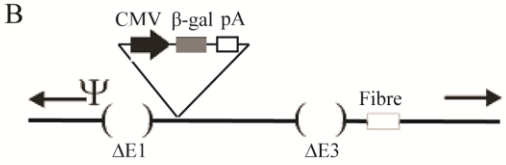

	Shaft	Knob	Modification	Shaft Length
Ad5LlacZ	Ad5	Ad5	---	37nm
Ad5SlacZ	Ad9	Ad5	---	11nm
Ad5SpklacZ	Ad9	Ad5	pk	11nm

Figure 3.1 *Viral constructs.*
Panel A: General capsid structure of the viruses used in this study.
Panel B: General genetic structure of the viruses used in this study. All viruses are deleted of E1 and E3, and contain the same *E.coli* lacZ gene under regulation by the human CMV immediate early enhancer/promoter and bovine growth hormone polyadenylation sequence (pA). Ad5LlacZ encodes the native Ad5 fibre protein. Ad5SlacZ encodes a chimeric fibre protein with an Ad9 shaft and Ad5 knob. Ad5SpKlacZ is similar in structure to Ad5SlacZ, but contains a poly-lysine motif in the H-I loop of the fiber knob domain.

cell membrane.

Throughout this chapter, I investigated: (i) which Ad construct best infects the desired tissues, i.e. the spinal cord and skeletal muscle, (ii) the most effective delivery method, and (iii) optimal viral dose. Initial experiments were done using a β-gal reporter gene for tracking. As all construct have the same promoter region, β-gal expression was used as a marker for infection efficiency. These studies will serve to establish the best vector and conditions for Ad-mediated gene therapy for SMA in the future. A manuscript for this project has been published in Virology (Appendix 2).

3.2 **Results**

3.2.a Ad vectors are able to infect both motor neurons and muscle cells *in vitro*

In vitro infections were preformed to ensure all Ad constructs were able to efficiently infected motor neurons and muscle cells. Viral titers were determined by particle count and their accuracy confirmed through immunoblot analysis of the major caspid protein hexon, Figure 3.2A. Immunoblot was further used to confirm differences in fiber size for the various viral constructs. As expected, the modified constructs containing an Ad9 shaft had significantly reduced fiber size compared to the control Ad5 virus, shown by the 15 kDa difference in Figure 3.2B. Next MN1, A549, undifferentiated and differentiated C2C12 cells were infected at a MOI of 10 with the various viruses and the infected cells harvested in lysis buffer (Applied Biosystems) at 24 hpi. Viral transgene expression was determined through a chemiluminescence β-gal assay. Our data showed all three viruses infected MN1 cells relatively consistently with a 10-fold increase in luminescence compared to the PBS control, Figure 3.3B. MN1 cell infection efficiency was lower than A549 cells, which expressed a 100-1000 fold increase in β-gal activity in the viral constructs relative to PBS, Figure 3.3A.

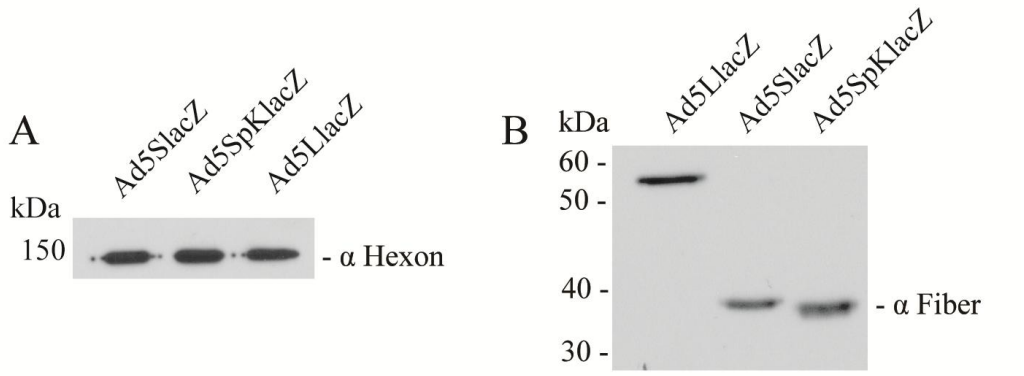
A
Ad5SlacZ
Ad5SpKlacZ
Ad5LlacZ
kDa
150
- α Hexon
B
kDa
Ad5LlacZ
Ad5SlacZ
Ad5SpKlacZ
60 -
50 -
40 -
30 -
- α Fiber

Figure 3.2 *Ad5LlacZ, Ad5SlacZ and Ad5SpKlacZ differ in fiber size.*
Panel A: Viral titers determined through particle count, were confirmed through separating 10^9 viral particles by SDS-PAGE, and probing the resulting membrane for hexon protein. Data represents n=3
Panel B: 10^9 virus particles were separated by SDS-PAGE and probed for fiber. Data represents n=2

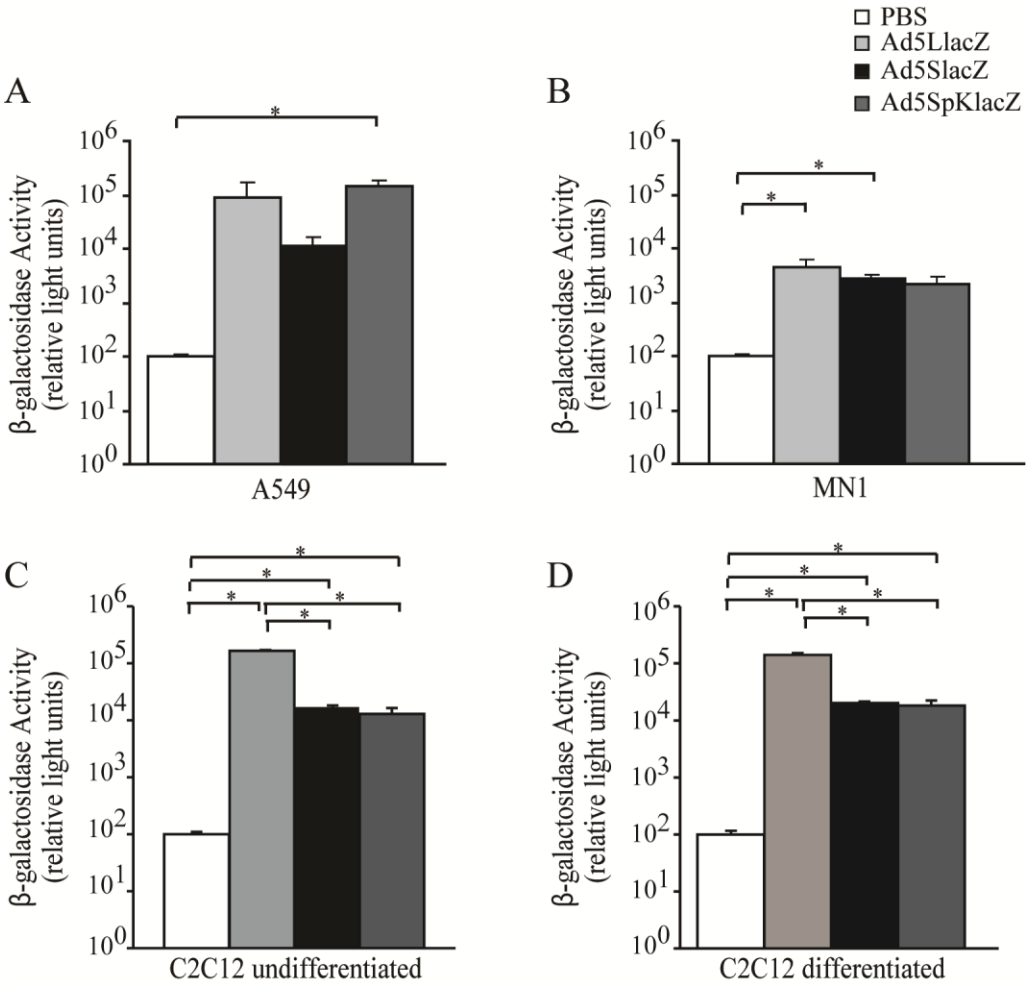
PBS
Ad5LlacZ
Ad5SlacZ
Ad5SpKlacZ
A
B
C
D
β-galactosidase Activity
(relative light units)
A549
MN1
C2C12 undifferentiated
C2C12 differentiated

Figure 3.3 *Infection of Ad5LlacZ, Ad5SlacZ and Ad5SpKlacZ in established cell lines derived from different tissues.* A549 (A), MN1 (B), and undifferentiated (C) or differentiated C2C12 (D) cells were infected at an MOI of 10 with Ad5LlacZ, Ad5SlacZ, Ad5SpKlacZ or mock infected with PBS. The quantity of β-gal expressed 24 hpi was assessed by chemiluminescent assay. Data represents n=3, with average and standard deviation shown. *= $p<0.05$.

Undifferentiated and differentiated C2C12 cells have nearly identical infection profiles, again with 100-1000 fold increase in luminesence compared to the PBS control, Figure 3.3C-D. Both Ad5LlacZ and Ad5SlacZ showed similar infection levels in C2C12 and A549 cells, while Ad5SpKlacZ had a 10-fold lower infection efficiency in C2C12 cells. All viruses showed enhanced infection efficiency in C2C12 cells compared to MN1 cells, with Ad5LlacZ demonstrating the most dramatic difference with a 10-fold increase. Overall, the results suggest that all the constructs were able to infect motor neuron and mature muscle cells *in vitro*, with Ad5LlacZ having a slightly higher degree of efficiency than the modified constructs.

3.2.b Ad vectors predominately localize to the liver and the site of injection

To examine viral spread *in vivo*, all 3 objectives - different constructs, injection methods and concentrations - were explored in parallel. As the constructs showed similar infection efficiency *in vitro,* experiments were continued with all three viruses. IP, IV and TA injections were investigated, as well as three viral concentrations $5x10^{11}$ VP/kg (low), $1x10^{12}$ VP/kg (middle) and $5x10^{12}$ VP/kg (high) however, only the high concentration was tested for TA injections. C57Bl/6J mice were chosen as they represent the background of the $SMN^{2B/-}$ SMA mouse model. Injections were preformed with mice between six and eight weeks of age. After a 24 hour exposure period, mice were euthanized and tissues harvested. Tissue infection was detected using a chemiluminescent assay and β-gal staining. Livers and TA muscles were homogenized for analysis via chemiluminescence assay, Figure 3.4. After systemic delivery Ad predominately accumulates in the liver, therefore high liver infection was expected. This was observed for both TA (Figure 3.4B) and IV injections (Figure 3.4F), where IV injections demonstrated increased transgene expression in a dose dependent

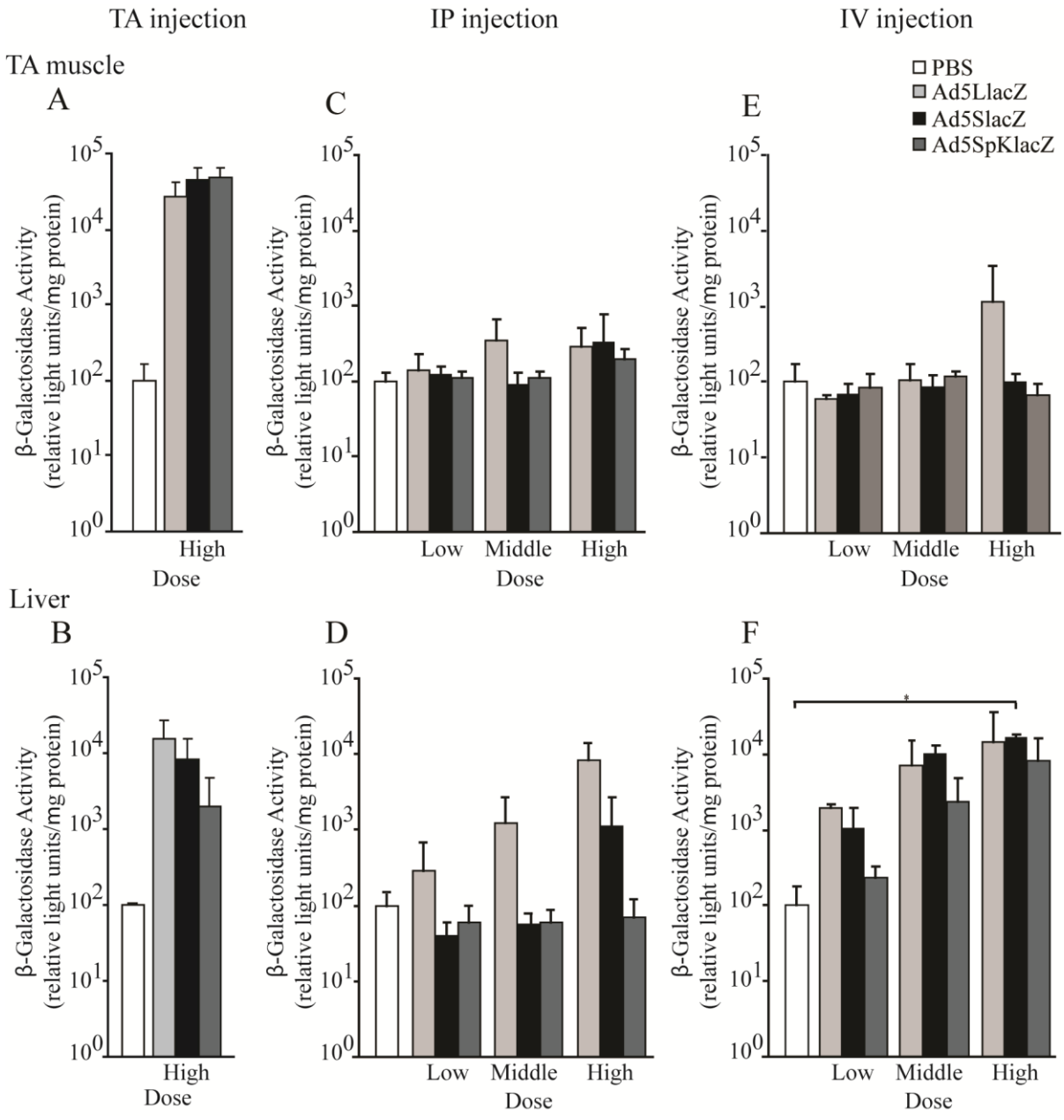
TA injection
IP injection
IV injection
TA muscle
Liver
PBS
Ad5LlacZ
Ad5SlacZ
Ad5SpKlacZ
A
B
C
D
E
F
β-Galactosidase Activity
(relative light units/mg protein)
Low
Middle
High
Dose
*

Figure 3.4 *Analysis of transgene expression from Ad5LlacZ, Ad5SlacZ and Ad5SpKlacZ in TA muscle and liver.* Six to eight week old C57Bl/6J mice (n=2-3 per treatment) were injected with a low ($5x10^{11}$ VP/kg), middle ($1x10^{12}$ VP/kg) or high ($5x10^{12}$ VP/kg) dose of Ad5LlacZ, Ad5SlacZ, Ad5SpKlacZ or PBS by either TA (Panel A and B), IP (Panel C and D) or IV (Panel E and F) injections. Twenty-four hours post injection, the TA muscle (n=2-5) or liver (n=2-3) were removed, processed, and assayed for β-gal activity (normalized to μg of protein in the sample). Average and standard deviation are shown. *= $p<0.05$.

manner. Surprisingly, high liver infection was not observed following IP injections, where expression for Ad5SlacZ and Ad5SpKlacZ in the liver remained similar to PBS, Figure 3.4D. This observation suggested that the viruses were mainly located elsewhere throughout the body. In all three injection methods, Ad5LlacZ resulted in the highest, while Ad5SpKlacZ had the lowest levels of liver infection; however, this was not statistically significant. We also determined Ad infection was prominent at the site of injection, as observed in the TA muscle following TA injections. In this case, all three viruses have roughly a equivalent 100-fold increased β-gal expression compared to PBS (Figure 3.4A). Both IV and IP injections showed minimal or no transgene expression in the TA muscle, suggesting neither fiber modification enhanced viral spread to distal muscle tissue (Figure 3.4C and 3.4E). Of note, there is a single outlier within the IV injections where at high concentration Ad5LlacZ shows significant TA infection. The reason for this outlier is unknown and was not reproducible. Taken together, these results indicate exclusive infection of the liver and site of injection with no enhancement in uptake by muscle tissue with these fiber modifications.

The overall trend of viral infection remaining localized at the site of injection was supported through β-gal staining of tissue sections. Tissues analyzed by staining were submerged in 2% PFA fixative for 1 hour, sectioned in transverse slices of 12 μm, and stained for approximately 24 hours at 37^{o}C in X-gal stain. β-gal expression was detected in the TA muscle following TA injections, Figure 3.5A, where enhanced infection is observed in Ad5LlacZ and Ad5SpKlacZ relative to Ad5SlacZ. Transgene expression was not detectable in the TA muscle following IP or IV injections, Figure 3.5B-C. The diaphragm was tested as an additional muscle tissue as it is in close proximity to the injection site for IP injections. Following IP injections, the lower edge of the diaphragm showed positive viral

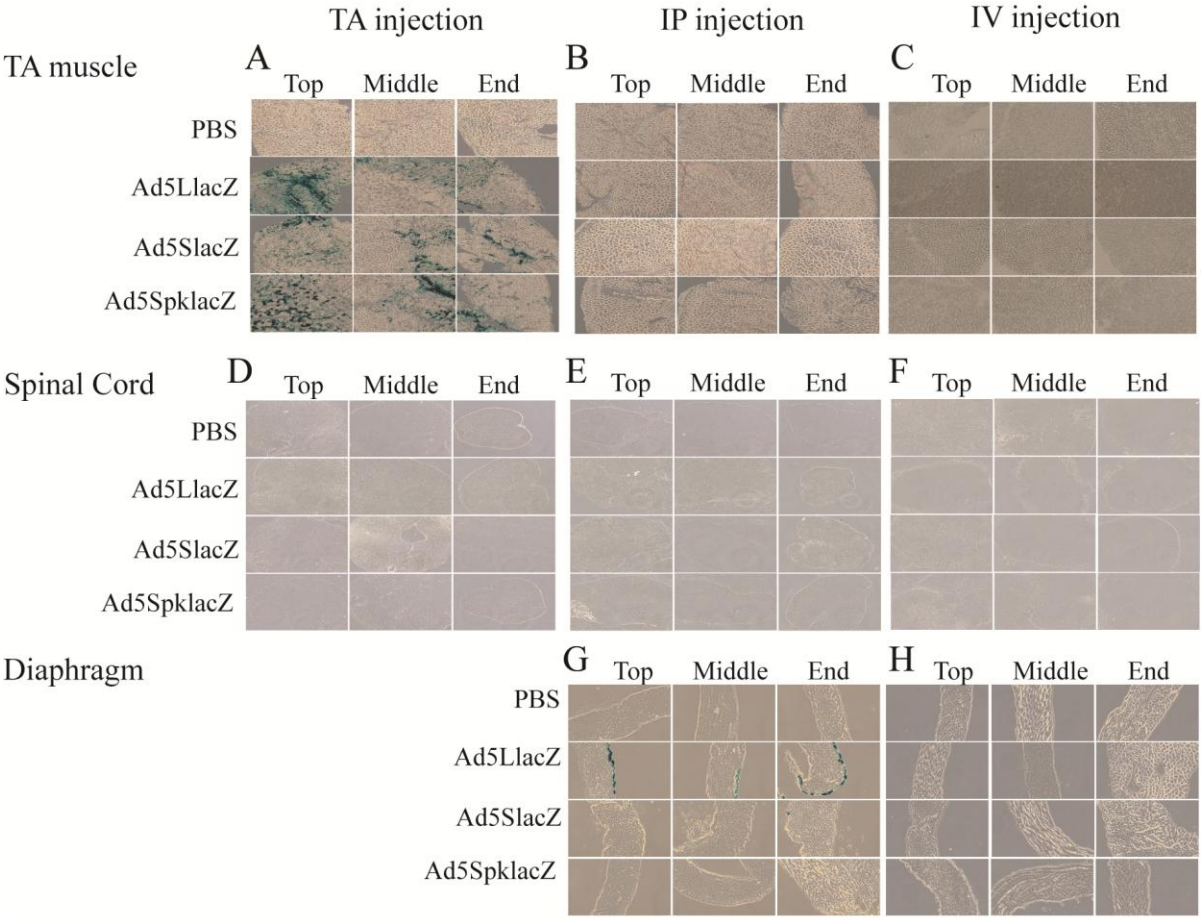
TA injection
IP injection
IV injection
TA muscle
A
B
C
Top
Middle
End
PBS
Ad5LlacZ
Ad5SlacZ
Ad5SpklacZ
Spinal Cord
D
E
F
Diaphragm
G
H

Figure 3.5 *Histological analysis of β-gal expression in the TA muscle, spinal cord and diaphragm of treated animals.* Six to eight weeks old C57Bl/6J mice were treated with $5x10^{12}$ VP/kg of Ad5LlacZ, Ad5SlacZ, Ad5SpKlacZ or PBS by either TA, IP or IV injections. The TA muscle (Panel A - C), spinal cord (Panel D - F) and diaphragm (Panel G and H) were removed 24 hours post-treatment, fixed, sectioned, and stained for β-gal activity. Sections were viewed using an AxioCam Axiophot2 light microscope at 10X magnification. Data represents n=2 biological replicates.

infection with Ad5LlacZ, however the virus appeared unable to penetrate through the tissue, Figure 3.5G. There was no significant viral infection with either of the modified constructs or following IV injections. Lastly, following transverse sectioning, infection in the spinal cord was analysed for all injection methods. Unfortunately, β-gal staining was undetectable in all cases, suggesting the viral constructs were unable to reach the motor neurons or unable to spread within the spinal cord. Thus, the site of injection played a key role in determining which tissues were accessible for infection. Overall, the data indicated that even with a reduced diameter the viral constructs could not spread to distal muscle tissue or the spinal cord regardless of injection method or viral dose.

3.2.c Increased exposure periods did not result in enhanced infection in muscle tissue or retrograde transport to motor neurons

A study preformed by Nakajima *et al* showed adenovirus is able to undergo retrograde transport and reach the CNS from various muscle groups in rats [79]. Retrograde transport is the movement up a neuron from a nerve ending to the CNS. Ads ability to undergo retrograde transport suggests Ad vectors may be useful in treating neuron diseases. We wished to further investigate if we could establish a method to achieve efficient retrograde transport into the spinal cord following TA injections. Literature suggests that an increased exposure period could allow for enhanced retrograde transport [46]. As such, TA injections were repeated with tissues harvested 48 or 72 hours after injection. It is possible that increased exposure periods may alter viral infection in other tissues and, as such, liver and TA muscles were again harvested and analyzed via chemiluminenesce assay. Liver samples showed a slight decrease in β-gal expression over time, Figure 3.6B, possibly due to the innate immune responses directed toward the vector. The same overall trend was

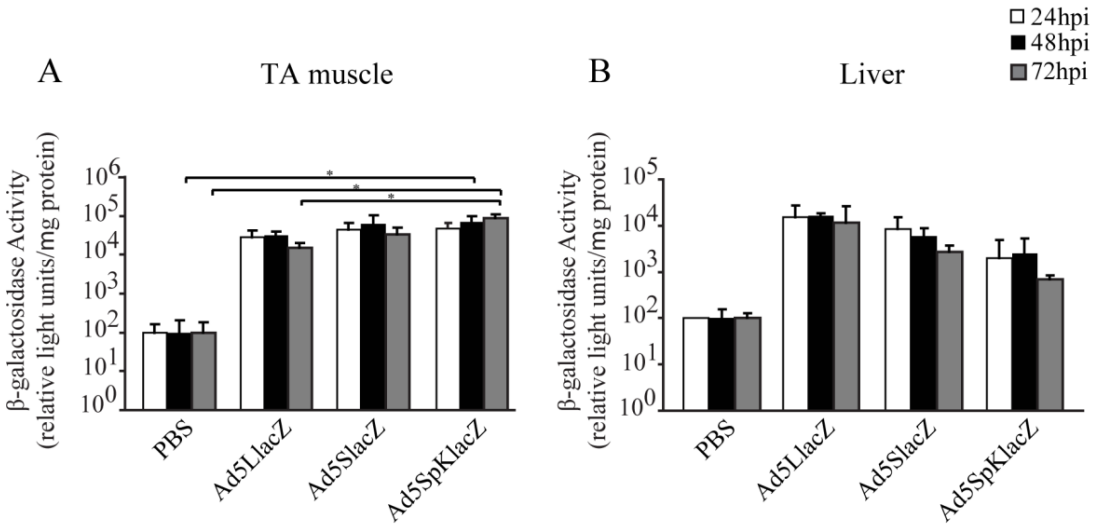
24hpi
48hpi
72hpi
A
TA muscle
B
Liver
β-galactosidase Activity
(relative light units/mg protein)
10^6
10^5
10^4
10^3
10^2
10^1
10^0
10^5
10^4
10^3
10^2
10^1
10^0
*
*
*
PBS
Ad5LlacZ
Ad5SlacZ
Ad5SpKlacZ

Figure 3.6 *Analysis of Ad5LlacZ, Ad5SlacZ and Ad5SpKlacZ in TA muscle and liver with extended exposure periods.* Six to eight week old C57Bl/6J mice were injected in the TA muscle with $5x10^{12}$ VP/kg of Ad5LlacZ, Ad5SlacZ, Ad5SpKlacZ or PBS. Mice were sacrificed 1, 2 or 3 days post injection and TA muscles (Panel A; n=3) and liver (Panel B; n=2) were collected. Samples were processed and analyzed for β-gal activity by chemiluminescence assay. Average and standard deviation the mean shown. *= $p<0.05$.

observed for all viruses, with Ad5LlacZ having the greatest transgene expression and Ad5SpKlacZ having the lowest. In the TA muscle, all three viruses showed equivalent β-gal expression with very little variation over the three day time period, Figure 3.6A. To confirm these results, TA muscles were harvested and analyzed by sectioning and β-gal staining. Figure 3.7 showed whole cross sections of the TA muscle from the top, middle, and end of the tissue. When viewing the muscle as a whole, there appeared to be no difference in viral infection between the three viruses or over the three day incubation period. The area of transgene expression was quantified using ImageJ, Table 3.1; however, the magnitude of staining varied significantly between mice. The overall trend showed increased β-gal staining at the top of the tissue, nearest to the point of injection, relative to the bottom of the tissue. Averaging the nine values for each viral construct suggested Ad5LlacZ and Ad5SlacZ had nearly identical infection efficiency, while Ad5SpKlacZ showed a marginal improvement compared to the other constructs. Lastly, we analysed the area of transduction in the tissue sections through indirect immunofluorescence. Primary β-gal and laminin antibodies were incubated overnight for viral detection and cellular identification, respectively. Positive transgene expression was again detected as seen in Figure 3.8. These outcomes imply all constructs were able to infect both the liver and the TA muscle at all three exposure periods. However, our results showed no improvement in viral spread throughout the muscle or degree of infection with longer incubations.

To study Ad retrograde transport into the CNS not only were exposure times extended but sectioning was done in a longitudinal orientation and injections were done in the presence of Dextran Texas Red Fixable dye. It is known that the TA muscle tracks through the sciatic nerve to the L4-L6 regions of the spinal cord [46]. However, it is very difficult to locate and isolate these specific lumbar regions via transverse sectioning. As

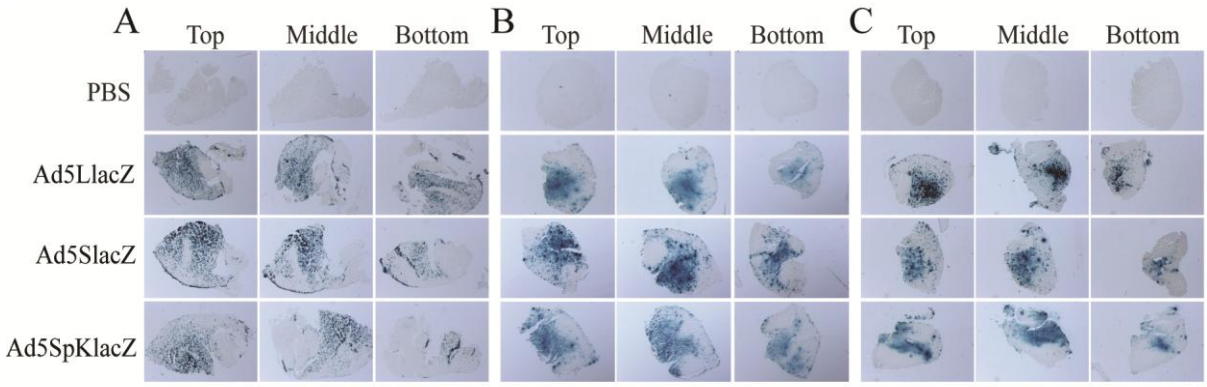
A
Top
Middle
Bottom
B
Top
Middle
Bottom
C
Top
Middle
Bottom
PBS
Ad5LlacZ
Ad5SlacZ
Ad5SpKlacZ

Figure 3.7 *Histological analysis of β-gal expression in the TA muscle after extended exposure periods.* Six to eight week old C57Bl/6J mice were treated with $5x10^{12}$ VP/kg of Ad5LlacZ, Ad5SlacZ, Ad5SpKlacZ or PBS by direct TA injection. The TA muscle was removed at 24 (Panel A), 48 (Panel B) or 72 (Panel C) hours post injection. Tissues were fixed, sectioned and stained for β-gal activity. Whole sections were viewed using a Leica M80 microscope. Data represents n=2 biological replicates.

Table 3.1 Area[a] of TA muscle expressing β-gal following TA injection.

	Ad5LlacZ			Ad5SlacZ			Ad5SpKlacZ		
	Top	Middle	Bottom	Top	Middle	Bottom	Top	Middle	Bottom
24h	25.1 ± 6.5	25.5 ± 4.2	35.9 ± 23.5	18.4 ± 10.7	20.4 ± 0.8	14.1 ± 5.1	20.6 ± 1.6	16.7 ± 1.4	21.3 ± 22.6
48h	27.0 ± 13.4	25.0 ± 14.6	22.1 ± 11.8	42.1 ± 1.2	43.1 ± 3.6	21.9 ± 11.7	31.6 ± 12.5	28.2 ± 15.5	21.7 ± 21.7
72h	20.0 ± 16.9	17.3 ± 10.6	13.3 ± 9.1	26.1 ± 5.1	21.8 ± 18.2	9.7 ± 8.6	30.9 ± 3.4	26.7 ± 18.1	9.9 ± 7.7

[a] Images from stained sections were analyzed using Image J. A color intensity threshold was applied to determine the area of the muscle section showing X-gal staining, which is reported as the percentage of the total cross-sectional area of the muscle.

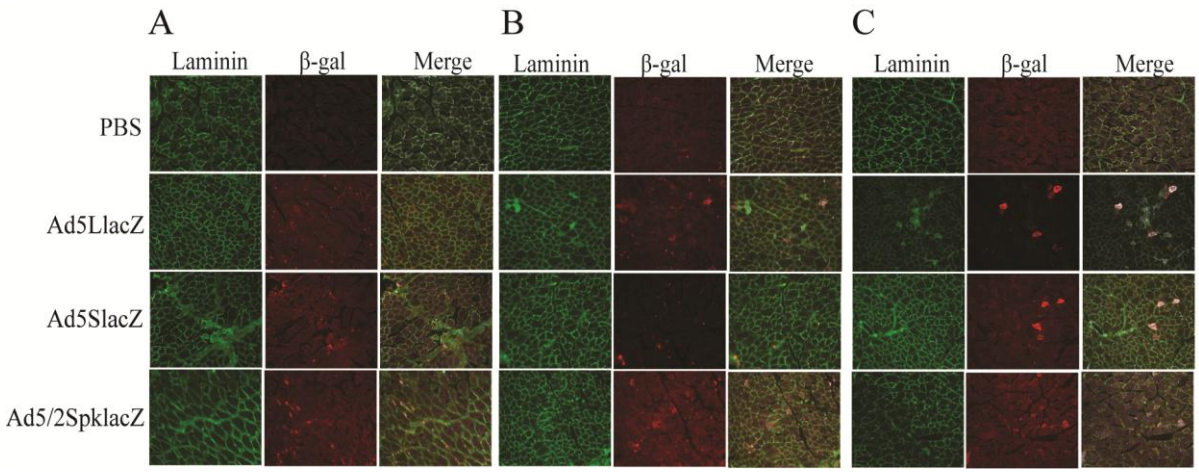
A
B
C
Laminin
β-gal
Merge
Laminin
β-gal
Merge
Laminin
β-gal
Merge
PBS
Ad5LlacZ
Ad5SlacZ
Ad5/2SpklacZ

Figure 3.8 *Immunofluorescence of TA muscles by α-β-gal and α-laminin.* Six to eight weeks old C57Bl/6J mice were treated with $5x10^{12}$ VP/kg of Ad5LlacZ, Ad5SlacZ, Ad5SpKlacZ or PBS by direct TA injection and the TA muscle was removed at 24 (Panel A), 48 (Panel B) or 72 (Panel C) hours post injection. Tissues were fixed, sectioned and analysed by immunofluorescence using antibodies to β-gal and laminin. Data represents n=2.

such, longitudinal sectioning was done, since it allows for a greater region of the spinal cord to be analysed and improves the probability of locating the motor neurons which innervate the TA muscle. Viral constructs were diluted in Dextran Texas Red Fixable dye to allow visualization of the motor neurons which innervate with the TA muscle. Dextran is a hydrophilic polysaccharide efficient at retrograde transport and therefore commonly employed for fluorescent neuronal tracking [59]. TA injections were done using 16 mg/mL Dextran Texas Red Fixable dye along with $5x10^{12}$ VP/kg of virus. Following a 48 hour incubation period, mice were euthanized and spinal cords collected. The lumbar region of the spinal cord was sectioned longitudinally until motor neurons were detected by the immunofluorescent Dextran dye, Figure 3.9A. Sections immediately following those positive for motor neurons were then stained for approximately 24 hours with X-gal stain. Panel B of Figure 3.9 showed that virus is detectable in the motor neurons and therefore Ad does undergo retrograde transport. Our results were quite variable between mice, but Ad5SpKlacZ was observed to have the least success at retrograde transport. Overall, we did observe β-gal staining in the motor neurons, it was relatively inefficient and none of the modified viruses showed a significant enhancement in retrograde transport or motor neuron transduction.

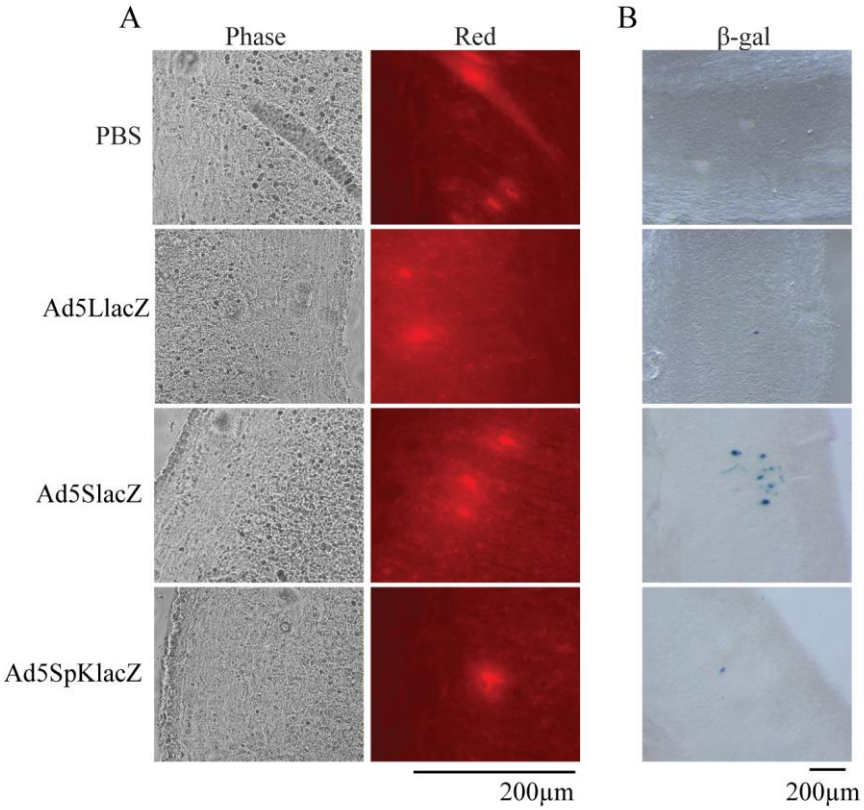
A
Phase
Red
B
β-gal
PBS
Ad5LlacZ
Ad5SlacZ
Ad5SpKlacZ
200μm
200μm

Figure 3.9 *Immunofluorescence analysis of motor neurons and histological analysis of β-gal expression.* Six to eight week old C57Bl/6J mice were treated with 16 mg/mL Dextran Texas Red Fixable dye in $5x10^{12}$ VP/kg of Ad5LlacZ, Ad5SlacZ, Ad5SpKlacZ or PBS by TA injection. Spinal cords were removed 48 hours post injection. Tissues were fixed and 12µm longitudinal sections were collected until motor neurons were detected by the immunofluorescent Dextran dye (Panel A). The next serial section was then stained for β-gal activity and viewed using a Leica M80 microscope (Panel B). Data represents n=2 biological replicates.

3.3 **Discussion**

3.3.a Overview

SMA is an autosomal recessive disorder with very early onset in children. The disease is characterized by the progressive deterioration of muscle tissue, leading to impaired mobility and breathing, often resulting in death [37]. SMA occurs due to low levels of the SMN protein generally resulting from a genetic mutation in the *SMN1* gene [56]. Several different treatment avenues are currently under investigation to increase the amount of SMN in the damaged tissues, specifically α-motor neurons and skeletal muscle. The goal in this chapter was to alter Ad vector distribution throughout the body and enhance infection in the damaged tissues. This improved Ad vector could then be used in the treatment of SMA. The Ad capsid protein, fiber, was modified with the hope of improving biodistribution and altering infection tropism. Unfortunately it was found that none of the modified constructs had improved infection relative to the control Ad5. In the majority of cases Ad constructs localized to the liver or remained at the site of injection.

3.3.b Ad localizes predominantly to the liver

Ad has been extensively studied over the past 60 years and its localization to the liver is well characterized [47]. This chapter investigated if modifications to the Ad fibre would show increased systemic spread by monitoring Ad accumulation within the liver. Analysis of the three different injection methods following a 24 hour incubation period, Figure 3.4, showed Ad5LlacZ gave the highest levels of liver infection. This result suggested that the modified constructs were infecting elsewhere throughout the body or being degraded and lost. Between the two modified constructs, Ad5SpKlacZ consistently showed the lowest levels of liver infection, implying the addition of poly-lysine to enhance viral interactions

with cellular heparan sulphate proteoglycans does increase the number of cellular targets. IV injections demonstrated the highest levels of liver infection and did so in a dose dependent manner for all constructs. Surprisingly, IP injections demonstrated very low liver transgene expression. In the case of low viral concentration ($5x10^{11}$ VP/Kg), β-gal expression levels were equivalent to the PBS control, implying the virus is being trapped elsewhere, most likely within the intraperitoneal space. Livers were analysed following TA injections from three different exposure periods, Figure 3.6B; however the same trend was observed, Ad5LlacZ and Ad5SpKlacZ had the highest and lowest infection levels, respectively. Although a decrease in β-gal expression was observed with increased exposure periods in the liver, there was no dramatic change in expression levels, suggesting minimal immune-mediated loss of the vector. Overall, these results suggest that the liver remains the primary site of infection for both TA and IV injections, and that the viral constructs are unable to reach the liver following IP injections. Furthermore, the three viral constructs did not have equivalent infection efficiencies, with Ad5LlacZ having the greatest and the modified constructs, in particular Ad5SpKlacZ, yielding slightly lower infection rates.

3.3.c Muscle infection is not enhanced through fiber modifications

As SMA affects the NMJ, it is currently debated whether SMA is a muscle disease or a neuron disease. Although it is ideal to have systemic SMN replacement, the replacement of SMN in α-motor neurons and skeletal muscle is vital. The addition of 7 lysine residues to the Ad5SpKlacZ construct was designed to increase muscle infection by enhancing specificity to cellular heparan sulphate proteoglycans, which has been shown previously by Bramson *et al.* [11]. Unfortunately, while Ad5SpKlacZ demonstrated the lowest rate of liver infection, this does not appear to be a result of enhanced muscle infection. *In vitro* experiments involving

C2C12 cells (Figure 3.3) showed no difference in viral infection between Ad5SpKlacZ and Ad5SlacZ, which lacks the poly-lysine motif. In fact, decreased infection efficiency was observed for Ad5SpKlacZ compared to the unmodified fiber, Ad5LlacZ. *In vivo* experiments were mainly analyzed using the TA muscle, where infection was detected following only TA injections (Figure 3.4 and Figure 3.5). Again, there was no significant difference between viral constructs suggesting the poly-lysine residue did not enhance muscle infection. The lack of viral infection in the TA muscle following IV and IP injections (Figure 3.4 and Figure 3.5) suggests that even at a reduced size the viral constructs are unable to spread systemically and rarely reach distal tissues. Likewise, lack of viral spread was observed in the diaphragm. Positive diaphragm staining was only observed following IP injections where the diaphragm is in close proximity to the site of injection. Transgene expression was observed with Ad5LlacZ in the bottom of the tissue indicating again the virus is unable to spread through muscle tissue. Surprisingly, infection was not detectable for the two modified viruses which had the lowest liver infection rate following IP injections and are smallest in size. The reason for this is unknown however, it is hypothesized that these viruses remain near the site of injection, infecting the membranes in the peritoneum.

It was thought that increased exposure periods may result in reduced β-gal activity due to activation of the murine immune system against the viral vector resulting in death of the transduced cells. However, this was not the case. Following TA injection, β-gal expression in the TA muscle remained constant over the 72 hour incubation period for all three viral constructs (Figure 3.6A and 3.7), implying Ad vectors are not cleared from muscle tissue for at least 72 hours. Rapid removal of Ad vectors is one of the major concerns in gene therapy however current studies suggest that helper dependent Ad is able to persist for years *in vivo* [12]. Overall, increased specificity to cellular heparan sulphate

proteoglycans did not enhance muscle infection relative to normal Ad5 fiber, nor did decreasing the virion size through changing the length of the fiber shaft. The lack of skeletal muscle infection following both IV and IP injections suggests that systemic spread did not occur and further modifications maybe be required to achieve efficient delivery to distant tissues using Ad vectors.

3.3.d Spinal cord infection is detectable in the α-motor neurons

For the proper treatment of SMA it is essential that the SMN protein be delivered to α-motor neurons. Previous studies have shown that Ad can undergo retrograde transport [79] and transport may be improved with increased exposure periods [46]. The TA muscle, representing the site of injection, tracks through the sciatic nerve to the L4-L6 regions of the spinal cord [46]. In cell culture, our studies showed that all constructs were able to infect MN1 cells (Figure 3.3B). However, in initial *in vivo* experiments, viral infection was not detectable within the spinal cord. This was attributed to the use of transverse sections which may not have contained α-motor neurons from the L4-L6 region. However, following TA injections at high viral concentration combined with Dextran dye, specific detection of motor neurons was possible and viral infection within the spinal cord was observed, Figure 3.9B. Dextran is a hydrophilic polysaccharide with low toxicity, commonly employed for neuron tracking due to its efficiency at anterograde and retrograde transport [59]. β-gal staining of sections positively identified with α-motor neurons confirmed positive viral infection at sites corresponding to the α-motor neurons. An accurate comparison between constructs was not possible due to large variability between samples and low sample size however potential trends were observed. Ad5SpKlacZ consistently had the weakest infection of α-motor neurons while Ad5SlacZ demonstrated minimal improved transgene expression over

Ad5LlacZ. It was thought that decreasing the overall size of the virion by changing the Ad5 shaft to the smaller Ad9 shaft could enhance retrograde transport and this was observed for Ad5SlacZ which showed slightly enhanced motor neuron staining. Ad5SpKlacZ did not result in enhance retrograde transport suggesting the reduced diameter may be beneficial only in the absence of poly-lysine residues. In all cases the viruses were able to reach the spinal cord and infect the motor neurons however viruses were unable to escape the motor neurons.

3.4 **Conclusions**

All constructs demonstrated positive infection *in vitro* with a variety of cell types, as well as, *in vivo* in the liver, TA muscle and motor neurons. No significant differences were observed between injection methods, as the viruses specifically infected the site of injection or the liver. Importantly, in terms of SMA, none of the viral constructs were sufficient for body-wide transduction. Overall despite reducing the vector size by changing the fiber shaft and increasing the number of cellular targets through the addition of poly-lysine residues the constructs were unable to specifically or effectively infect the desired tissues. These studies suggest that additional modifications to the Ad vector system are required to enhance its utility for treatment of SMA.

Chapter 4 - Exosome transport of SMN

4.1 Introduction

The goal of this project was to utilize the natural accumulation of virus in the liver as a protein production factory and investigate how this newly synthesised SMN protein can spread body-wide. Such an approach has been explored for diseases involving secreted proteins, as such as factor IX for the treatment of hemophilia [113]. It was determined in the previous chapter that IV injections result in significant dose dependent delivery to the liver. It is hypothesized that following infection significant amounts of viral encoded SMN will be transcribed. The challenge in treating SMA is to find a mechanism for this newly synthesized SMN to be released from hepatocytes, spread throughout the body and be taken up by recipient cells.

In order to address the issue of protein release a previous student in the lab created vectors encoding modifications to the SMN gene, Figure 4.1A [14]. These additions included an N-terminal secretory peptide (SP) to enhance release of the SMN protein from hepatic cells, as well as various tags. To verify the release of the SMN protein from cells, A549 cells were infected with Ad-SMN and Ad-SP-SMN at an MOI of 25, 100 or mock infected. Cells were harvested at 24 hpi using 2x LD, and cellular SMN and tubulin were detected using immunoblot. The 24 hour old media was also collected and, following TCA protein precipitation [45], the secreted proteins were analyzed by immunoblot. Figure 4.1B showed that SMN was present in both cells (bottom panel) and media (top panel) following infection from the two different viral constructs. It was determined that although Ad-SP-SMN contained a secretory peptide and Ad-SMN does not, significant amounts of SMN were observed in the media from Ad-SMN infected cells. This suggests that native SMN is released from A549 cells, and modifications to the SMN gene to enhance secretion of the

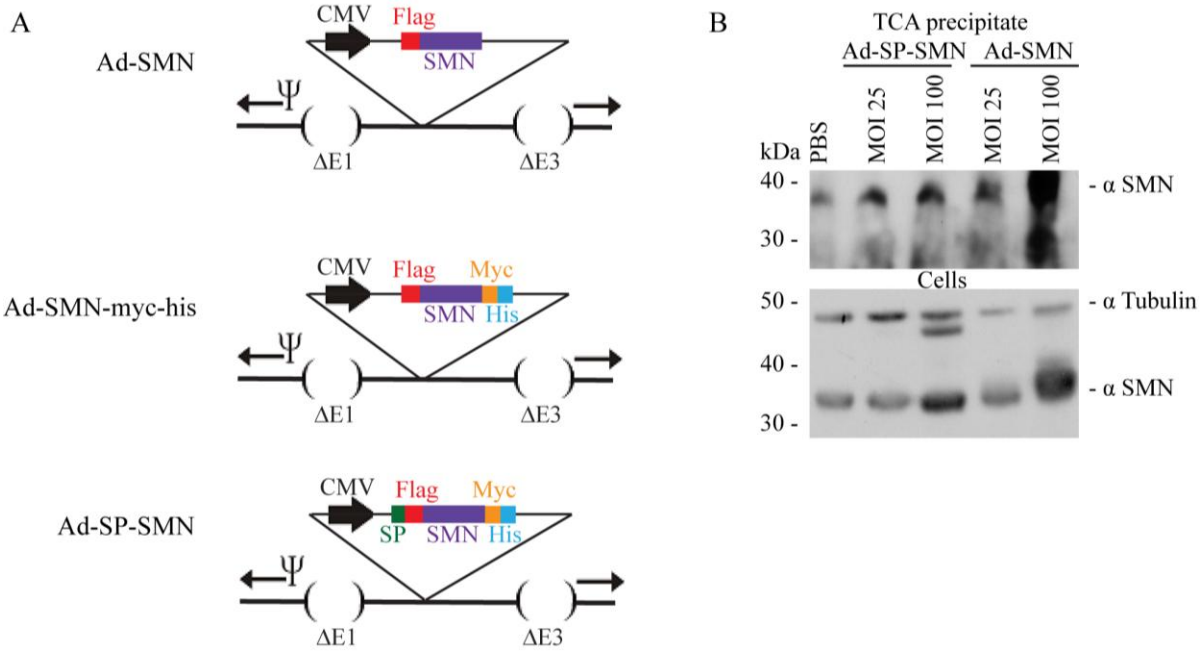
A
Ad-SMN
CMV
Flag
SMN
Ψ
ΔE1
ΔE3
Ad-SMN-myc-his
CMV
Flag
Myc
SMN
His
Ψ
ΔE1
ΔE3
Ad-SP-SMN
CMV
Flag
Myc
SP
SMN
His
Ψ
ΔE1
ΔE3
B
TCA precipitate
Ad-SP-SMN
Ad-SMN
PBS
MOI 25
MOI 100
MOI 25
MOI 100
kDa
40 -
30 -
- α SMN
Cells
50 -
40 -
30 -
- α Tubulin
- α SMN

Figure 4.1 *Analysis of SMN levels in cells and media for cell treated with Ad-SP-SMN or Ad-SMN.*
Panel A: General structure of the viruses used in this study. All viruses are deleted of E1 and E3, and express Flag-SMN under regulation by the human CMV immediate early enhancer/promoter. Ad-SMN-myc-his encodes additional myc and his tags while Ad-SP-SMN encodes all three tags and a SP.
Panel B: A549 cells were infected at an MOI of 25 or 100 with Ad-SP-SMN and Ad-SMN (or mock infected), 24 hpi SMN expression was detected by immunoblot for both the cell lysates (bottom) and media following TCA precipitation (top). Equivalent volumes of cell lysate and TCA precipitate were applied to the gel. Data represents n=3.

protein may be unnecessary. This is further confirmed by the presences of SMN in the media of the mock infected cells observed in Lane 1 of Figure 4.1B. Additional experiments were performed to establish that SMN is secreted from cells and is not a consequence of the FBS in complete MEM. Media following a 24 hour incubation on A549 cells was compared to media not used for culturing, Figure 4.2A. After TCA precipitation, it was observed that media incubated on cells had enhanced SMN signal relative to media never exposed to cells. This corroborates our previous observation of natural SMN release however, it is unknown how SMN is being released. SMN is also released into the media from various other cell lines, Figure 4.2B. These cell lines are a mixture of both human and mouse cells as well as normal and cancerous cells together representing a variety of tissue types. Again SMN was detected in the media following TCA precipitation suggesting protein release. This novel knowledge may be useful in the development of an SMA therapeutic, therefore in this chapter I investigated: (i) how SMN is released (ii) how SMN release can be enhanced (iii) if secreted SMN is taken up by recipient cells and (iv) analysed this process *in vivo*.

4.2 **Results**

4.2.a SMN is present in exosomes

We first investigated how SMN is released into the media. Cells produce a variety of microvesicles which, depending on their size, are capable of carrying large numbers of proteins. Exosomes, the smallest of the microvesicles can carry up to 100 proteins and 10,000 nucleotides [70]. The exosome field is currently very active due to their new found role in cellular communication and immune function [52]. Studies have found that hepatocytes, like most cells, are able to produce and release exosomes [85]. Therefore, we investigated if SMN, a cytosolic protein, may be packaged into exosomes during MVB

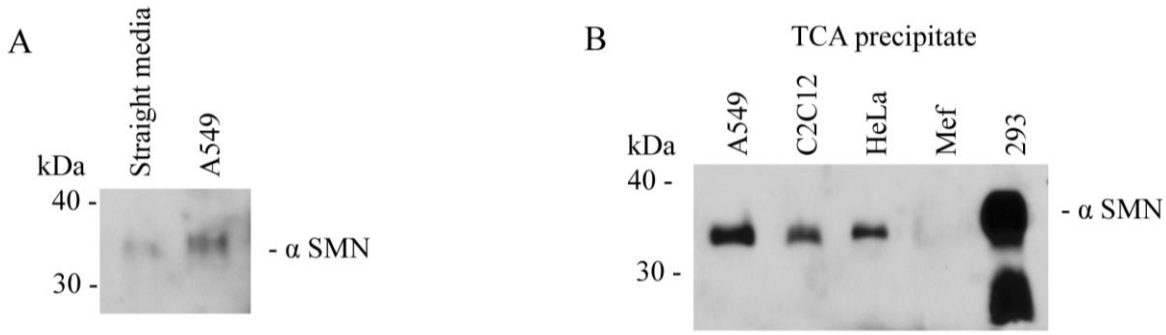
A
Straight media
A549
kDa
40 -
30 -
- α SMN
B
TCA precipitate
A549
C2C12
HeLa
Mef
293
kDa
40 -
30 -
- α SMN

Figure 4.2 *Native SMN is detectable in media following TCA precipitation.*
Panel A: Media following a 24 hour incubation with A549 cells or media without incubation was subjected to TCA precipitation, separated by SDS-PAGE, and the resulting immunoblot probed for SMN. Equivalent volumes of TCA precipitate were applied to the gel. Data represents n=3.
Panel B: SMN expression after TCA precipitation of media following a 24 hour incubation on A549, C2C12, HeLa, Mef or 293 cells. Equivalent volumes of TCA precipitate were applied to the gel however cells were not plated at equal confluences. Data represents n=3.

internal budding. SMN's natural expression in exosomes could potentially simplify the process of delivering this protein to recipient cells.

Exosome isolation was preformed using an exosome collection protocol involving a series of ultra centrifugation steps. The final sample representing exosomes was analyzed via Nanosight, Figure 4.3A. These particles were found to have a mean size of 260 nm. As exosomes are between 30-100 nm in diameter, our analysis indicates possible microparticle contamination. The exosome collection protocol was modified by exchanging the 10,000 xg centrifugation step with filtration through a 0.2 μm filter. This approach successfully reduced the mean particle size to 160 nm, Figure 4.3B. Although this does suggest a decreased amount of microparticles in the exosome sample, the preparation likely still contained a mix of exosomes and microparticles. The harvested exosomes were then analyzed by immunoblot using exosome positive, ALIX and Flotillin-2, and exosome negative, Calnexin and SMAC, markers. Figure 4.3C showed that the positive marker ALIX is detectable in both 293 and A549 harvested exosomes. In Figure 4.3D, A549 exosomes were compared to that of A549 cell lysates, loaded at equivalent concentrations. Of note, this blot was cut in order to place the A549 exosomes and A549 cell lysates side by side. Here we observed the exosome positive control Flotillin-2 is in the exosome sample, however at a lower concentration then that of the cell lysate. The negative exosome markers were not detectable in the exosome sample, but were present in the A549 cell lysate. Lastly Flotillin-2 was used to confirm no vesicles remained in the media following exosome collection, which suggested complete particle harvest, Figure 4.3E. Overall, although the harvested exosome samples may not be pure, exosomes represent a large proportion of the microvesicles collected.

The next step was to determine if exosomes represent a mechanism for SMN release. These newly acquired exosomes were investigated via immunoblot for the presence of SMN.

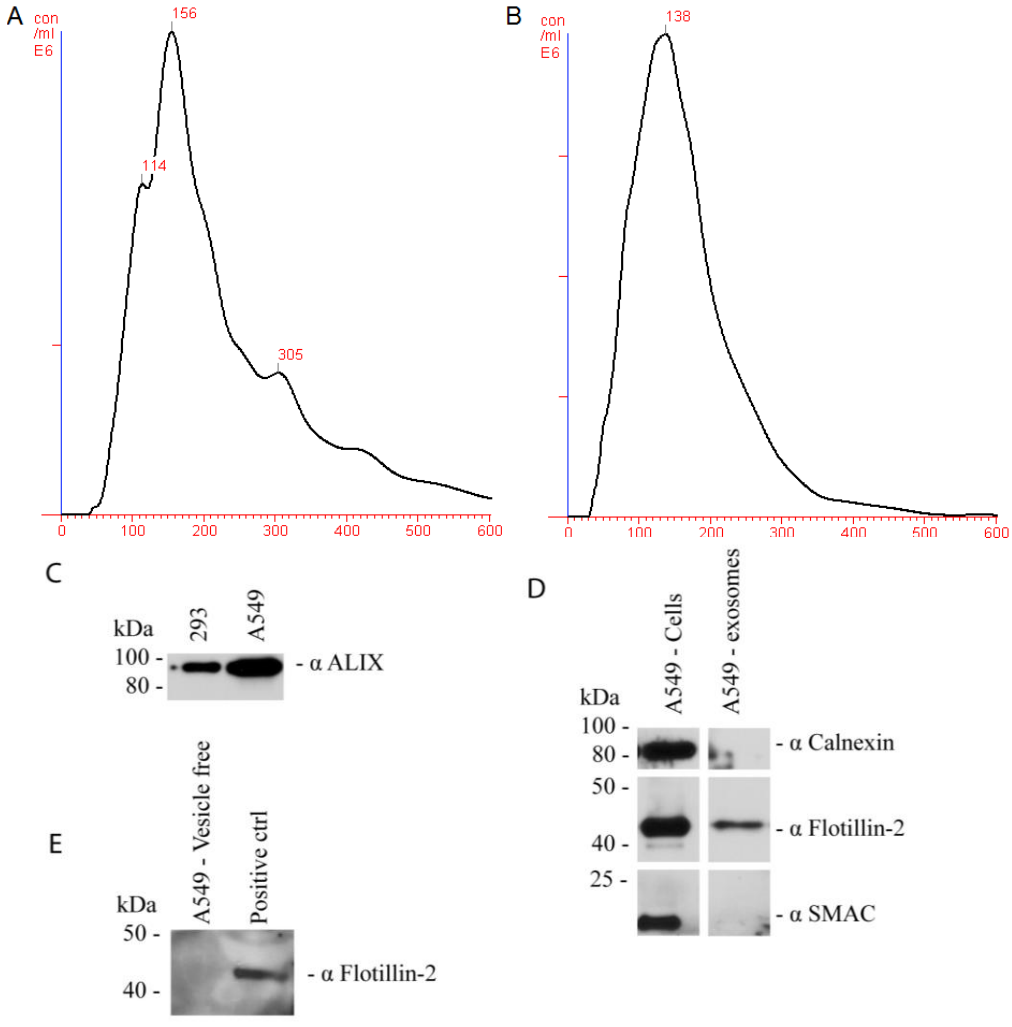
A
con
/ml
E6
156
114
305
0
100
200
300
400
500
600
B
con
/ml
E6
138
0
100
200
300
400
500
600
C
kDa
293
A549
100 -
80 -
- α ALIX
D
A549 - Cells
A549 - exosomes
kDa
100 -
80 -
- α Calnexin
50 -
40 -
- α Flotillin-2
25 -
- α SMAC
E
A549 - Vesicle free
Positive ctrl
kDa
50 -
40 -
- α Flotillin-2

Figure 4.3 *Size of harvested exosomes and detection with various markers.*
Panel A: Particle size as determined via Nanosight. A549 exosomes purified through ultracentrifugation including a 10,000 xg centrifugation step.
Panel B: Particle size as determined via Nanosight. A549 exosomes purified through ultracentrifugation including a 0.2 µm filtration step. This method of purification was done for all following exosome experiments unless otherwise stated.
Panel C: Harvested A549 (2.4µg) and 293 (0.15µg) exosomes were separated by SDS-PAGE, and the resulting immunoblot probed for the positive exosome marker ALIX. Exosome concentration was determined by Bradford assay with non-lysed samples. Data represents n=3.
Panel D: Exosomes from A549 cells and A549 cell lysates were diluted to a concentration of 15µg/mL and separated by SDS-PAGE. The immunoblot was probed with the positive exosome marker Flotillin-2 and the negative exosome markers SMAC and Calnexin. Exosome and cell lysate concentrations were determined using Bradford assay with lysed samples. Data represents n=2.
Panel E: TCA precipitation was preformed on A549 media post exosomes collection. This vesicle-free media was subject to SDS-PAGE and immunoblot with Flotillin-2. TCA precipitated media from A549 cells infected with Ad-SMN at MOI 100 for 24 hours was used as a positive control. Data represents n=2.

Figure 4.4A showed that SMN is detectable in all particles isolated during exosome purification. Furthermore, it was determined that SMN is detectable in exosomes harvested from different cells lines including A549, 293, and HUVEC, Figure 4.4B. Differences in SMN levels suggest exosomes produced from different cell lines vary in protein content, which agrees with current literature. Together this indicates that SMN is naturally found in exosomes and this can function as a method for SMN release from cells.

We next investigated if we could increase the quantity of SMN in exosomes, using two different approaches. First, a new cell line which over expresses Flag-SMN, A549::SMN, was created from A549 cells by cloning and necleofection. Figure 4.5 showed this new A549::SMN cell line overexpresses SMN relative to the parental A549 cell line in cell lysates (A), media following TCA precipitation (B) and harvested exosomes (C). The N-terminal Flag tag was also detectable in cells via immunoblot and immunofluorescence. The cells were examined by immunofluorescence to determine the cellular localization of the SMN protein. Figure 4.6 showed that the Flag-SMN was found inside as well as surrounding the nucleus, which is in agreement with native SMN [61]. The Flag tag was also detectable in A549::SMN exosomes (bottom panel of Figure 4.5C), however the Flag signal is much weaker then that of the SMN signal suggesting the Flag tag is being modified. The second method to enhance the amount of SMN in exosomes was to infect A549 cells with an Ad vector expressing Flag-SMN, Ad-SMN (Figure 4.1). A549 cells were infected at a MOI 50 and incubated for 24 hours prior to exosome harvest. Infection with Ad-SMN resulted in enhanced amounts of SMN as well as the presence of the Flag tag in cells (Figure 4.7A), media precipitates (B) and exosomes (C). Again, detection of the Flag tag appeared to be reduced as the signal in media was significantly lower compared to SMN and the Flag signal in the exosome sample was sporadic and unreliable. Overall it was determined that SMN is

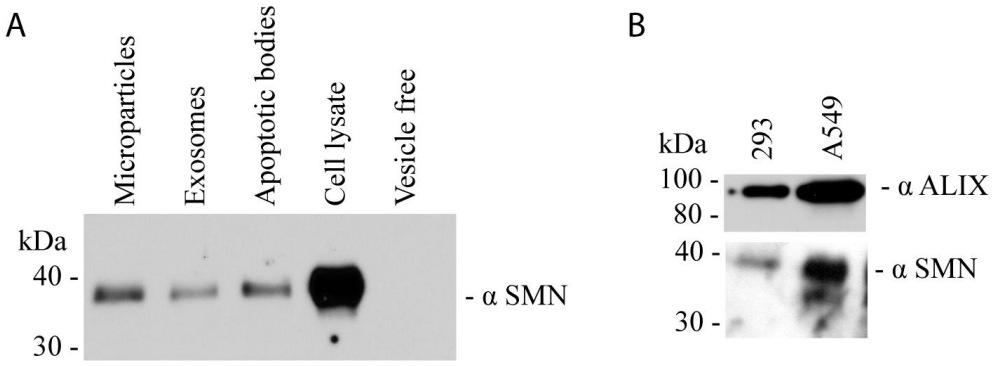
A
Microparticles
Exosomes
Apoptotic bodies
Cell lysate
Vesicle free
kDa
40 -
30 -
- α SMN
B
kDa
293
A549
100 -
80 -
- α ALIX
40 -
30 -
- α SMN

Figure 4.4 *SMN is present in microvesicles, including exosomes, from various cell lines.*
Panel A: Vesicles from HUVEC by Dr. Dylan Burger were collected at each step of the exosome purification protocol. HUVEC samples were lysed and stored in RIPA buffer. Five µg of each sample was separated by SDS-PAGE and probed for SMN. Concentrations were determined using a Bradford assay. Data represents n=2.
Panel B: Exosomes harvested from A549 (2.4µg) and 293 (0.15µg) cells were separated by SDS-PAGE, and the resulting immunoblot was probed for SMN and ALIX. Exosome concentration was determined using Bradford assay with non-lysed samples. Top panel is the same as Figure 4.3C. Data represents n=3.

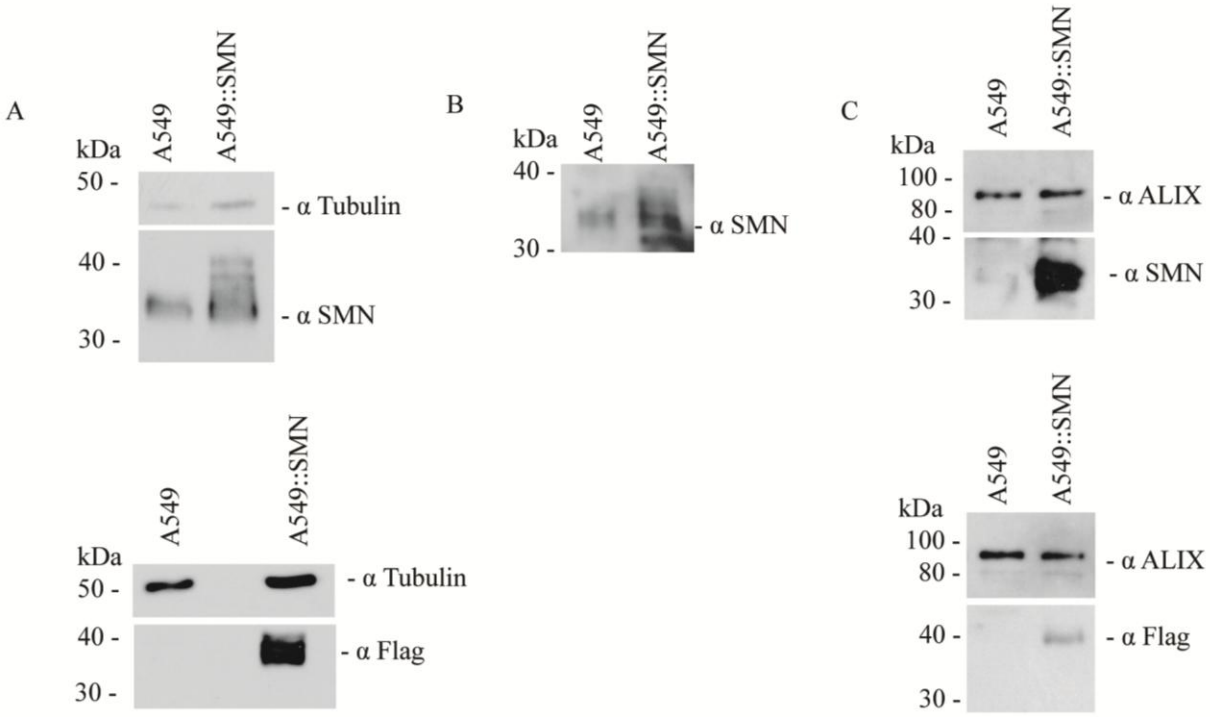
A
kDa
A549
A549::SMN
50 -
- α Tubulin
40 -
- α SMN
30 -
A549
A549::SMN
kDa
50 -
- α Tubulin
40 -
- α Flag
30 -
B
kDa
A549
A549::SMN
40 -
- α SMN
30 -
C
kDa
A549
A549::SMN
100 -
80 -
- α ALIX
40 -
- α SMN
30 -
A549
A549::SMN
kDa
100 -
80 -
- α ALIX
40 -
- α Flag
30 -

Figure 4.5 *SMN expression can be enhanced in exosomes using an SMN-over expressing cell line.* A new cell line A549::SMN was created from A549 cells, which over expresses Flag-SMN through hygromycin selection

Panel A: A549 and A549::SMN cells were lysed in 2x LD and separated by SDS-PAGE. The resulting immunoblot was probed for SMN, tubulin and Flag. Equivalent volumes of cell lysates were used. Data represents n=3.

Panel B: A549 and A549::SMN TCA media precipitates were separated by SDS-PAGE, and the resulting immunoblot was probed for SMN. Equivalent volumes of TCA precipitate were applied to the gel. Data represents n=3.

Panel C: 0.5µg of both A549 and A549::SMN exosomes were separated by SDS-PAGE, and the resulting immunoblot was probed for SMN, Flag and ALIX. Exosome concentration was determined using a Bradford assay with non-lysed samples. Data represents n=3.

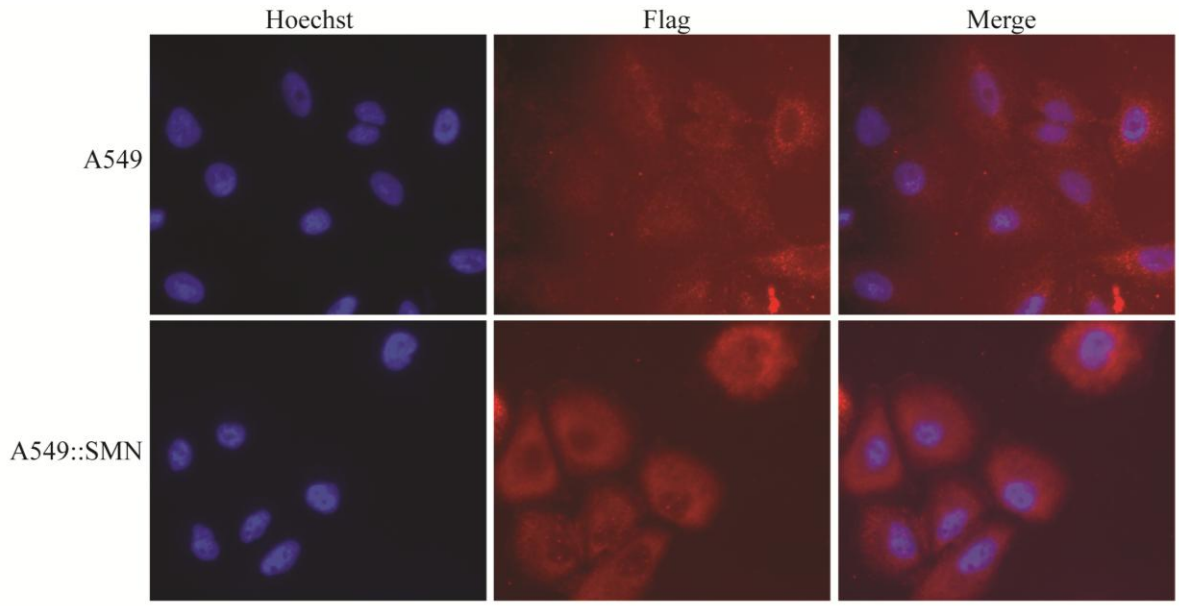
Hoechst
Flag
Merge
A549
A549::SMN

Figure 4.6 *A549::SMN cells express Flag tagged SMN.* A549 and A549::SMN cells were examined by immunofluorescence using both Hoechst (left) and Flag (middle). Images were merged (right) to determine cellular localization of Flag-SMN. Data represents n=3.

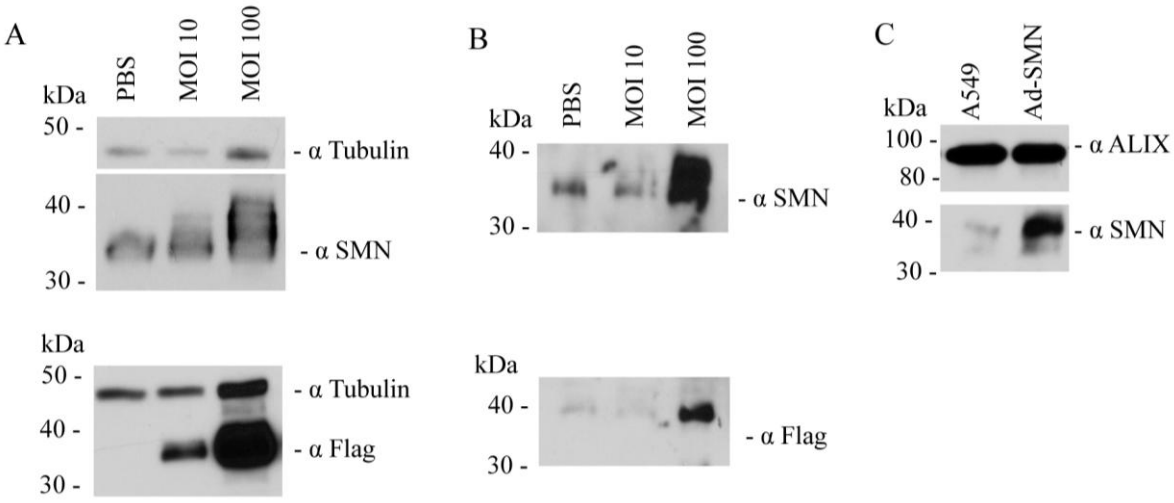
A
PBS
MOI 10
MOI 100
kDa
50 -
- α Tubulin
40 -
- α SMN
30 -
kDa
50 -
- α Tubulin
40 -
- α Flag
30 -
B
PBS
MOI 10
MOI 100
kDa
40 -
- α SMN
30 -
kDa
40 -
- α Flag
30 -
C
A549
Ad-SMN
kDa
100 -
- α ALIX
80 -
40 -
- α SMN
30 -

Figure 4.7 *The level of SMN protein is enhanced in exosomes isolated from Ad-SMN infected cells.* A549 cells were infected at an MOI of 10, 50 or 100 with Ad-SMN (or mock infected), 24 hpi cells were harvested and media was collected for TCA precipitation or in the case of MOI 50 media was collect for exosome purification.

Panel A: A549 or Ad-SMN infected A549 cells were separated by SDS-PAGE, and the resulting immunoblot was probed for SMN, tubulin and Flag. Equivalent volumes of cell lysate were applied to the gel. Data represents n=3.

Panel B: A549 or Ad-SMN infected A549 TCA media precipitates were separated by SDS-PAGE, and the resulting immunoblot was probed for SMN and Flag. Equivalent volumes of TCA precipitate were applied to the gel. Data represents n=3.

Panel C: A549 or Ad-SMN infected A549 exosomes were separated by SDS-PAGE, and the resulting immunoblot was probed for SMN and ALIX. 2.4µg of A549 and 2.8µg of A549::SMN exosomes were applied to the gel. Exosome concentration was determined using a Bradford assay with non-lysed samples. Data represents n=3.

contained within exosomes and the level of SMN protein can be enhanced through genetic modification or viral infection. Of note, the Flag tag used for tracking SMN appears to be less readily detectable in exosome samples versus samples isolated from cells.

4.2.b Exosomes associate with recipient cells

In order to act as a therapeutic it is essential that SMN-containing exosomes are able to enter recipient cells and this newly acquired SMN must be functional. Exosome entrance was tested through a variety of different means. Each process involved incubating 5 µg A549::SMN exosomes on recipient A549 cells for approximately 4 hours at 37ºC. Immunoblot was preformed to determine if Flag-SMN associates with the recipient cells. Figure 4.8 showed that there is a unique Flag signal in the A549::SMN exosome treated recipient cells. This flag signal indicates our harvested exosomes are able to successfully attach to other cells. Immunofluorescence was used to confirm exosome entrance as well as determine cellular localization of the protein. Unfortunately, we were unable to detect a flag signal in recipient cells, but it is unclear if this is due to lack of entry of the exosomes or poor Flag signal, as shown above. To further explore this issue, a Co-IP was preformed to determine if Flag-SMN from delivered exosomes interacted with its normal cellular components. The pull down was preformed with Flag to isolate exosome-derived SMN and association with the normal cellular partner Gemin-2 was analyzed via immunoblot. Unfortunately again the weak Flag signal compromised our ability to obtain a clear answer (data not shown). Overall Flag-SMN is able to associate with recipient cells; however, further experiments are needed to determine whether the exosomes are capable of delivering SMN to the interior of the cell.

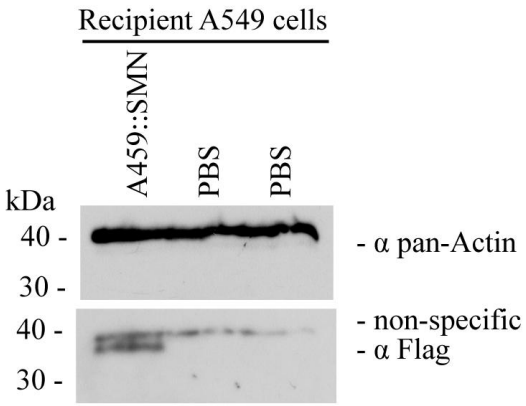
Recipient A549 cells
A459::SMN
PBS
PBS
kDa
40 -
30 -
- α pan-Actin
40 -
30 -
- non-specific
- α Flag

Figure 4.8 *Exosomes associate with A549 recipient cells.* 5 µg A549::SMN exosomes were incubated on recipient A549 cells for 4 hours then harvested using 2x LD. Cell lysates were separated by SDS-PAGE, and the resulting immunoblot was probed for Flag. A non-specific flag signal is detectable in all samples. Pan-actin was used as a loading control. Data represents n=2.

SMN is found in exosomes isolated from mouse serum

The first step for *in vivo* studies was to determine if exosomes could be harvested from murine serum. Exoquick was used to concentrate exosomes instead of ultra centrifugation as it is effective with very small volumes. Exoquick functions through a key polymer decreasing available water molecules forcing less-soluble components like vesicles to precipitate out of solution [59]. Following the Exoquick protocol, serum derived exosomes were analyzed via Nanosight Tacking analysis, Figure 4.9B. Due to the high concentration of the particles, significant levels of background noise were observed. However, the mean particle size, 105 nm, was smaller then achieved from the *in vitro* harvested exosomes. Next, the exosome samples were tested for the positive exosome marker Flotillin-2 by immunoblot. Figure 4.9A showed the presence of Flotillin-2 in the serum sample suggesting the pellet acquired from Exoquick does represent exosomes. We next investigated whether SMN was contained within these exosomes and therefore normally released from cells *in vivo*. We observed that SMN was found within the serum derived exosomes and this signal was enhanced in exosomes relative to that of pure serum, Figure 4.10B. Also surprising was the difference in endogenous SMN expression levels between homogenized liver and spinal cord, where the spinal cord expressed approximately 10x more SMN when equal quantities of protein were applied to the gel, Figure 4.10A. This finding agrees with previous literature suggesting different tissues may vary in there SMN levels and thresholds. Overall, this agrees with our *in vitro* data suggesting natural release of SMN. The fact that SMN is normally found circulating in the body lends support to the overall projects goal to use the liver as a SMN production factory.

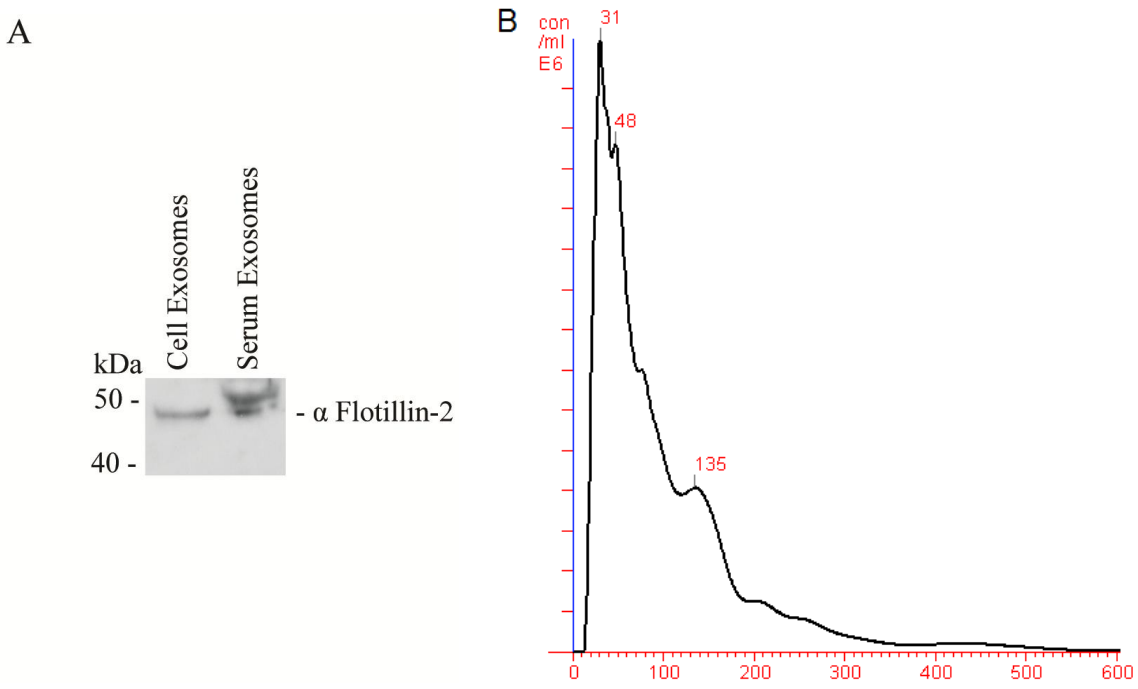
A
Cell Exosomes
Serum Exosomes
kDa
50 -
40 -
- α Flotillin-2
B
con
/ml
E6
31
48
135
0
100
200
300
400
500
600

Figure 4.9 *Isolation of serum-derived exosomes*.
Panel A: Media incubated on A549 cells for 24 hours was subjected to Exoquick to be comparable to serum derived exosomes. Equivalent volumes of exosomes derived from media and serum were separated by SDS-PAGE, and the resulting immunoblot was probed for Flotillin-2. Data represents n=2.
Panel B: Particle size as determine via Nanosight. Serum exosomes were purified through Exoquick for all experiments.

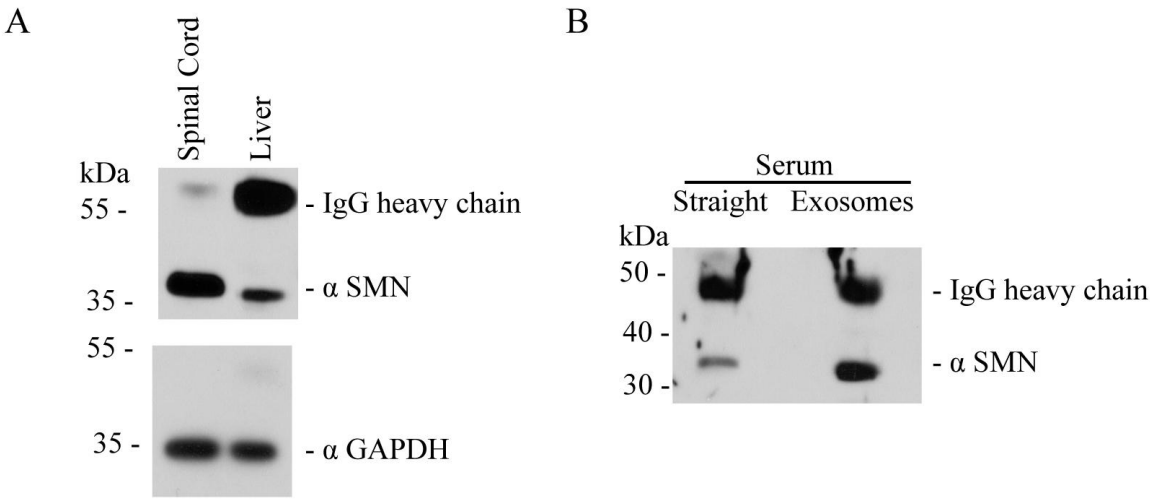
A
Spinal Cord
Liver
kDa
55 -
- IgG heavy chain
35 -
- α SMN
55 -
35 -
- α GAPDH
B
Serum
Straight
Exosomes
kDa
50 -
- IgG heavy chain
40 -
- α SMN
30 -

Figure 4.10 *Endogenous SMN is detectable in tissues and serum.*

Panel A: Six to eight week old C57Bl/6J mice liver and spinal cord samples were homogenized and 15µg of protein was separated by SDS-PAGE. The resulting immunoblot was probed for SMN and GAPDH as a loading control. Of note, the IgG heavy chain is also detectable. Data represents n=3.

Panel B: C57Bl/6J mouse serum and serum exosomes were separated by SDS-PAGE, and the resulting immunoblot was probed for SMN. Equivalent volumes were applied to the gel. Note the IgG heavy chain is also detectable. Data represents n=3.

4.2.c Virally-derived β-gal can be loaded into exosomes *in vivo*

Now that serum exosomes can be harvested, the Ad5LlacZ construct from Chapter 3 was used to determine if virus-derived proteins could be loaded within these exosomes. Ad5LlacZ was chosen due to its high β-gal expression and the ease of β-gal detection. The virus was delivered to six to eight week old CD1 mice at a high viral dose, $5x10^{12}$ VP/kg, via IV injection. Mice were then euthanized 24 hours later by cardiac puncture and chest opening to allow for maximum blood collection. Exosomes were harvested by Exoquick and analyzed via chemiluminescence assay (Applied Biosystems) and immunoblot in 2x LD. For comparison A549 cells were infected with Ad5LlacZ at MOI 50, the concentration used for all *in vitro* exosome preparations. Twenty-four hpi, the media was collected and exosomes harvested using the corresponding media Exoquick protocol. Figure 4.11A shows that β-gal is present in Exoquick derived exosomes isolated from both cells and serum when anaylized by chemiluminescence assay. The difference in β-gal expression relative to the PBS controls was considerably larger for cellular-derived exosomes than serum derived exosomes. This difference was also reflected in the immunoblot experiments where β-gal was detectable in cellular-derived exosomes, Figure 4.11B, but no significant signal in serum-derived exosomes was observed compared to the PBS control, Figure 4.11C. Together these results suggest that virally produced proteins are present in serum exosomes but at very low levels, levels below the sensitivity of western blot.

4.2.d Virally-derived SMN is undetectable in serum exosomes with anti-Flag

Finally, we investigated whether viral derived SMN could be detected in serum exosomes. Six to eight week old C57Bl/6J or CD1 mice were treated with $5x10^{12}$ VP/kg of Ad-SMN through an IV injection. After a 24 hour exposure period, several tissues were

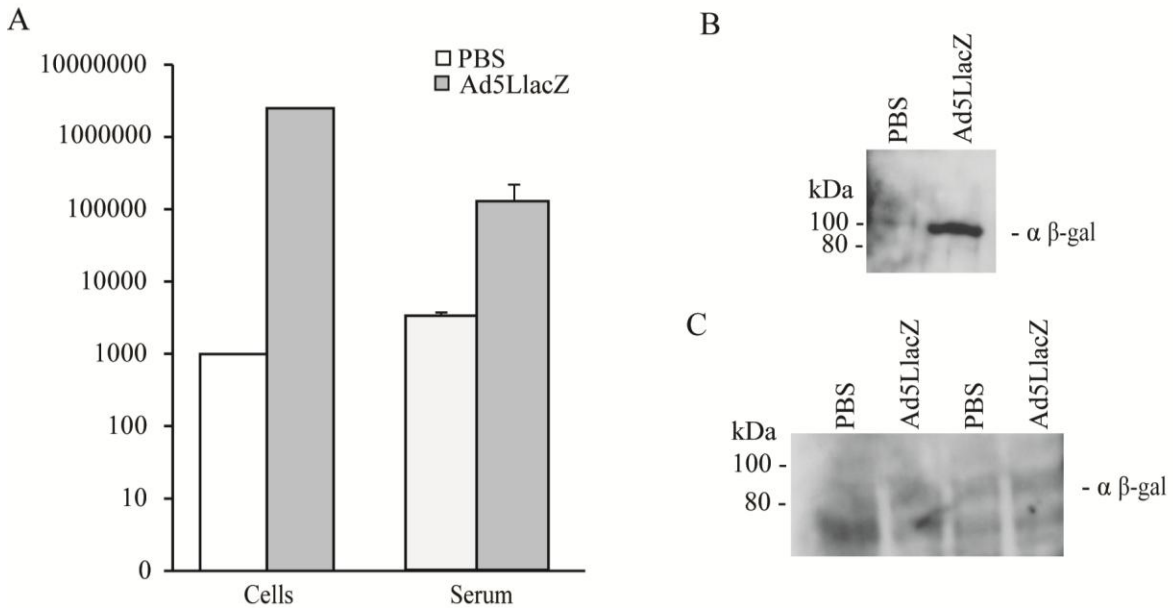
A
10000000
1000000
100000
10000
1000
100
10
0
PBS
Ad5LlacZ
Cells
Serum
B
PBS
Ad5LlacZ
kDa
100 -
80 -
- α β-gal
C
PBS
Ad5LlacZ
PBS
Ad5LlacZ
kDa
100 -
80 -
- α β-gal

Figure 4.11 *Virally produced β-gal is detectable in both cellular- and serum-derived exosomes.* A549 cell were infected with Ad5LlacZ at an MOI 50 or mock infected. Twenty-four hpi media was collected and exosomes harvest via Exoquick. Six to eight week old CD1 mice were injected with Ad5LlacZ or PBS at a concentration of $5x10^{12}$ VP/kg via IV injection. Twenty-four hours post injection mice were sacrificed by cardiac puncture and serum exosomes harvest using Exoquick.

Panel A: β-gal expression of exosomes derived from serum from mice treated with or cells infected with Ad5LlacZ was assessed by chemiluminscent assay. Data represents n=1-2.

Panel B: Exosomes isolated from A549 or Ad-SMN infected A549 were separated by SDS-PAGE and the resulting immunoblot was probed for β-gal. Data represents n=2.

Panel C: Serum derived exosomes from mice treated with Ad5LlacZ were separated by SDS-PAGE and the resulting immunoblot was probed for β-gal. Equivalent volumes of serum exosomes were applied to the gel. Data represents n=2.

removed and serum collected by cardiac puncture. Tissues were homogenized, subjected to immunoblot and probed for both SMN and Flag. While Ad-SMN liver samples showed significantly enhanced SMN expression relative to the control mice, Figure 4.12A, the difference in Flag expression in the same 3 Ad-SMN infected mice was not nearly as dramatic, Figure 4.12B. For example, in the middle lane of Figure 4.12B the Ad-SMN injected mouse had no detectable Flag signal, the reason for this is unknown however, it is thought to be a result of the Flag tag being altered. The TA muscle, diaphragm and spinal cord were also examined although none had any detectable Flag expression or change in SMN levels (data not shown). Lastly serum exosomes were tested for the presence of SMN derived from Ad-SMN however as expected no Flag signal was detectable (data not shown). Nor did serum exosomes yield any enhancement in SMN levels, Figure 4.12C. Next, we examined whether increasing the time before isolation of the exosomes from the mice could result in enhanced levels of SMN in the exosomes. The experiment was repeated with cardiac puncture taking place 72 hours post injection. The expression profiles are consistent with that of the 24 hour incubation. The liver still contained high SMN levels, Figure 4.12D, with marginal Flag expression, Figure 4.12E, while the TA muscle, diaphragm, spinal cord and serum exosomes had no change in SMN levels (Figure 4.12F) or detectable Flag signal (data not shown). The lack of enhanced SMN levels in serum exosomes suggests that SMN derived from the Ad vector is not being efficiently packaged into exosomes or possibly liver exosomes do not represent a large proportion of the exosomes in the circulatory system or detection issues. Further studies must be done to ensure that (1), virally transcribed SMN can be packaged into exosomes and (2), the liver functions to release a significant proportion of the circulating exosomes.

We also examined whether changing the tag contained on the SMN protein may

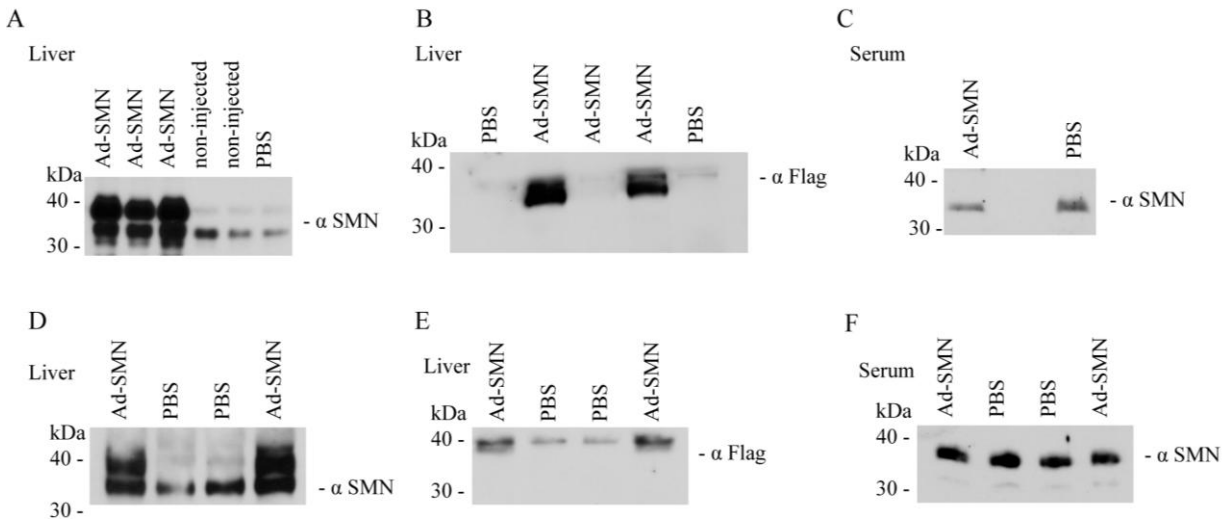
A
Liver
Ad-SMN
Ad-SMN
Ad-SMN
non-injected
non-injected
PBS
kDa
40 -
30 -
- α SMN
B
Liver
PBS
Ad-SMN
Ad-SMN
Ad-SMN
PBS
kDa
40 -
30 -
- α Flag
C
Serum
Ad-SMN
PBS
kDa
40 -
30 -
- α SMN
D
Liver
Ad-SMN
PBS
PBS
Ad-SMN
kDa
40 -
30 -
- α SMN
E
Liver
Ad-SMN
PBS
PBS
Ad-SMN
kDa
40 -
30 -
- α Flag
F
Serum
Ad-SMN
PBS
PBS
Ad-SMN
kDa
40 -
30 -
- α SMN

Figure 4.12 *In vivo Ad-SMN injection results in elevated SMN levels in the liver but not in serum-derived exosomes.* Six to eight week old mice were treated with Ad-SMN or PBS at a concentration of $5x10^{12}$ VP/kg via IV injection. After 24 hours (C57Bl/6J mice) or 72 hours (CD1 mice), mice were sacrificed by cardiac puncture. Tissues were removed, homogenized and serum exosomes were harvest using Exoquick.

Panel A: Liver samples from mice subjected to a 24 hour incubation period were homogenized and 20µg of protein was separated by SDS-PAGE. The resulting immunoblot was probed for SMN. Data represents n=3.

Panel B: Liver samples from mice subjected to a 24 hour incubation period were homogenized and 20µg of protein was separated by SDS-PAGE. The resulting immunoblot was probed for Flag. Data represents n=3.

Panel C: Serum exosomes from mice subjected to a 24 hour incubation period were separated by SDS-PAGE and the resulting immunoblot was probed for SMN. Equivalent volumes of serum exosomes were applied to the gel. Data represents n=3.

Panel D: Liver samples from mice subjected to a 72 hour incubation period were homogenized and 20µg of protein was separated by SDS-PAGE. The resulting immunoblot was probed for SMN. Data represents n=2.

Panel E: Liver samples from mice subjected to a 72 hour incubation period were homogenized and 20µg of protein was separated by SDS-PAGE. The resulting immunoblot was probed for Flag. Data represents n=2.

Panel F: Serum exosomes from mice subjected to a 72 hour incubation period were separated by SDS-PAGE and the resulting immunoblot was probed for SMN. Equivalent volumes of serum exosomes were applied to the gel. Data represents n=3.

allow for detection of virus-derived SMN in serum exosomes. Six to eight week old CD1 mice were injected under the same conditions as described above with Ad-SMN-myc-his, a viral vector containing SMN and the following tags: N-terminal Flag and C-terminal myc-his (Figure 4.1A). Twenty-four hours after injection, mice were euthanized, serum collected and exosomes purified through Exoquick. Immunoblot was preformed with the serum exosomes; however neither myc nor his antibodies resulted in a significant signal over background, Figure 4.13. Taken together these results indicate that endogenous SMN is naturally contained within exosomes isolated from serum. Furthermore, Ad-SMN was able to enhance SMN levels within the liver however; low proteins levels make detection of virally-derived SMN in serum exosomes inconclusive.

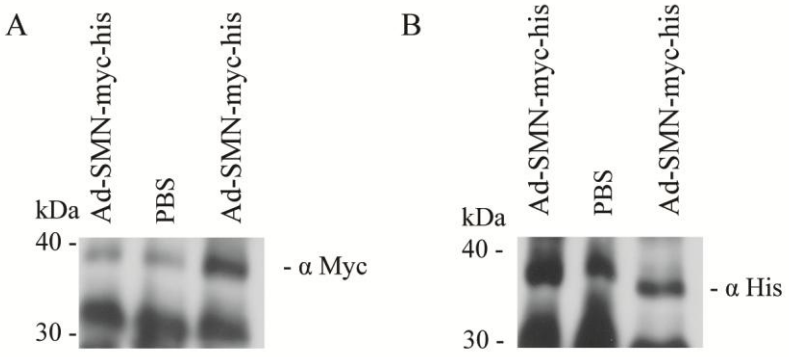
A
Ad-SMN-myc-his
PBS
Ad-SMN-myc-his
kDa
40 -
30 -
- α Myc
B
Ad-SMN-myc-his
PBS
Ad-SMN-myc-his
kDa
40 -
30 -
- α His

Figure 4.13 *Myc and his tags contained on Ad-SMN-myc-his are not detectable in serum exosomes.* CD1 mice were injected with Ad-SMN-myc-his or PBS at a concentration of $5x10^{12}$ VP/kg via IV injection. Twenty-four hours post injection mice were euthanized and exosomes collected via Exoquick. Serum derived exosomes were separated by SDS-PAGE and the resulting immunoblot was probed for myc (Panel A) or his (Panel B). Equivalent volumes of serum exosomes were applied to the gel. Data represents n=2.

4.3 **Discussion**

4.3.a Overview

It was determined in Chapter 3 that the reduced virion size of the modified Ad vectors were unsuccessful at enhancing infection of spinal cord or skeletal muscle. However, as observed in many studies, we detected high-level uptake in liver. This observation suggested that one approach might be to use the liver as a protein production factory, as has been used successfully for other systemic diseases such as hemophilia [113]. The goal of this chapter was to produce an SMN protein that was able to spread systemically. Following Ad-SMN vector liver infection, significant amounts of the virally encoded SMN will be transcribed. In this study it was determined that SMN can be released naturally from cells through means of microvesicles. Exosomes can enter and deliver proteins to recipient cells suggesting this approach may be appropriate for treatment of SMA.

4.3.b Microparticle contamination

Exosomes were harvested using an established protocol [103] and analyzed via Nanosight. Nanosight relates the rate of Brownian motion to particle size [25]. However, we observed that the mean particle size was larger than expected for a pure exosome population. This may be a result of technical issues with evaluating the samples as the Nanosight used was not on an air table or in an isolated area. Regardless, the Nanosight set-up cannot fully explain the large particle size. As such, it was thought that the exosome sample might be contaminated with microparticles. Microparticles are larger than exosomes with a size range between 100-1000 nm and bud from the plasma membrane instead of MVB [101]. Fortunately both exosomes and microparticles share a role in cell-to-cell communication [25], therefore microparticles will not hinder the overall goal of systemic SMN delivery.

Nevertheless, steps were taken to increase the purity of the exosome sample by changing the method of purification from a 10,000 xg centrifugation step to filtration through a 0.2 µm membrane (Figure 4.3). Although this approach resulted in some success, the microparticle contamination was not eliminated. Other studies have shown that size readings from Nanosight are slightly larger than the reported exosome size; for example, exosomes harvested by Ramteke *et al* had a Nanosight reading of 141-187 nm while electron microscopy suggested the exosomes were 50-100 nm [86]. Differences in size readings from these two methods may be a result of particle aggregation [86]. Taken together we believe our harvested particles do represent a relatively pure exosome population.

4.3.c Exosome yield

Studies have shown that 1-2 µg of exosomes can be harvested from 10^6 immature dendritic cells, where dendritic cells are known to produce very high quantities of exosomes [103]. Our harvested exosomes preparation, however, gave lower yields of only 1 µg per $2.4x10^6$ A549 cells, approximately half as much. This was surprising as the exosome collection protocol used is well established and had fewer steps than other protocols, hence a decreased risk of sample loss [33]. One possible reason for this difference is that A549 cells, used in the majority of this study, are not an ideal cell type for studying exosomes. It is known that cells release over six times more exosomes in suspension than when attached to a plate [53]. This was shown by Koumangoye *et al*, who demonstrated that the addition of EDTA, to detach adherent cells, resulted in abundant exosome release [53]. With this in mind, exosomes could be harvested from 293N3S cells or another cell line in suspension to increase exosome yield. Therefore future studies should use cells in suspension or a non adherent liver cell line which would be more physiologically relevant.

4.3.d Exosome markers

Several different exosome markers were used to test the harvested particle samples (Figure 4.3). Positive controls include proteins more commonly found within exosomes, which are proteins involved in vesicle development and transport. Negative exosome markers are endoplasmic reticulum or mitochondrial based proteins that have minimal interactions with a forming MVB. Unfortunately, due to the process of exosome formation the presence of a positive exosome markers does not confirm the particle is actually an exosome. As well, since cytosolic proteins can be captured in exosomes, it is possible, though rare, for negative exosome markers to be found within exosomes. Overall, appropriate or definitive controls for exosome detection are lacking and need to be developed to further the exosome research field.

4.3.e SMN containing exosomes *in vitro*

We were fortunate to detect SMN within exosomes, indicating no modifications were necessary for the protein to be packaged into these structures. This is not uncommon of cytosolic proteins [104, 33]. We were also able to demonstrate that when SMN is over expressed within the cell there is an enhancement of the protein within exosomes. Overall, these findings suggest that SMN is naturally released from cells in exosomes and the amount of SMN within the exosomes can be altered through viral vectors. Of note, it was also found that SMN was released in apoptotic bodies and microparticles; however, due to the small size of our harvested microvesicles we believe that SMN is released from live cells and is not just an artefact of cell death represented by apoptotic bodies.

4.3.f Exosome-mediated delivery of proteins to recipient cells

For our therapeutic strategy to be successful it is vital for hepatocyte-derived exosomes to enter recipient cells, principally α-motor neuron and skeletal muscle, the damaged tissues in SMA. Immunoblot results suggest our SMN-containing exosomes are able to associate with recipient A549 cells (Figure 4.8). However, both immunofluorescent and Co-IP experiments proved unsuccessful at showing detectable levels of exosome-delivered SMN within recipient cells. Studies have shown that exosome entrance can be as efficient as transfection [2], though this was demonstrated using immune recipient cells, known to be superior at exosome up-take [62]. Our low levels of association may be a result of two factors: (i) exosomes remaining attached to the outer cell surface and (ii) a weak Flag signal. Throughout this chapter, issues with Flag detection has occurred, compromising our ability to effectively track exosomes. It is thought that a post-translational modification must be occurring to result in this loss of signal. Previous studies by Schmidt *et al* have shown that the tyrosine at position two in the Flag tag is highly susceptible to tyrosine sulfation in insect cells and this significantly abolishes Flag-anti-Flag interactions [96]. Although the means of post-translation modification occuring within our cells remains unknown, it is thought to significantly reduce the efficiency of detection of the Flag tag.

Until further experiments are preformed to determine the success of exosome up-take, the functionality of the delivered SMN cannot be properly assessed. It is believed that the delivered SMN protein will be functional as studies have shown exosomes are able to deliver functional mRNA [112]. Thus once the SMN tags are optimized exosome entrance and protein function can be more accurately assessed.

4.3.g Detection of virus derived SMN *in vivo*

The Ad-SMN viral vector could be used directly to treat SMA patients, as the Ad vector is deleted of essential viral genes (E1 and E3), preventing viral replication. Following infection, virally derived SMN could be packaged into exosomes which would then spread throughout the body. Due to significant localization of Ad to the liver, detection of both enhanced SMN levels and the Flag tag were possible in the liver at both 24 and 72 hours post-treatment (Figure 4.12). However, the difference in expression between Flag and SMN suggests the Flag tag is again being modified. No elevation of SMN or detection of the Flag tag was observed in serum exosomes following Ad-SMN delivery to mice. Yet, this was expected as initial experiments with β-gal-expressing viruses indicated that immunoblot experiments were not sensitive enough to detect low levels of virus-derived proteins contained in the exosomes (Figure 4.11). Other tags were tested, *i.e.* myc and his, yet they too were unsuccessful at tracking SMN derived from the Ad vector *in vivo* (Figure 4.13). Regardless, it is expected that the SMN protein is present in serum exosomes at very low levels, well below the detection limits of western blot.

4.4 **Conclusion**

SMN is naturally released and carried within exosomes from a variety of cell lines and *in vivo*. This is important in the treatment of SMA where the lack of SMN in α-motor neurons and skeletal muscle results in muscle deterioration and death. Using SMN over expressing cells or Ad vectors, the amount of SMN within exosomes can be enhanced, leading to a possible SMA therapeutic.

Chapter 5 – Overview of SMA treatments

5.1 Summary

Ad has great potential as a viral vector for gene therapy due to its high safety profile and its large cloning capacity [116]. Current studies have shown that helper-dependent Ad has the ability to persist and express a trangene *in vivo* for extended time periods, up to at least 7 years in non-human primates [12]. Thus Ad vectors are an ideal therapeutic for SMA, a progressive disease caused by insufficient levels of the SMN protein. Disease onset occurs early in life and is seen as deterioration of the α-motor neurons and skeletal muscle.

Given that Ad predominately localizes to the liver the initial goal was to enhance vector spread through decreasing the overall size of the virion. The virion diameter was reduced through producing a chimeric Ad5 vector with an Ad9 shaft, as the Ad9 shaft is roughly one third the length of an Ad5 shaft. Additional modifications to the chimeric vector included addition of 7 lysine residues to enhance interactions with heparan sulphate proteoglycans while also increasing the overall virion charge. Unfortunately, neither modification resulted in enhanced systemic spread. All viral constructs localized to the liver or remained at the site of injection. Although infection, determined via transgene expression, was detected in both the desired tissues, the α-motor neurons and skeletal muscle, the lack of viral spread suggests that multiple injections would be required to prevent deterioration of each muscle group. As such, further modifications to Ad vectors are needed to achieve efficient systemic biodistribution of Ad.

Preliminary experiments indicated that SMN is found outside the cell. Follow-up studies determined that this is a result of SMN release in microvesicles. Exosomes, a type of microvesicle which functions in cellular communication, are released from cells under normal conditions, travel throughout the body and are taken up by recipient cells. This

observation led to the second goal of using exosomes to achieve systemic biodistribution of the SMN protein produced from an SMN-expressing Ad vector. It was found that SMN is contained in all microvesicles including exosomes and SMN levels could be enhanced within exosomes. Unfortunately due to issues with the Flag tag used to track vector-derived SMN, it could not be determined if SMN associating with recipient cells was able to enter the nucleus or function properly. It was also not possible to determine if vector derived SMN was contained in exosomes *in vivo*. However vector-derived β-gal was detectable in serum exosomes by chemiluenescence as such it is likely that virally-derived SMN is present in serum exosomes as well. This project has great promise and investigations are still ongoing.

5.2 **Future directions**

All viruses tested in Chapter 3 were able to infect both α-motor neurons and skeletal muscle, yet were unable to spread within these tissues in any capacity. We therefore suggest that additional approaches should be examined to further modify the fiber protein until enhanced viral spread is achieved. These modifications include further altering the size of the Ad virion, increasing the number of poly-lysine residues and decreasing the tropism to CAR. Exchanging the Ad5 shaft with an Ad9 decreased the virion size by approximately 50 nm however this did not result in enhanced viral spread. Other chimeric vectors could be explored to determine if the Ad size can be further reduced allowing for greater spread *in vivo*. Increasing the number of poly-lysine residues could result in two benefits (1) amplify interactions with mature muscle tissue and other cells with low CAR expression and (2) increase the overall charge of the virion, thereby decreasing the repulsion from the negative cell membrane. Finally, action could be taken to abolish fiber's specificity to CAR. This would result in the virus relying on alternate primary or secondary interactions, such as

penton, to associate with host cells. These interactions may occur more slowly, increasing the amount of time the vector is free-floating throughout the body and potentially enhancing systemic spread.

The project discussed in Chapter 4, Exosome transport of SMN, remains ongoing with several avenues yet to be investigated. First, experiments could be done to enhance SMN within exosomes. This may be possible through the addition of a C1C2 lactadherin domain. Studies have shown the C1C2 domain results in higher rates of exosome packaging due to the formation of high affinity complexes between the C1C2 domain and membranes, including MVB [39]. Second, experiments could be done to improve exosome entrance in recipient cells. Exosomes could be modified with targeting ligands, such as Nerve Growth Factor, known to interact with the Trk family of neurotrophin receptors expressed on motor neurons [4]. These receptors could assist not only in exosome uptake but also enhance uptake in desired tissues, as demonstrated previously by Alvarez *et al* [2]. Lastly, although we believe SMN derived from Ad-SMN is packaged in exosomes *in vivo* this was not confirmed due to the detection limits of western blot. Additional experiments with increased detection specificity must be done to determine if Ad-SMN enhances SMN levels in serum exosomes. Sanchez *et al* suggested SMN interacts with translational machinery affecting some mRNAs including CARM1 [43], as such a functional assay involving serum exosomes and CARM1 could be done to functionally determine changes in SMN levels.

Alternatively, instead of loading exosomes with SMN through an Ad-vector, exosomes could be harvested from an individual and the SMN protein directly loaded or attached, as observed in current clinical trials [112]. This approach would involve the isolation and purification of human exosomes which are then modified through attaching the desired protein to the exterior of the exosome. These loaded exosomes are then reintroduced

into the original donor. Unfortunately this type of exosome treatment has two drawbacks (i) it must be done on an individual basis to prevent immune reactions and (ii) this requires isolation and purification of large quantities of the desired SMN protein, a process for which is still being established.

5.3 **Conclusions**

Overall, it was found that body-wide distribution of the Ad constructs tested was not achieved even with significantly reduced virion size. However, we determined that SMN is naturally release from cells in exosomes and protein levels can be enhanced through Ad vectors. Experiments are ongoing to determine if SMN-expressing Ad vectors can be used in conjunction with exosomes for systemic protein spread and the treatment of SMA.

6. References

1. Addison, C. L., Hitt, M., Kunsken, D., & Graham, F. L. (1997). Comparison of the human versus murine cytomegalovirus immediate early gene promoters for transgene expression by adenoviral vectors. Journal of General Virology, 78, 1653-1661.
2. Alvarez-Erviti, L., Seow, Y., Yin, H., Betts, C., Lakhal, S., & Wood, M. J. A. (2011). Delivery of siRNA to the mouse brain by systemic injection of targeted exosomes. Nature Biotechnology, 29(4), 341-U179.
3. Baietti, M. F., Zhang, Z., Mortier, E., Melchior, A., Degeest, G., Geeraerts, A. David, G. (2012). Syndecan-syntenin-ALIX regulates the biogenesis of exosomes. Nature Cell Biology, 14(7), 677-685.
4. Barbacid, M. (1994). The TRK family of neurotrophin receptors. Journal of Neurobiology, 25(11), 1386-1403.
5. Bebee, T. W., Dominguez, C. E., & Chandler, D. S. (2012). Mouse models of SMA: tools for disease characterization and therapeutic development. Human Genetics, 131(8), 1277-1293.
6. Benkhelifa-Ziyyat, S., Besse, A., Roda, M., Duque, S., Astord, S., Carcenac, R. Barkats, M. (2013). Intramuscular scAAV9-SMN Injection Mediates Widespread Gene Delivery to the Spinal Cord and Decreases Disease Severity in SMA Mice. Molecular Therapy, 21(2), 282-290.
7. Blau, H. M., Pavlath, G. K., Hardeman, E. C., Chiu, C. P., Silberstein, L., Webster, S. G.,Webster, C. (1985). Plasticity of the differentiated state. Science, 230(4727), 758-766.
8. Bowerman, M., Anderson, C. L., Beauvais, A., Boyl, P. P., Witke, W., & Kothary, R. (2009). SMN, profilin IIa and plastin 3: A link between the deregulation of actin dynamics and SMA pathogenesis. Molecular and Cellular Neuroscience, 42(1), 66-74.
9. Bowerman, M., Murray, L. M., Beauvais, A., Pinheiro, B., & Kothary, R. (2012). A critical smn threshold in mice dictates onset of an intermediate spinal muscular atrophy phenotype associated with a distinct neuromuscular junction pathology. Neuromuscular Disorders, 22(3), 263-276.
10. Bowerman, M., Murray, L. M., Boyer, J. G., Anderson, C. L., & Kothary, R. (2012). Fasudil improves survival and promotes skeletal muscle development in a mouse model of spinal muscular atrophy. Bmc Medicine, 10.
11. Bramson, J. L., Grinshtein, N., Meulenbroek, R. A., Lunde, J., Kottachchi, D., Lorimer, I. A., Parks, R. J. (2004). Helper-dependent adenoviral vectors containing modified fiber for improved transduction of developing and mature muscle cells. Human Gene Therapy, 15(2), 179-188.
12. Brunetti-Pierri, N., Ng, T., Iannitti, D., Cioffi, W., Stapleton, G., Law, M., Ng, P. (2013). Transgene Expression up to 7 Years in Nonhuman Primates Following Hepatic Transduction with Helper-Dependent Adenoviral Vectors. Human Gene Therapy, 24(8), 761-765.
13. Burnett, B. G., Munoz, E., Tandon, A., Kwon, D. Y., Sumner, C. J., & Fischbeck, K. H. (2009). Regulation of SMN Protein Stability. Molecular and Cellular Biology, 29(5), 1107-1115.
14. Burns, J. (2013). Development of a protein-based therapy for the treatment of spinal muscular strophy, in Biochemistry with specialization in Human and Molecular Genetics. University of Ottawa: Ottawa.
15. Caby, M. P., Lankar, D., Vincendeau-Scherrer, C., Raposo, G., & Bonnerot, C. (2005). Exosomal-like vesicles are present in human blood plasma. International Immunology, 17(7), 879-887.
16. Carayon, K., Chaoui, K., Ronzier, E., Lazar, I., Bertrand-Michel, J., Roques, V., Joly, E. (2011). Proteolipidic Composition of Exosomes Changes during Reticulocyte Maturation. Journal of Biological Chemistry, 286(39), 34426-34439.

17. Carissimi, C., Baccon, J., Straccia, M., Chiarella, P., Maiolica, A., Sawyer, A., Pellizzoni, L. (2005). Unrip is a component of SMN complexes active in snRNP assembly. Febs Letters, 579(11), 2348-2354.
18. Chartier, C., Degryse, E., Gantzer, M., Dieterle, A., Pavirani, A., & Mehtali, M. (1996). Efficient generation of recombinant adenovirus vectors by homologous recombination in Escherichia coli. Journal of Virology, 70(7), 4805-4810.
19. Chen, T. H., Chang, J. G., Yang, Y. H., Mai, H. H., Liang, W. C., Wu, Y. C., Wang, H. Y., Huang, Y. B., Wu, S. M., Chen, Y. C., Yang, S. N., Jong, Y. J. [29]. Randomized, double-blind, placebo-controlled trail of hydroxyurea in spinal muscular atrophy. Neurology 75(24), 2190-7.
20. Clayton, A., Turkes, A., Dewitt, S., Steadman, R., Mason, M. D., & Hallett, M. B. (2004). Adhesion and signaling by B cell-derived exosomes: the role of integrins. Faseb Journal, 18(6), 977.
21. Coady, T. H., & Lorson, C. L. (2010). Trans-Splicing-Mediated Improvement in a Severe Mouse Model of Spinal Muscular Atrophy. Journal of Neuroscience, 30(1), 126-130.
22. Corti, S., Nizzardo, M., Simone, C., Falcone, M., Nardini, M., Ronchi, D., Comi, G. P. (2012). Genetic Correction of Human Induced Pluripotent Stem Cells from Patients with Spinal Muscular Atrophy. Science Translational Medicine, 4(165).
23. Crystal, R. G. (2014). Adenovirus: The First Effective In Vivo Gene Delivery Vector. Human Gene Therapy, 25(1), 3-11.
24. DiDonato, C. J., Parks, R. J., Kothary, R. (2003). Development of a gene therapy strategy for the restoration of survival motor neuron protein expression: Implications for spinal muscular atrophy therapy. Human Gene Therapy, 14(2), 179-188.
25. Dragovic, R. A., Gardiner, C., Brooks, A. S., Tannetta, D. S., Ferguson, D. J. P., Hole, P., Sargent, I. L. (2011). Sizing and phenotyping of cellular vesicles using Nanoparticle Tracking Analysis. Nanomedicine-Nanotechnology Biology and Medicine, 7(6), 780-788.
26. Duque, S., Joussemet, B., Riviere, C., Marais, T., Dubreil, L., Douar, A. M., Barkats, M. (2009). Intravenous Administration of Self-complementary AAV9 Enables Transgene Delivery to Adult Motor Neurons. Molecular Therapy, 17(7), 1187-1196.
27. Echaniz-Laguna, A., Miniou, P., Bartholdi, D., & Melki, J. (1999). The promoters of the survival motor neuron gene (SMN) and its copy (SMNc) share common regulatory elements. American Journal of Human Genetics, 64(5), 1365-1370.
28. Escudier, B., Dorval, T., Chaput, N., Andre, F., Caby, M. P., Novault, S., Zitvogel, L. (2005). Vaccination of metastatic melanoma patients with autologous dendritic cell (DC) derived-exosomes: results of the first phase I clinical trial. Journal of Translational Medicine, 3.
29. Feldkotter, M., Schwarzer, V., Wirth, R., Wienker, T. F., & Wirth, B. (2002). Quantitative analyses of SMN1 and SMN2 based on real-time LightCycler PCR: Fast and highly reliable carrier testing and prediction of severity of spinal muscular atrophy. American Journal of Human Genetics, 70(2), 358-368.
30. Feng, D., Zhao, W. L., Ye, Y. Y., Bai, X. C., Liu, R. Q., Chang, L. F., Sui, S. F. (2010). Cellular Internalization of Exosomes Occurs Through Phagocytosis. Traffic, 11(5), 675-687.
31. Frugier, T., Tiziano, F. D., Cifuentes-Diaz, C., Miniou, P., Roblot, N., Dierich, A., Melki, J. (2000). Nuclear targeting defect of SMN lacking the C-terminus in a mouse model of spinal muscular atrophy. Human Molecular Genetics, 9(5), 849-858.
32. Ginn, S. L., Alexander, I. E., Edelstein, M. L., Abedi, M. R., & Wixon, J. (2013). Gene therapy clinical trials worldwide to 2012 an update. Journal of Gene Medicine, 15(2), 65-77.
33. Gomes, C., Keller, S., Altevogt, P., & Costa, J. (2007). Evidence for secretion of Cu,Zn superoxide dismutase via exosomes from a cell model of amyotrophic lateral sclerosis. Neuroscience Letters, 428(1), 43-46.
34. Goulet, B. (2013). Two-way Approach to Spinal Muscular Atrophy Therapy Development, in Microbiology and Immunology. University of Ottawa: Ottawa.

35. Graham, F. L. (1987). Growth of 293 cells in suspension-culture. Journal of General Virology, 68, 937-940.
36. Graham, F. L., Smiley, J., Russell, W. C., & Nairn, R. (1977). Characteristics of a human cell line transformed by DNA from human adenovirus type-5. Journal of General Virology, 36(JUL), 59-72.
37. Gubitz, A. K., Feng, W. Q., & Dreyfuss, G. (2004). The SMN complex. Experimental Cell Research, 296(1), 51-56.
38. Harding, C., Heuser, J., & Stahl, P. (1983). Receptor-mediated endocytosis of transerrin and recycling of the transferring receptor in rat reticulocytes. Journal of Cell Biology, 97(2), 329-339.
39. Hartman, Z. C., Wei, J. P., Glass, O. K., Guo, H. T., Lei, G. J., Yang, X. Y., Lyerly, H. K. (2011). Increasing vaccine potency through exosome antigen targeting. Vaccine, 29(50), 9361-9367.
40. Hassani, K., & Olivier, M. (2013). Immunomodulatory Impact of Leishmania-Induced Macrophage Exosomes: A Comparative Proteomic and Functional Analysis. Plos Neglected Tropical Diseases, 7(5).
41. He, W. A., Calore, F., Londhe, P., Canella, A., Guttridge, D. C., & Croce, C. M. (2014). Microvesicles containing miRNAs promote muscle cell death in cancer cachexia via TLR7. Proceedings of the National Academy of Sciences of the United States of America, 111(12), 4525-4529.
42. Heier, C. R., & DiDonato, C. J. (2009). Translational readthrough by the aminoglycoside geneticin (G418) modulates SMN stability in vitro and improves motor function in SMA mice in vivo. Human Molecular Genetics, 18(7), 1310-1322.
43. Hua, Y. M., Sahashi, K., Hung, G. N., Rigo, F., Passini, M. A., Bennett, C. F., & Krainer, A. R. (2010). Antisense correction of SMN2 splicing in the CNS rescues necrosis in a type III SMA mouse model. Genes & Development, 24(15), 1634-1644.
44. Hua, Y. M., Sahashi, K., Rigo, F., Hung, G., Horev, G., Bennett, C. F., & Krainer, A. R. (2011). Peripheral SMN restoration is essential for long-term rescue of a severe spinal muscular atrophy mouse model. Nature, 478(7367), 123-126.
45. Jiang, L, He L, Fountoulakis, M. (2004). Comparison of protein precipitation methods for sample preparation prior to proteomic analysis. Journal Chromatography A, 1023(2), 317-20.
46. Jovanovic, K., Pastor, A. M., & O'Donovan, M. J. (2010). The Use of PRV-Bartha to Define Premotor Inputs to Lumbar Motoneurons in the Neonatal Spinal Cord of the Mouse. Plos One, 5(7).
47. Kalyuzhniy, O., Di Paolo, N. C., Silvestry, M., Hofherr, S. E., Barry, M. A., Stewart, P. L., & Shayakhmetov, D. M. (2008). Adenovirus serotype 5 hexon is critical for virus infection of heptocytes in vivo. Proceedings of the National Academy of Sciences of the United States of America, 105(14), 5483-5488.
48. Kobayashi, D. T., Shi, J., Stephen, L., Ballard, K. L., Dewey, R., Mapes, J., Pediat Neuromuscular Clinical, R. (2013). SMA-MAP: A Plasma Protein Panel for Spinal Muscular Atrophy. Plos One, 8(4).
49. Kolb, S. J., Battle, D. J., & Dreyfuss, G. (2007). Molecular functions of the SMN complex. Journal of Child Neurology, 22(8), 990-994.
50. Kosaka, N., Iguchi, H., Hagiwara, K., Yoshioka, Y., Takeshita, F., & Ochiya, T. (2013). Neutral Sphingomyelinase 2 (nSMase2)-dependent Exosomal Transfer of Angiogenic MicroRNAs Regulate Cancer Cell Metastasis. Journal of Biological Chemistry, 288(15), 10849-10859.
51. Kosaka, N., Iguchi, H., Yoshioka, Y., Hagiwara, K., Takeshita, F., & Ochiya, T. (2012). Competitive Interactions of Cancer Cells and Normal Cells via Secretory MicroRNAs. Journal of Biological Chemistry, 287(2), 1397-1405.

52. Kosaka, N., Iguchi, H., Yoshioka, Y., Takeshita, F., Matsuki, Y., & Ochiya, T. (2010). Secretory Mechanisms and Intercellular Transfer of MicroRNAs in Living Cells. Journal of Biological Chemistry, 285(23), 17442-17452.
53. Koumangoye, R. B., Sakwe, A. M., Goodwin, J. S., Patel, T., & Ochieng, J. (2011). Detachment of Breast Tumor Cells Induces Rapid Secretion of Exosomes Which Subsequently Mediate Cellular Adhesion and Spreading. Plos One, 6(9).
54. Le, T. T., Pham, L. T., Butchbach, M. E. R., Zhang, H. L., Monani, U. R., Coovert, D. D., Burghes, A. H. M. (2005). SMN Delta 7, the major product of the centromeric survival motor neuron (SMN2) gene, extends survival in mice with spinal muscular atrophy and associates with full-length SMN. Human Molecular Genetics, 14(6), 845-857.
55. Lefebvre, S., Burglen, L., Frezal, J., Munnich, A., & Melki, J. (1998). The role of the SMN gene in proximal spinal muscular atrophy. Human Molecular Genetics, 7(10), 1531-1536.
56. Lefebvre, S., Burglen, L., Reboullet, S., Clermont, O., Burlet, P., Viollet, L., Melki, J. (1995). Identification and characterization of a spinal muscular atrophy-determining gene. Cell, 80(1), 155-165.
57. Lefebvre, S., Burlet, P., Liu, Q., Bertrandy, S., Clermont, O., Munnich, A., Melki, J. (1997). Correlation between severity and SMN protein level in spinal muscular atrophy. Nature Genetics, 16(3), 265-269.
58. Li, J. H., Liu, K. C., Liu, Y., Xu, Y., Zhang, F., Yang, H. J.. Yuan, Z. H. (2013). Exosomes mediate the cell-to-cell transmission of IFN-alpha-induced antiviral activity. Nature Immunology, 14(8), 793-+.
59. Life technologies. (2014). Thermo Fisher Scientific.
60. Ling, K. K. Y., Gibbs, R. M., Feng, Z. H., & Ko, C. P. (2012). Severe neuromuscular denervation of clinically relevant muscles in a mouse model of spinal muscular atrophy. Human Molecular Genetics, 21(1), 185-195.
61. Liu, Q., Fischer, U., Wang, F., & Dreyfuss, G. (1997). The spinal muscular atrophy disease gene product, SMN, and its associated protein SIP1 are in a complex with spliceosomal snRNP proteins. Cell, 90(6), 1013-1021.
62. Lopez-Verrilli, M. A., & Court, F. A. (2013). Exosomes: mediators of communication in eukaryotes. Biological Research, 46(1), 5-11.
63. Lorson, C. L., & Androphy, E. J. (2000). An exonic enhancer is required for inclusion of an essential exon in the SMA-determining gene SMN. Human Molecular Genetics, 9(2), 259-266.
64. Lorson, C. L., Hahnen, E., Androphy, E. J., & Wirth, B. (1999). A single nucleotide in the SMN gene regulates splicing and is responsible for spinal muscular atrophy. Proceedings of the National Academy of Sciences of the United States of America, 96(11), 6307-6311.
65. Lorson, M. A., Spate, L. D., Samuel, M. S., Murphy, C. N., Lorson, C. L., Prather, R. S., & Wells, K. D. (2011). Disruption of the Survival Motor Neuron (SMN) gene in pigs using ssDNA. Transgenic Research, 20(6), 1293-1304.
66. Lotti, F., Imlach, W. L., Saieva, L., Beck, E. S., Hao, L. T., Li, D. K., Pellizzoni, L. (2012). An SMN-Dependent U12 Splicing Event Essential for Motor Circuit Function. Cell, 151(2), 440-454.
67. Maguire, C., Balaj, L., Sivaraman, S., Crommentuijn, M., Ericsson, M., Mincheva-Nilsson, L., Baranov, V., Gianni, D., Tannous, B., Sena-Esteves, M., Breakefield, X., Skog, J. (2011). Microvesicles-associated AAV vector as a novel gene delivery system. Molecular Therapy.
68. Martin, C. S. (2012). Latest Insights on Adenovirus Structure and Assembly. Viruses-Basel, 4(5), 847-877.
69. Martinez-Hernandez, R., Soler-Botija, C., Also, E., Alias, L., Caselles, L., Gich, I., Tizzano, E. F. (2009). The Developmental Pattern of Myotubes in Spinal Muscular Atrophy Indicates Prenatal Delay of Muscle Maturation. Journal of Neuropathology and Experimental Neurology, 68(5), 474-481.

70. Masyuk, A. I., Masyuk, T. V., & LaRusso, N. F. (2013). Exosomes in the pathogenesis, diagnostics and therapeutics of liver diseases. Journal of Hepatology, 59(3), 621-625.
71. Mathivanan, S., Fahner, C. J., Reid, G. E., & Simpson, R. J. (2012). ExoCarta 2012: database of exosomal proteins, RNA and lipids. Nucleic Acids Research, 40(D1), D1241-D1244.
72. Medina-Kauwe, L. K. (2003). Endocytosis of adenovirus and adenovirus capsid proteins. Advanced Drug Delivery Reviews, 55(11), 1485-1496.
73. Miskovic, M., Lalic, T., Radivojevic, D., Cirkovic, S., Ostojic, S., & Guc-Scekic, M. (2014). Ten years of experience in molecular prenatal diagnosis and carrier testing for spinal muscular atrophy among families from Serbia. International Journal of Gynecology & Obstetrics, 124(1), 55-58.
74. Mittal, B. (2012). Rapid molecular diagnosis of spinal muscular atrophy. Indian Journal of Medical Research, 135(1), 6-8.
75. Miyajima, H., Miyaso, H., Okumura, M., Kurisu, J., & Imaizumi, K. (2002). Identification of a cis-acting element for the regulation of SMN exon 7 splicing. Journal of Biological Chemistry, 277(26), 23271-23277.
76. Monani, U. R., Lorson, C. L., Parsons, D. W., Prior, T. W., Androphy, E. J., Burghes, A. H. M., & McPherson, J. D. (1999). A single nucleotide difference that alters splicing patterns distinguishes the SMA gene SMN1 from the copy gene SMN2. Human Molecular Genetics, 8(7), 1177-1183.
77. Morelli, A. E., Larregina, A. T., Shufesky, W. J., Sullivan, M. L. G., Stolz, D. B., Papworth, G. D,. Thomson, A. W. (2004). Endocytosis, intracellular sorting, and processing of exosomes by dendritic cells. Blood, 104(10), 3257-3266.
78. Murray, L. M., Beauvais, A., Bhanot, K., & Kothary, R. (2013). Defects in neuromuscular junction remodelling in the Smn(2B/-) mouse model of spinal muscular atrophy. Neurobiology of Disease, 49, 57-67.
79. Nakajima, H., Uchida, K., Kobayashi, S., Inukai, T., Yayama, T., Sato, R., Baba, H. (2008). Target muscles for retrograde gene delivery to specific spinal cord segments. Neuroscience Letters, 435(1), 1-6.
80. Nurputra, D. K., Lai, P. S., Harahap, N. I. F., Morikawa, S., Yamamoto, T., Nishimura, N., Nishio, H. (2013). Spinal Muscular Atrophy: From Gene Discovery to Clinical Trials. Annals of Human Genetics, 77, 435-463.
81. Pane, M. P., Staccioli, S. S., Messina, S. M., d'Amico, A. D., Pelliccioni, M. P., Mazzone, E. M., Mercuri, E. M. (2008). Daily salbutamol in young patients with SMA type II. Neuromuscular Disorders, 18(9-10), 762-762.
82. Parks, R. J., & Graham, F. L. (1997). A helper-dependent system for adenovirus vector production helps define a lower limit for efficient DNA packaging. Journal of Virology, 71(4), 3293-3298.
83. Pearn, J. (1978). Incidence, prevalence, and gene frequency studies of chronic childhood spinal muscular-atrophy. Journal of Medical Genetics, 15(6), 409-413.
84. Poulin, K. L., Lanthier, R. M., Smith, A. C., Christou, C., Quiroz, M. R., Powell, K. L., Parks, R. J. (2010). Retargeting of Adenovirus Vectors through Genetic Fusion of a Single-Chain or Single-Domain Antibody to Capsid Protein IX. Journal of Virology, 84(19), 10074-10086.
85. Ramakrishnaiah, V., Thumann, C., Fofana, I., Habersetzer, F., Pan, Q. W., de Ruiter, P. E.,van der Laan, L. J. W. (2013). Exosome-mediated transmission of hepatitis C virus between human hepatoma Huh7.5 cells. Proceedings of the National Academy of Sciences of the United States of America, 110(32), 13109-13113.
86. Ramteke, A., Ting, H., Agarwal, C., Mateen, S., Somasagara, R., Hussain, A., Graner, M., Frederick, B., Agarwal, R., Deep, G. (2013). Exosomes secreted under hypoxia enhance invasiveness and stemness of prostate cancer cells by targeting adherens junction molecules. Molecular Carcinogensis.

87. Raposo, G., Nijman, H. W., Stoorvogel, W., Leijendekker, R., Harding, C. V., Melief, C. J. M., & Geuze, H. J. (1996). B lymphocytes secrete antigen-presenting vesicles. Journal of Experimental Medicine, 183(3), 1161-1172.
88. Rochette, C. F., Surh, L. C., Ray, P. N., McAndrew, P. E., Prior, T. W., Burghes, A. H. M., Simard, L. R. (1997). Molecular diagnosis of non-deletion SMA patients using quantitative PCR of SMN exon 7. Neurogenetics, 1(2), 141-147.
89. Ross, P.J. and R.J. Parks. (2009). Construction and characterization of adenovirus vectors. CSH Protoc, (5), 149-165.
90. Rossoll, W., Jablonka, S., Andreassi, C., Kroning, A. K., Karle, K., Monani, U. R., & Sendtner, M. (2003). Smn, the spinal muscular atrophy-determining gene product, modulates axon growth and localization of beta-actin mRNA in growth cones of motoneurons. Journal of Cell Biology, 163(4), 801-812.
91. Rudnik-Schoneborn, S., Heller, R., Berg, C., Betzler, C., Grimm, T., Eggermann, T., Zerres, K. (2008). Congenital heart disease is a feature of severe infantile spinal muscular atrophy. Journal of Medical Genetics, 45(10), 635-638.
92. Russman, B. S. (2007). Spinal muscular atrophy: Clinical classification and disease heterogeneity. Journal of Child Neurology, 22(8), 946-951.
93. Salazar-Grueso, E. F., Kim, S., & Kim, H. (1991). Embryonic mouse spinal-cord motor neuron hybrid-cells. Neuroreport, 2(9), 505-508.
94. Sanchez, G., Dury, A. Y., Murray, L. M., Biondi, O., Tadesse, H., El Fatimy, R., Cote, J. (2013). A novel function for the survival motoneuron protein as a translational regulator. Human Molecular Genetics, 22(4), 668-684.
95. Saunderson, S. C., Schuberth, P. C., Dunn, A. C., Miller, L., Hock, B. D., MacKay, P. A., McLellan, A. D. (2008). Induction of exosome release in primary B cells stimulated via CD40 and the IL-4 receptor. Journal of Immunology, 180(12), 8146-8152.
96. Schmidt, P. M., Sparrow, L. G., Attwood, R. M., Xiao, X. W., Adams, T. E., & McKimm-Breschkin, J. L. (2012). Taking down the FLAG! How Insect Cell Expression Challenges an Established Tag-System. Plos One, 7(6).
97. Schneider, A., & Simons, M. (2013). Exosomes: vesicular carriers for intercellular communication in neurodegenerative disorders. Cell and Tissue Research, 352(1), 33-47.
98. Shayakhmetov, D. M., & Lieber, A. (2000). Dependence of adenovirus infectivity on length of the fiber shaft domain. Journal of Virology, 74(22), 10274-10286.
99. Simons, M., & Raposo, G. (2009). Exosomes - vesicular carriers for intercellular communication. Current Opinion in Cell Biology, 21(4), 575-581.
100. Strauss, K., Goebel, C., Runz, H., Mobius, W., Weiss, S., Feussner, I., Schneider, A. (2010). Exosome Secretion Ameliorates Lysosomal Storage of Cholesterol in Niemann-Pick Type C Disease. Journal of Biological Chemistry, 285(34), 26279-26288.
101. Suetsugu, A., Honma, K., Saji, S., Moriwaki, H., Ochiya, T., & Hoffman, R. M. (2013). Imaging exosome transfer from breast cancer cells to stroma at metastatic sites in orthotopic nude-mouse models. Advanced Drug Delivery Reviews, 65(3), 383-390.
102. Takahashi, Y., Nishikawa, M., Shinotsuka, H., Matsui, Y., Ohara, S., Imai, T., & Takakura, Y. (2013). Visualization and in vivo tracking of the exosomes of murine melanoma B16-BL6 cells in mice after intravenous injection. Journal of Biotechnology, 165(2), 77-84.
103. Théry, C., Amigorena, S., Raposo, G., Clayton, A. (2006). Isolation and characterization of exosomes from cell culture supernatants and biological fluids. Current Protocols in Cell Biology, 3.22.1-3.22.29.
104. Théry, C., Boussac, M., Veron, P., Ricciardi-Castagnoli, P., Raposo, G., Garin, J., & Amigorena, S. (2001). Proteomic analysis of dendritic cell-derived exosomes: A secreted subcellular compartment distinct from apoptotic vesicles. Journal of Immunology, 166(12), 7309-7318.

105. Théry, C., Duban, L., Segura, E., Veron, P., Lantz, O., & Amigorena, S. (2002). Indirect activation of naive CD4(+) T cells by dendritic cell-derived exosomes. Nature Immunology, 3(12), 1156-1162.
106. Ting, C. H., Wen, H. L., Liu, H. C., Hsieh-Li, H. M., Li, H., & Lin-Chao, S. (2012). The Spinal Muscular Atrophy Disease Protein SMN Is Linked to the Golgi Network. Plos One, 7(12).
107. Trams, E. G., Lauter, C. J., Salem, N., & Heine, U. (1981). Exfoliation of membrane ecto-enzyms in the form of micro-vesicles. Biochimica Et Biophysica Acta, 645(1), 63-70.
108. Valadi, H., Ekstrom, K., Bossios, A., Sjostrand, M., Lee, J. J., & Lotvall, J. O. (2007). Exosome-mediated transfer of mRNAs and microRNAs is a novel mechanism of genetic exchange between cells. Nature Cell Biology, 9(6), 654-U672.
109. Vanlandingham, P. A., & Ceresa, B. P. (2009). Rab7 Regulates Late Endocytic Trafficking Downstream of Multivesicular Body Biogenesis and Cargo Sequestration. Journal of Biological Chemistry, 284(18), 12110-12124.
110. Vellinga, J., Van der Heijdt, S., & Hoeben, R. C. (2005). The adenovirus capsid: major progress in minor proteins. Journal of General Virology, 86, 1581-1588.
111. Vidal, M., Mangeat, P., & Hoekstra, D. (1997). Aggregation reroutes molecules from a recycling to a vesicle-mediated secretion pathway during reticulocyte maturation. Journal of Cell Science, 110, 1867-1877.
112. Vlassov, A. V., Magdaleno, S., Setterquist, R., & Conrad, R. (2012). Exosomes: Current knowledge of their composition, biological functions, and diagnostic and therapeutic potentials. Biochimica Et Biophysica Acta-General Subjects, 1820(7), 940-948.
113. Wang, L., Takabet, K., Bidlingmaier, S. M., Ill C. R., Verma, I. M. (1999). Sustained correction of bleeding disorder in hemophilia B mice by gene therapy. Medical Sciences, 96, 3906–3910.
114. Willemsen, K. (2009). Improving adenoviral vectors for muscle-directed gene therapy, in Biochemistry, Microbiology and Immunology. University of Ottawa: Ottawa, 145.
115. Wu, E., Pache, L., Von Seggern, D. J., Mullen, T. M., Mikyas, Y., Stewart, P. L., & Nemerow, G. R. (2003). Flexibility of the adenovirus fiber is required for efficient receptor interaction. Journal of Virology, 77(13), 7225-7235.
116. Yamamoto, M., & Curiel, D. T. (2010). Current Issues and Future Directions of Oncolytic Adenoviruses. Molecular Therapy, 18(2), 243-250.
117. Yoshioka, Y., Konishi, Y., Kosaka, N., Katsuda, T., Kato, T., Ochiya, T. (2013). Comparative marker analysis of extracellular vesicles in different human cancer types. Journal of Extracellular vesicles, 18;2.
118. Young, P. J., Le, T. T., Dunckley, M., Man, N. T., Burghes, A. H. M., & Morris, G. E. (2001). Nuclear gems and cajal (coiled) bodies in fetal tissues: Nucleolar distribution of the spinal muscular atrophy protein, SMN. Experimental Cell Research, 265(2), 252-261.
119. Zhang, Y. M., & Bergelson, J. M. (2005). Adenovirus receptors. Journal of Virology, 79(19), 12125-12131.
120. Zhang, Z., Lotti, F., Dittmar, K., Younis, I., Wan, L., Kasim, M., & Dreyfuss, G. (2008). SMN deficiency causes tissue-specific perturbations in the repertoire of snRNAs and widespread defects in splicing. Cell, 133(4), 585-600.

7. Appendix 1 – Chemicals and Reagents

Cell culture

- Complete medium:
  - MEM or DMEM (Life Technologies)
  - 10% FBS (Sigma)
  - 1% antibiotic/antimycotic (Life Technologies)
    0.1 mg/ml streptomycin and 100 U/ml penicillin
  - 1% glutamax (Life Technologies)

- Differentiation medium: DMEM (Life Technologies)
  - 2% horse serum (Life Technologies)
  - 1% antibiotic/antimycotic (Life Technologies)
  - 1% glutamax (Life Technologies)

- Hygromycin medium:
  - MEM (Life Technologies)
  - 10% FBS (Sigma)
  - 150 mg hygromycin (Invitrogen)
  - 1% antibiotic/antimycotic (Life Technologies)
  - 1% glutamax (Life Technologies)

- Unmodified MEM:
  - MEM (Life Technologies)

- 10x Citric Saline:
  - 1.35 M KCl (Fisher)
  - 150 mM sodium citrate (Fisher)
  - In ddH_2O, autoclave 45 minutes at 121^0C

- 1x Citric Saline:
  - 50 mL 10x citric saline in 500 mL ddH_2O

- 1x Trypsin:
  - 20 mL 10x Trypsin (Life Technologies)
  - In 200 mL PBS (Sigma)

Particle count

- Assay solution:
  - 1 mM EDTA, (Fisher)
  - 0.1% SDS (Fisher)

TCA media precipitation

- 100% Trichloroacetic acid (Sigma-Aldrich)

Tissues

- RIPA buffer:
  - 0.5% sodium deoxycholate (Fisher)
  - 100 mM NaCl (Fisher)
  - 50 mM Tris pH8 (Fisher)
  - 0.1% SDS (Fisher)

- 20% PFA stock:
  - 20% PFA in RNAse-free H_2O (BDH)

- 2% PFA fixative:
  - 10 mL of 20% PFA
  - 81 mM Na_2HPO_4 (Sigma-Aldrich)
  - 19 mM NaH_2PO_4 (Sigma-Aldrich)
  - 2 mM $MgCl_2$ (BDH)
  - 1.25 mM Ethylene glycol tetraacetic acid pH 7.4 (Sigma-Aldrich)

- X-gal Stain:
  - 39 mL X-gal wash buffer
  - 4% X-gal stock (Fisher)
  - 0.2% Potassium ferrocyanide (BDH)
  - 0.15% Potassium ferricyanide (BDH)

- X-gal wash buffer:
  - 2 mM $MgCl_2$ (BDH)
  - 1% sodium deoxycholate (Fisher)
  - 2% NP-40 (GBioSciences)
  - 97.8 mM Phosphate buffer

- Phosphate buffer:
  - 23 mM Na_2HPO_4 (Sigma-Aldrich)
  - 77 mM NaH_2PO_4 (Sigma-Aldrich)

Immunofluorescence

- 4% PFA fix:
  - 4% formaldehyde (Sigma-Aldrich)
  - In PBS

- BSA Blocking buffer:
  - 0.5% BSA (Sigma)
  - 0.4% Triton X-100 (Fisher)
  - In PBS

Western Blot

- 2x Laemmli loading dye (LD):
  - 62.5 mM Tris-HCl pH6.8 (Fisher)
  - 25% glycerol (Fisher)
  - 2% SDS (Fisher)
  - 0.01 g bromophenol blue (EM Science)
  - 5% β-mercaptoethanol (Fisher)

- Stacking Solution:
  - 50% 2x Stacking Buffer
  - 3.75% Acrylamide (Fisher)
  - 0.016% Ammonium persulfate (Fisher)
  - 0.16% N,N,N’,N’,-tetramethylethylenediamine (Sigma-Aldrich)
  - In ddH_2O

- 2x Stacking Buffer:
  - 250 mM Tris-HCL pH 6.8 (Fisher)
  - 0.2% SDS (Fisher)

- 12% Separating Solution: - 49.5% 2x Separating Buffer
  - 8.9% Acrylamide (Fisher)
  - 0.09% Ammonium persulfate (Fisher)
  - 0.1% N,N,N',N',-tetramethylethylenediamine (Sigma-Aldrich)
  - In ddH_2O

- 15% Separating Solution: - 49.5% 2x Separating Buffer
  - 11.2% Acrylamide (Fisher)
  - 0.09% Ammonium persulfate (Fisher)
  - 0.1% N,N,N',N',-tetramethylethylenediamine (Sigma-Aldrich)
  - In ddH_2O

- 2x Separating Buffer: - 750 mM Tris-HCl pH 8.8 (Fisher)
  - 0.2% SDS (Fisher)

- Running Buffer: - 1.44% glycine (Fisher)
  - 0.1% SDS (Fisher)
  - 50 mM Tris-HCl (Fisher)

- Transfer Buffer (Semi Dry): - 0.293% glycine (Fisher)
  - 20% MeOH (Fisher)
  - 0.0375% SDS (Fisher)
  - 48 mM Tris-HCl (Fisher)

- Wash buffer (0.1% TBST): - 0.1% TWEEN-20 (Fisher)
  - 150 mM NaCl (Fisher)
  - 10 mM Tris-HCl pH 8.0 (Fisher)

- Milk Blocking Solution: - 5% skim milk powder
  - In 0.1% TBST

Virology 468-470 (2014) 444–453

Contents lists available at ScienceDirect

Virology

journal homepage: www.elsevier.com/locate/yviro

A reduction in the human adenovirus virion size through use of a shortened fibre protein does not enhance muscle transduction following systemic or localised delivery in mice

Emily R. McFall [a,b], Lyndsay M. Murray [a,1], John A. Lunde [c], Bernard J. Jasmin [c,d], Rashmi Kothary [a,c,d,e], Robin J. Parks [a,b,d,e,*]

[a] Regenerative Medicine Program, Ottawa Hospital Research Institute, Ottawa, Ontario, Canada K1H 8L6
[b] Department of Biochemistry, Microbiology and Immunology, University of Ottawa, Ottawa, Ontario, Canada
[c] Department of Cellular and Molecular Medicine, University of Ottawa, Ottawa, Ontario, Canada
[d] University of Ottawa Centre for Neuromuscular Disease, Ottawa, Ontario, Canada
[e] Department of Medicine, University of Ottawa, Ottawa, Ontario, Canada

ARTICLE INFO

Article history:
Received 17 June 2014
Returned to author for revisions
28 July 2014
Accepted 22 August 2014
Available online 20 September 2014

Keywords:
Adenovirus
Transduction
Viral vector
Muscle

ABSTRACT

We have investigated whether reducing the overall size of adenovirus (Ad), through use of a vector containing a shortened fibre, leads to enhanced distribution and dissemination of the vector. Intravenous or intraperitoneal injection of Ad5SlacZ (12 nm fibre *versus* the normal Ad5 37 nm fibre) or Ad5SpKlacZ (shortened fibre with polylysine motif in the *H–I* loop of fibre knob domain) led to similar levels of lacZ expression compared to Ad5LlacZ (native Ad5 fibre) in the liver of treated animals, but did not enhance extravasation into the tibialis anterior muscle. Direct injection of the short-fibre vectors into the tibialis anterior muscle did not result in enhanced spread of the vector through muscle tissue, and led to only sporadic transgene expression in the spinal cord, suggesting that modifying the fibre length or redirecting viral infection to a more common cell surface receptor does not enhance motor neuron uptake or retrograde transport.

Introduction

Human adenovirus (Ad) is the most common platform for delivery of therapeutic genes in gene therapy applications, and has been used in approximately 23% of all human clinical trials to date (Ginn et al., 2013). Ad has many advantages that have allowed it to become so widely utilised. Deletion of the Ad early region 1 (E1) renders the vector replication defective and together with additional deletion of the non-essential E3 region provides a relatively large cloning capacity of ~8 kb (Bett et al., 1993). Ad vectors devoid of all viral protein sequences, termed helper-dependent Ad (Palmer and Ng, 2005; Parks et al., 1996), further increase this cloning limit to ~36 kb (Parks and Graham, 1997). Ad vectors remain predominantly episomal in transduced cells (Harui et al., 1999; Hillgenberg et al., 2001; Jager and Ehrhardt, 2009; Stephen et al., 2010; Wong et al., 2013), greatly reducing the risk of insertional inactivation or activation of cellular genes. Ad has a relatively good safety profile (Amalfitano and Parks, 2002), although at very high doses Ad can cause acute inflammation and toxicity, which can be lethal (Brunetti-Pierri et al., 2004; Morral et al., 2002; Raper et al., 2003). Upon systemic delivery in most species, human Ad serotype 5 (the most commonly used subtype) preferentially accumulates in the liver (Guo et al., 1996; Nicol et al., 2004; Worgall et al., 1997). This preferential uptake in the liver is due in part to the physical architecture of this tissue (Ad becomes trapped in the liver sinusoids and fenestrations (Bernt et al., 2003; Ross and Parks, 2003)), and the rapid scavenging of Ad vectors by Kupffer cells in the liver triggers a robust pro-inflammatory cytokine response (Lieber et al., 1997; Muruve et al., 1999). A unique mechanism of Ad5 uptake in liver hepatocytes also contributes to Ad-induced inflammation. The Ad5 hexon protein interacts with coagulation factor X which provides a bridging interaction for binding to heparan sulphate proteoglycans expressed on the surface of hepatocytes, allowing internalisation (Alba et al., 2012; Bradshaw et al., 2010; Kalyuzhniy et al., 2008; Waddington et al., 2008). Detection of internalised Ad-associated factor X by toll-like receptor 4 in the endosome triggers an innate immune response and inflammatory signalling (Doronin

* Corresponding author at: Regenerative Medicine Program, Ottawa Hospital Research Institute, 501 Smyth Road, Room C4115, Ottawa, Ontario, Canada, K1H 8L6. Tel.: +1 613 737 8123; fax: +1 613 737 8803.
E-mail address: rparks@ohri.ca (R.J. Parks).
[1] Current Address: Centre for Integrative Physiology, and the Euan MacDonald Centre for Motor Neurone Disease Research, University of Edinburgh, Edinburgh, UK.

http://dx.doi.org/10.1016/j.virol.2014.08.026

et al., 2012). However, Ad vectors containing mutations in the hexon protein that prevent its interaction with factor X still localise to the liver, although uptake by hepatocytes is dramatically reduced (Alba et al., 2010; Kalyuzhniy et al., 2008). These results suggest that physical constraints, other than receptor binding, contribute significantly to vector biodistribution.

The virion of Ad5 is a non-enveloped icosahedral capsid with a diameter of ~95 nm (for the main "body" of the virion, measured vertex to vertex), and is composed of three major (II, III, and IV) and five minor (IIIa, IVa2, VI, VIII, and IX) polypeptides (Berk, 2007; San Martin, 2012). Protein IV, more commonly known as fibre, forms trimers that project from the capsid surface at each of the 12 vertices, and is the viral protein predominantly responsible for interacting and binding to the cell surface through the coxsackie–adenovirus receptor (CAR) (Bergelson et al., 1997, 1998). For Ad5, the fibre protein is 37 nm in length (Ruigrok et al., 1990; van Raaij et al., 1999), thus increasing the overall size of the virus to about ~169 nm. Other human serotypes differ in the length of fibre and the cell surface proteins with which they interact, which can significantly influence the cell types that they preferentially infect (Havenga et al., 2002). For example, the Ad35 fibre protein is only 13 nm in length (for an overall virion size of ~110 nm), and binds CD46 rather than CAR (Gaggar et al., 2003; Saban et al., 2005). The ability of Ad to infect is intimately tied to its ability to bind to the target cell. Cells with no or low levels of either the primary or secondary Ad5 receptors are transduced at a greatly reduced frequency (Goldman et al., 1996; Nalbantoglu et al., 1999). CAR is frequently developmentally downregulated, thus reducing Ad infection efficiency of mature tissues such as muscle and neurons (Ahn et al., 2008; Nalbantoglu et al., 1999). Indeed, numerous groups have improved Ad transduction of a variety of cell types and tissues through introducing protein motifs into the fibre protein that redirect attachment to cell surface receptors prevalent on most cells, such as a poly-lysine motif which allows Ad to bind heparan sulphate proteoglycans (Bramson et al., 2004; Wickham et al., 1997).

The preferential accumulation of Ad in the liver of treated animals has meant that many of the gene therapy "successes" when using Ad in animal models involve transduction of the liver either to restore a functional deficiency to hepatocytes, or to use this organ as a protein production factory to produce large amounts of secreted protein (Brunetti-Pierri and Ng, 2011). Use of Ad for therapy in other tissues has not been as successful. For example, since Ad does not efficiently extravasate from vasculature (Su et al., 2005), localised injections are required for efficient delivery to skeletal muscle (Quantin et al., 1992), unlike adeno-associated virus-based vectors which can escape circulation and transduce into all muscle groups after systemic delivery (Gregorevic et al., 2004). Even after direct skeletal muscle injection, Ad remains relatively localised and does not disperse within the muscle (Meulenbroek et al., 2004; Quantin et al., 1992). Thus, improvements in Ad vector design are necessary to improve Ad utility for treating diseases of tissues other than liver.

In this study, we asked whether decreasing the overall size of the Ad vector, through substitution of the native Ad5 fibre with a chimeric fibre containing the shorter shaft region from Ad9 (37 *versus* 12 nm fibre, respectively) could enhance the ability of Ad to extravasate from the vasculature into surrounding tissues, or improve spread after direct injection in muscle. This reduction in fibre length results in a 30% decrease in the overall diameter of the virus. We also address whether addition of a pK motif on the knob domain of the shortened fibre, to redirect infection to more ubiquitous cell surface receptors, also enhanced vector distribution, relative to vector containing the wildtype Ad5 fibre protein.

Results and discussion

Rationale and viral constructs

Ad-based vectors have a poor ability to extravasate into surrounding tissue after systemic delivery and also a poor ability to disperse beyond the site of injection after localised delivery in most tissues. In part, the inability to spread is due to the relatively large size of the Ad virion, which for Ad5 is approximately 169 nm. For comparison, AAV6, which can effectively spread to all tissues following systemic delivery (Gregorevic et al., 2004), is ~25 nm in diameter. We therefore investigated whether reducing the overall size of the Ad vector, by decreasing the length of the fibre protein, could enhance its dispersion in mice. We generated an Ad vector containing the short Ad9 shaft region of fibre fused to the native Ad5 fibre knob domain (Shayakhmetov and Lieber, 2000), designated Ad5SlacZ, which decreased the overall size of the virus by ~30% relative to a normal Ad5-based vector (Ad5LlacZ) (Fig. 1A). Since the natural receptor for Ad, CAR, is downregulated on many mature tissues, we also designed a derivative of Ad5SlacZ which contained a poly-lysine motif in the *HI* loop of the knob domain,

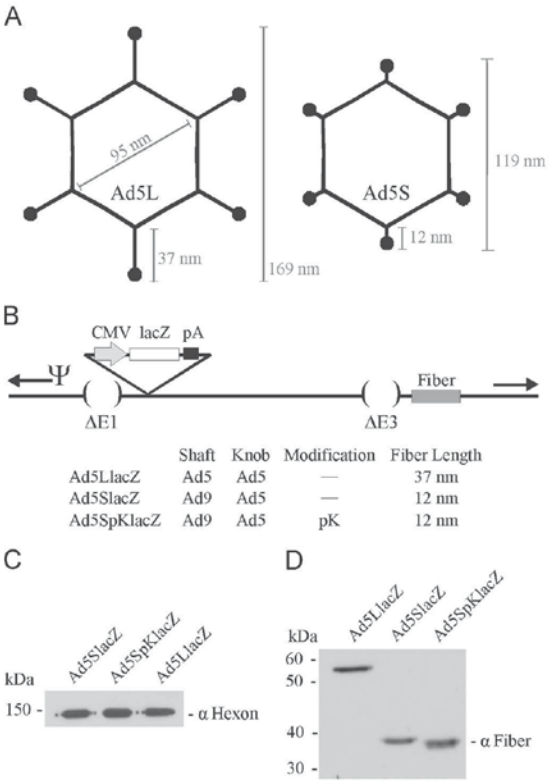

Fig. 1. Adenovirus vectors used in this study. Panel A: wildtype Ad5 has a fibre length of ~37 nm which, together with the main virion size of 95 nm, provide an overall virion diameter of 169 nm. Substitution of the Ad5 shaft region for that of Ad9 reduces the length of fibre to ~12 nm, and reduces the overall virion diameter to 119 nm, or 30% smaller than Ad5. Viruses are drawn to approximate scale. Panel B: all viruses are deleted of the Ad early region 1 (E1) and E3, and encode the *E. coli lacZ* gene under the regulation of the human cytomegalovirus (CMV) immediate early enhancer/promoter and bovine growth hormone polyadenylation sequence (pA). Ad5SpKlacZ also contains a polylysine motif within the *HI* loop of the knob domain of fibre. Panels C and D: virus particles (10^9) were lysed in SDS–protein loading buffer, separated by SDS–PAGE, and the amount of hexon (Panel C) and fibre (Panel D) was determined by immunoblot.

designated Ad5SpKlacZ. Attachment for this virus occurs through binding to heparan sulphate proteoglycans which are present on the surface of most cells. Ad5SpKlacZ is not ablated for binding to CAR. All of these viruses are deleted of the Ad E1 and E3 regions, and encode the *Escherichia coli lacZ* gene under regulation by the human cytomegalovirus immediate early enhancer/promoter and bovine growth hormone polyadenylation sequence (Fig. 1B). These viruses were tested in tissue culture and mice for enhanced uptake and dispersion to a number of specific tissues.

All three viruses grew well and gave a similar yield upon large scale virus purification (data not shown). Since the viruses may have different inherent ability to infect cells, including the 293 cell lines typically used for virus titering, we quantified the amount of virus by particle count and verified the accuracy of the particle counts by analysing the same number of particles of each virus by immunoblot. Similar signal intensity was obtained for each virus (Fig. 1C). We also verified the size of the fibre protein for each of these viruses (Fig. 1D).

Infection of cell lines in vitro

We next compared the ability of the viruses to infect several different common cell lines derived from specific tissues: A549 (human lung adenocarcinoma), MN1 (rat motor neuron-like), and undifferentiated or differentiated C2C12 (mouse myoblasts). Cells grown in 35 mm dishes were infected in triplicate with an MOI of 10, and cell lysates were assayed 24 h postinfection for β-gal activity using a chemiluminescence assay. All viruses infected A549 cells with very high efficiency, and gave rise to β-gal activity significantly above background (Fig. 2A), which is perhaps not surprising given the high-level of expression of CAR on these cells (Hidaka et al., 1999). Substituting the long fibre shaft of Ad5 for the short shaft of Ad9 reduced the infection efficiency of A549 cells by about 10-fold, but addition of the pK motif to the short-fibre virus restored the infection level, as gauged by β-gal activity, to that of native Ad5 fibre.

In the motor neuron-like MN1 cells, expression from all viruses was equal and approximately 10-fold higher than background, but the overall level of β-gal activity was approximately 10- to 100-fold lower than that observed in A549 cells (Fig. 2B). This latter observation is consistent with the apparent developmental down-regulation of CAR expression in spinal cord of mice (Hotta et al., 2003) and with our previous data showing that Ad5 does not infect MN1 cells well (Goulet et al., 2013b). Addition of the pK motif on the Ad5S knob did not enhance infection of MN1 cells. Similar to A549 cells, viruses infected both undifferentiated and differentiated C2C12 cells with very high efficiency, and cells treated with the vector containing the native Ad fibre showed an approximately 10 fold higher level of β-gal activity than the other viruses (Fig. 2C and D).

Virus infection in vivo

To examine whether reducing the length of fibre protein, and thus the overall size of the virus, enhanced extravasation into surrounding tissue, we evaluated β-galactosidase expression in liver (a site for high level uptake of virus, regardless of injection route) and in TA muscle by chemiluminescence activity assay (Fig. 3). We used three doses of virus: 5×10^{11} VP/kg (low), 1×10^{12} VP/kg (middle) and 5×10^{12} VP/kg (high), and either IP

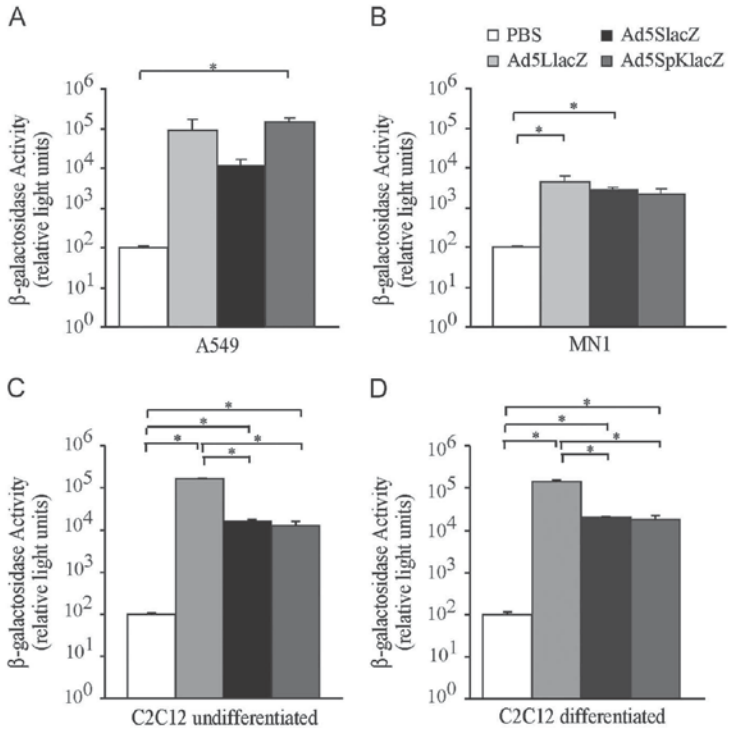

Fig. 2. Analysis of transgene expression from Ad5LlacZ, Ad5SlacZ and Ad5SpKlacZ in tissue culture. A549 (Panel A), MN1 (Panel B) or undifferentiated (Panel C) or differentiated (Panel D) C2C12 cells in 35 mm dishes were infected at a multiplicity of infection (MOI) of 10 with Ad5LlacZ, Ad5SlacZ and Ad5SpKlacZ and, 24 h later, crude protein extracts were prepared and assayed for β-gal activity using a commercial chemiluminescent assay. Data is shown as average and standard deviation of the mean ($n=3$). *$=p<0.05$.

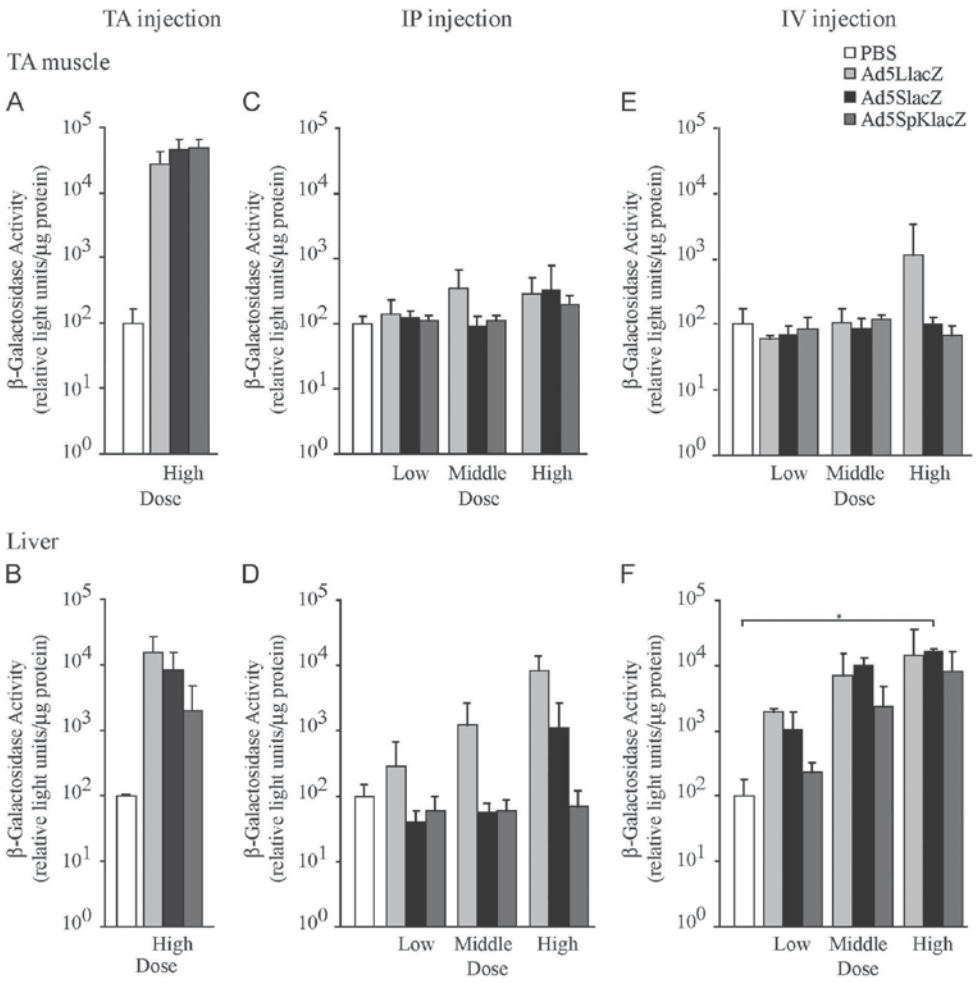

Fig. 3. Analysis of transgene expression from Ad5LlacZ, Ad5SlacZ and Ad5SpKlacZ in TA muscle and liver after *in vivo* vector administration. Mice (n=2–3 per treatment) were injected with a low (5×10^{11} VP/kg), middle (1×10^{12} VP/kg) or high (5×10^{12} VP/kg) dose of Ad5LlacZ, Ad5SlacZ, Ad5SpKlacZ, or PBS by direct TA injection (Panels A and B) or systemically by intraperitoneal (IP, Panels C and D), or intravenous (IV, Panels E and F) injection. 24 h post-injection, the TA muscle and liver were removed, processed, and assayed for β-gal activity (normalised to μg of protein in the sample). Average and standard deviation of the mean are shown, *=$p < 0.05$.

or IV injection. As a control, we injected the TA muscle directly with the highest dose of the three viruses. The data shows that the viruses were capable of infecting muscle and gave rise to very high levels of β-galactosidase activity (Fig. 3A). Of note, when normalised to the amount of protein in the sample, after direct TA muscle injection, approximately 20% of the β-gal activity was detected in the liver (Fig. 3B), suggesting there is significant escape from the site of injection to the liver. IP injection of the three viruses led to only a modest increase in β-gal activity in the TA muscle at the highest virus dose (Fig. 3C), and a dose dependent increase in expression in the liver for Ad5SlacZ and Ad5LlacZ (Fig. 3D). Interestingly, after IP injection, no liver expression was observed for Ad5SpKlacZ, regardless of dose, suggesting that the virus may efficiently and preferentially infect the peritoneum and is not available for infection elsewhere. IV injection of the viruses did not result in a significant increase in β-gal activity in the TA muscle, with the exception of the highest dose of Ad5LlacZ (Fig. 3E). For all viruses, following IV injection there was a significant dose-dependent increase in β-gal activity in the liver of treated animals, with an approximately equal level of expression for all viruses (Fig. 3F).

We also examined β-gal expression by histochemistry in tissue sections of TA muscle after TA, IP or IV injection of the viruses (Fig. 4). Mice were injected with the highest dose of virus (5×10^{12} VP/kg), the tissue was isolated 24 h later, fixed, sectioned and stained for β-gal activity. For the TA muscle, representative images from the top, middle and bottom of the muscle are shown. Consistent with our chemiluminesence activity assays, we observed significant levels of β-gal activity after direct injection of the three viruses into the TA muscle, but very limited expression after IP or IV injection (Fig. 4). Thus, systemic delivery of either Ad vector containing wildtype fibre or a shortened fibre does not lead to enhanced transduction of muscle.

Dispersion of virus after TA muscle injection

We next examined whether a decrease in virus size resulted in improved dispersion throughout the muscle following TA

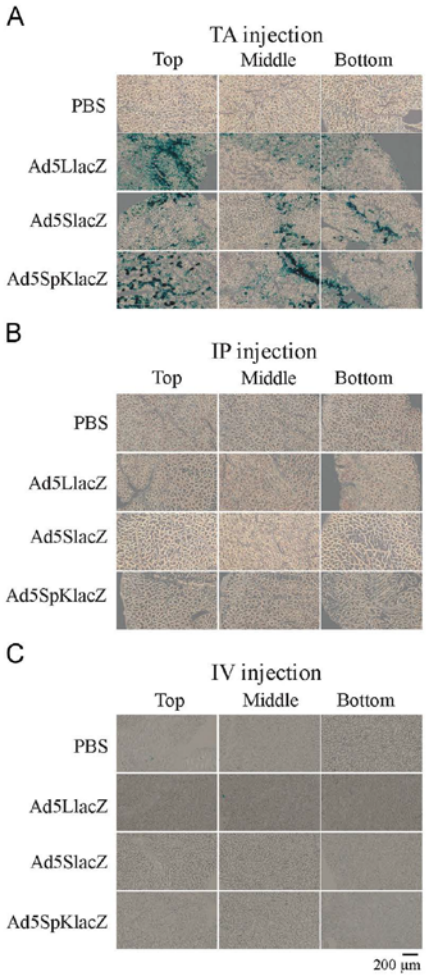

Fig. 4. Histological analysis of β-gal expression in the TA muscle of treated animals. Mice were treated with 5×10^{12} VP/kg of Ad5LlacZ, Ad5SlacZ and Ad5SpKlacZ by direct TA injection or systemically by intraperitoneal (IP) or intravenous (IV) injection. The TA muscle was removed 24 h post-treatment, fixed, sectioned and stained for β-gal activity. Sections were viewed using an AxioCam Axiophot2 light microscope at 10× magnification.

injection. To examine the kinetics of expression, mice were injected in the TA muscle with our highest dose of vector (5×10^{12} VP/kg), and expression analysed in muscle and liver at 1, 2 and 3 days post-injection. In the TA muscle, all viruses produced a level of β-gal activity approximately 100-fold above background, and expression was relatively stable over the 3-day time course (Fig. 5A). In contrast, β-gal activity in the liver was highest at day 1, and steadily declined by about 1 log over the next 2 days, with all three viruses showing a similar trend (Fig. 5B). This latter observation is consistent with previous studies that have shown a robust anti-Ad inflammatory response in liver, in part due to uptake and activation of liver Kupffer cells, leading to a dramatic reduction in viral genomes within the first 24 hpi, and a more gradual decline over the next several days (Lieber et al., 1997; Wolff et al., 1997; Worgall et al., 1997). Histochemical analysis of TA muscle sections from treated mice showed that all viruses resulted in a significant level of β-gal activity (Fig. 5C), with no significant difference in the per cent of the cross sectional area transduced by each virus (Table 1). These results suggest that reducing the size of the virus, through reduced fibre length, does not significantly alter dispersion of the virus in muscle after localised delivery.

Retrograde transport of Ad to the spinal cord after TA muscle injection is inefficient

Studies in rats have shown that injection of muscle with Ad can lead to efficient retrograde transport of the virus to motor neuron cell bodies in the spinal cord (Baumgartner and Shine, 1998; Ghadge et al., 1995; Nakajima et al., 2008). Retrograde transport has also been observed for a number of different viral vectors including adeno-associated virus (Bockstael et al., 2011) and lentivirus (Hirano et al., 2013). To determine if our modified viruses demonstrated altered retrograde transport, we injected TA muscle with 5×10^{12} VP/kg of the various viruses in a solution containing Texas-Red conjugated Dextran. Dextran is taken up by motor neurons, which would fluoresce red, and allows us to identify the appropriate region of the spinal cord for β-gal staining (Nance and Burns, 1990). Spinal cords from treated mice were sectioned until fluorescent motor neurons were visible (Fig. 6A), and the next adjacent section was stained with X-gal to visualise the efficiency of Ad transduction. As shown in Fig. 6B, we only observed sparse and sporadic expression of β-gal in motor neurons, regardless of virus identity. These results suggest that the efficiency of uptake and retrograde transport of Ad in mice is low, and is not improved by reduced fibre size or the presence of a heparan sulphate proteoglycan binding region on the fibre knob. Given that Ad does not infect motor neuron-like cells in culture very efficiently (Fig. 2B), it is perhaps not surprising that the efficiency of uptake and transduction of motor neurons *in vivo* is low. An enhancement in motor neuron uptake may be achieved through introduction of peptide motifs into the Ad capsid that specifically target infection to neurons (Poulin et al., 2011; Terashima et al., 2009), but this has yet to be examined. Alternatively, canine adenovirus has shown an enhanced ability to infect neurons and undergo retrograde transport (Soudais et al., 2001), suggesting it may be more amenable for the treatment of diseases of the motor neuron such as spinal muscular atrophy or amyotrophic lateral sclerosis (Goulet et al., 2013a; San Sebastian et al., 2013).

In this study, we have examined whether reducing the size of the adenovirus vector, through reduction in the length of the fibre protein, could result in enhanced delivery and distribution to muscle after systemic delivery. In general, reduction in the size of the fibre protein, with or without a polylysine motif to redirect virus binding to cell surface heparan sulphate proteoglycans, had little effect on enhancing muscle cell transduction following systemic or localised delivery. Previous studies have suggested that the Ad2 fibre protein, which is very similar to the Ad5 fibre protein, may naturally bend, which would effectively reduce the overall diameter of Ad5LlacZ to closer to that of Ad5SlacZ. The Ad2 (and Ad5) fibre protein shaft region contains 22 β-repeats. The twenty-first repeat, located just before the knob domain, is a non-consensus repeat that may allow for a small degree of bending between knob and shaft (van Raaij et al., 1999). More importantly, the third β-repeat is also non-consensus, and may provide significant flexibility to the fibre protein. In cryo-EM images, Ad2 fibre appears "kinked" in this approximate region (Chiu et al., 2001; Stewart et al., 1997). Replacing these flexible repeats with the corresponding regions of the more rigid fibre from Ad37 abolished infection suggesting that bending of fibre does occur naturally and is important for Ad5 infection (Wu et al., 2003). Molecular modelling showed that the fibre protein would need to bend at an angle of at least ~70° to allow proper alignment of the RGD motif contained in penton protein with surface exposed integrins (Wu et al., 2003). If fibre is capable of folding back

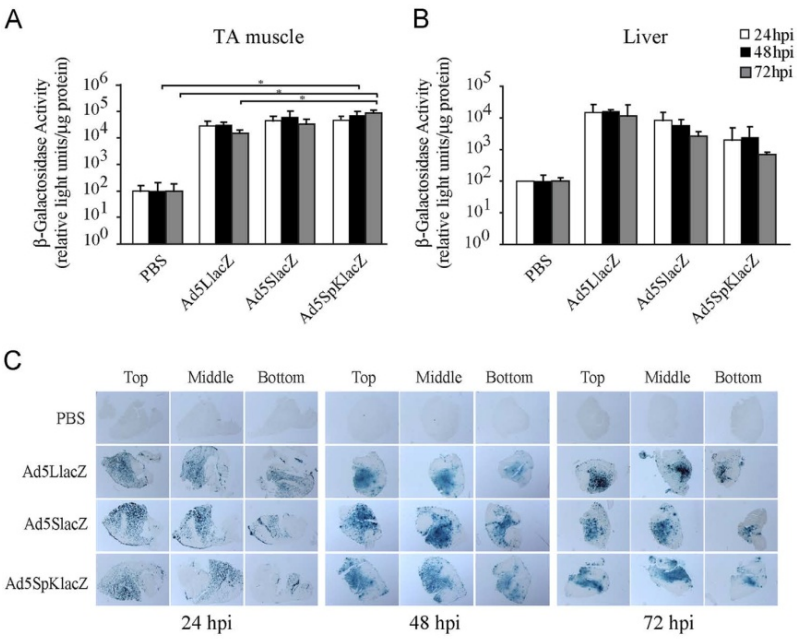

Fig. 5. Kinetics and area of transgene expression in the TA muscle of treated mice. Mice were injected in the TA muscle with 5×10^{12} VP/kg of Ad5LlacZ, Ad5SlacZ and Ad5SpKlacZ, and the TA muscle and liver was removed at 1, 2 or 3 days post-injection. Muscle (Panel A) and liver (Panel B) were processed and analysed for β-gal activity by chemiluminescence assay. Shown is the average and standard deviation ($n=2$–3), $^*p < 0.05$. Panel C: TA muscles were processed for histology to examine β-gal expression.

Table 1
Area[a] of TA muscle expressing β-gal following TA injection.

	Ad5LlacZ			Ad5SlacZ			Ad5SpKlacZ		
	Top	Middle	Bottom	Top	Middle	Bottom	Top	Middle	Bottom
24 h	25.1 ± 6.5	25.5 ± 4.2	35.9 ± 23.5	18.4 ± 10.7	20.4 ± 0.8	14.1 ± 5.1	20.6 ± 1.6	16.7 ± 1.4	21.3 ± 22.6
48 h	27.0 ± 13.4	25.0 ± 14.6	22.1 ± 11.8	42.1 ± 1.2	43.1 ± 3.6	21.9 ± 11.7	31.6 ± 12.5	28.2 ± 15.5	21.7 ± 21.7
72 h	20.0 ± 16.9	17.3 ± 10.6	13.3 ± 9.1	26.1 ± 5.1	21.8 ± 18.2	9.7 ± 8.6	30.9 ± 3.4	26.7 ± 18.1	9.9 ± 7.7

[a] Images from stained sections were analysed using Image J. A colour intensity threshold was applied to determine the area of the muscle section showing X-gal staining, which is reported as the percentage of the total cross-sectional area of the muscle.

towards the body of the Ad virion at such an acute angle, it would reduce the distance that the Ad5 fibre protrudes from the main body of the Ad virion from 37 nm to only ~16 nm. Short fibre shaft proteins, such as that of Ad9 used in this study, are predicted to be rigid (Chiu et al., 2001). Thus, the effective difference in length of the short and long fibre proteins used in this study may not be dramatically different, which could contribute to the similar transduction profiles observed for these viruses.

Another factor that could contribute to the similar transduction efficiencies of Ad5SlacZ and Ad5LlacZ may be the impact of the negative charge conferred on the virion by the Ad5 hexon protein. As discussed by Shayakhmetov and Lieber (2000), the surface exposed hypervariable regions of hexon from Ad serotypes with naturally short fibre proteins tend to be neutral or positively charged (Crawford-Miksza and Schnurr, 1996), allowing for the relatively close apposition of the Ad virion and negatively-charged cell membrane. In contrast, the hypervariable regions on the Ad5 hexon have a strong negative charge that may act as a significant repulsive force when combined with the short fibre protein, compromising efficient interaction of virus with the cell (Shayakhmetov and Lieber, 2000).

As others have also shown (Guo et al., 1996; Worgall et al., 1997), we observed that regardless of the route of administration, Ad naturally preferentially accumulates in the liver, leading to high level gene expression in this tissue. Many of the successes in preclinical studies using Ad-mediated gene transfer involve diseases of the liver or use the liver as a protein-production factory for secreted protein (Brunetti-Pierri and Ng, 2011). Ad vectors have a natural tropism for liver and can persist and express a transgene for greater than 7 years after a single IV injection in non-human primates (Brunetti-Pierri et al., 2013). However, as demonstrated in this study, use of Ad vectors to target gene expression to alternative tissues remains a challenging aspect of Ad vector development.

Materials and methods

Cell culture

All cell culture media and reagents were obtained from Invitrogen (Burlington, ON). 293 (Graham et al., 1977), 293N3S (Graham, 1987) and A549 (American Type Culture Collection) cells were grown in monolayer in minimum essential medium (MEM) supplemented with 2 mM Glutamax, 0.1 mg/ml streptomycin and 100 U/ml penicillin, and 10% foetal bovine serum (FBS). MN1 cells

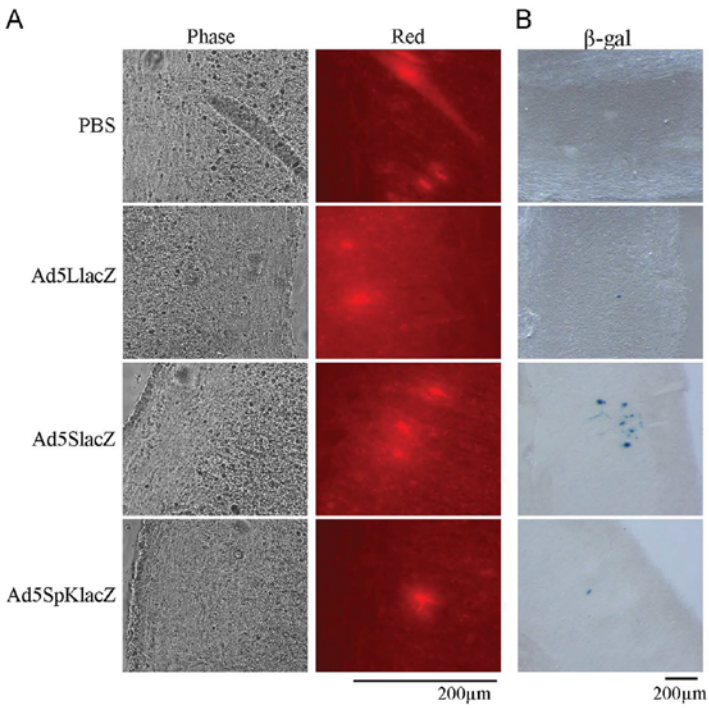

Fig. 6. Inefficient retrograde transport of Ad vectors in motor neurons after TA muscle injection in mice. Mice were injected in the TA muscle with 5×10^{12} VP/kg of Ad5LlacZ, Ad5SlacZ and Ad5SpKlacZ in a solution containing 16 mg/ml Texas Red-conjugated Dextran. Spinal cords were removed 48 h post-injection, fixed, and longitudinal sections were collected until motor neurons were detected by immunofluorescence. The next sequential section was then stained for β-gal activity, and viewed using a Leica M80 microscope.

(Salazar-Grueso et al., 1991) were maintained in Dulbecco's modified Eagle's medium (DMEM, Sigma-Aldrich) supplemented with 10% FBS, 2 mM L-Glutamax, 0.1 mg/ml streptomycin and 100 U/ml penicillin, and were a kind gift of Dr. Jocelyn Cote (University of Ottawa). C2C12 cells (Blau et al., 1985) were grown in DMEM supplemented with 10% FBS, 2 mM L-glutamine, 0.1 mg/ml streptomycin and 100 U/ml penicillin, and confluent plates were switched to medium supplemented with 2% horse serum to induce differentiation. C2C12 cells were allowed to differentiate for 4 days before infection.

Generation and propagation of viruses

All of the viruses used in this study are deleted of the Ad5 early region 1 (E1) and E3 regions, and were generated and propagated using standard techniques (Ross and Parks, 2009). A plasmid containing an Ad5 genome encoding a modified fibre protein with the Ad9 shaft and Ad5 knob was obtained from Drs. Dmitry Shayakhmetov and Andre Lieber (University of Washington) (Shayakhmetov and Lieber, 2000). The modified fibre gene was subcloned into an E1/E3-deleted Ad genomic plasmid, pRP2014 (Christou and Parks, 2011; Poulin et al., 2010), and a cytomegalovirus immediate early enhancer/promoter-lacZ expression cassette (pCA38, (Addison et al., 1997)) was introduced to replace the E1-deletion, using RecA-mediated recombination (Chartier et al., 1996), as detailed previously (Willemsen, 2009), and designated Ad5SlacZ. To introduce the poly-lysine motif into the *H–I* loop of the knob domain of the short fibre, a BglII/PstI fragment containing part of the knob domain was first subcloned into pSP72 (Promega). This plasmid was PCR amplified with the synthetic oligonucleotides 5′ ata gcc ggc aaa aag aaa aag aaa aag aaa gga gca cca agt gca tac tct atg tca ttt tca tg 3′ and 5′ taa gcc ggc agt tgt gtc tcc tgt ttc ctg tgt acc g 3′, which prime in opposite directions around the plasmid, creating a linear molecule with compatible NgoMIV ends. Recircularization of the plasmid creates a molecule encoding a short fibre knob domain that has been changed from amino acids GDTT-PSAY to GDTT-AGKKKKKKKGA-PSAY. The modified fibre protein was recombined into pRP2014 to replace the native Ad5 fibre, and the CMV-lacZ expression cassette added to replace the E1-deletion, and designated Ad5SpKlacZ. Recombination of pCA38 and pRP2014 generated the control virus Ad5LlacZ. Particle counts were used to determine the titre of the vector; an aliquot of virus was diluted in assay buffer (1 mM EDTA, 0.1 SDS), heated for 20 min at 65 °C, and the absorbance determined as 1 $A_{260} = 1.1 \times 10^{12}$ particles.

Immunoblot analysis

To examine the level of incorporation of the modified fibre proteins, we assayed dilutions of the virus stock for hexon (loading control) and fibre signal by immunoblot. Viruses were diluted to 10^9 viral particles in a total of 10 μl of PBS, and combined with equal volume of 2× SDS/PAGE protein loading buffer (62.5 mM Tris HCl pH 6.8, 25% glycerol, 2% SDS, 0.01% bromophenol blue, 5% β-mercaptoethanol). Samples were boiled for 5 min, and separated by electrophoresis on a 12% SDS–polyacrylamide gel. The separated proteins were transferred to a polyvinylidene difluoride membrane (Immobilon-P, Millipore) and the membrane was probed with an antibody raised against all Ad capsid proteins (ab6982, 1/10,000; Abcam) or fibre (MS-1027-P0, 1/1000, NeoMarkers). Binding of the primary antibody was detected using a goat or mouse anti-rabbit secondary antibody conjugated to

horseradish peroxidase (BioRad) and visualised by chemiluminescence reaction (Thermo Scientific ECL western blotting substrate) and autoradiography.

Infection assays in vitro

Triplicate 35 mm dishes of A549, MN1, or undifferentiated or differentiated C2C12 were seeded at a density of 0.3×10^6 cells per dish. The next day cells were infected at an multiplicity of infection (MOI) of 10 with Ad5LlacZ, Ad5SlacZ or Ad5SpKlacZ (or mock infected), except for one series of C2C12 cells, which was switched to differentiation medium (DMEM+2%HS), and infected after 4 days of differentiation. Crude protein extracts were prepared from the infected cells 24 h later by lysing the cells with 175 μl of Lysis Solution (Applied Biosystems). The samples were centrifuged at 9400*g* for 2 min at room temperature (RT) and the supernatant collected and stored at −80 °C. The samples were thawed and assayed for β-galactosidase (β-gal) activity using a commercial chemiluminescence assay (Galacto-star, Applied Biosystems) and a 20/20n luminometer (Turner BioSystems).

In vivo injections and tissue harvest

All animal experiments were approved by and performed according to the guidelines set by the Animal Research Ethics Board at the University of Ottawa (Ottawa, ON, Canada). Six to eight week-old C57Bl/6J mice (Charles River) were injected intravenously (IV) through the tail vein or intraperitoneally (IP) with 100 μl virus or PBS, or anaesthetised with halothane, and injected with virus or PBS in a volume of 25–30 μl in both the right and left tibialis anterior (TA) muscles. Three viral concentrations were used: 5×10^{11} VP/kg (low), 1×10^{12} VP/kg (middle) and 5×10^{12} VP/kg (high). One, two or three days later (as indicated in the specific experiment described below), the mice were euthanized with 100 μl euthanyl (CDMV Inc., Quebec City, QC). For determining the level of β-gal activity, liver and TA muscles from treated animals were removed and immediately frozen in liquid nitrogen and stored at −80 °C until processed as described below. For immunohistochemistry, TA muscles and the spinal cord were removed and immediately incubated in 2% paraformaldehyde (PFA) for 1 h, washed 3 times with PBS, and then incubated in 30% sucrose in PBS for 24–72 h. Tissues were equilibrated in 50:50 30% sucrose/OCT (Tissue-Tek 4583, VWR) for 1–2 h on a rocking platform. Samples were embedded in the same 50:50 mixture by flash freezing in liquid nitrogen and stored at −80 °C until sectioning. The tissues were sectioned using a cryostat in transverse or longitudinal 12 μm sections, mounted on a glass slide, and stored at −20 °C.

β-galactosidase staining

Tissue sections were hydrated in PBS for 1–2 min then fully submerged in X-gal stain (5 mM $K_4Fe(CN)_6$, 5 mM $K_3Fe(CN)_6$, 2 mM $MgCl_2$, 1 mg/ml 5-bromo-4-chloro-3-indolyl-β-d-galactopyranoside in PBS) for 24 h at 37 °C. Slides were washed in PBS for 1 min and covered with a glass cover slip in a 1:1 mixture of PBS and 30% glycerol. Quantification of the stained areas was performed using Image J (Wayne Rasband, Research Services Branch, National Institute of Mental Health, Bethesda, Maryland, USA). A colour intensity threshold was applied to determine the area of the muscle section showing X-gal staining, which is reported as the percentage of the total cross-sectional area of the muscle.

To examine the efficiency of retrograde transport to motor neurons after TA injection, mice were injected with 5×10^{12} VP/kg of Ad5LlacZ, Ad5SlacZ and Ad5SpKlacZ in a solution containing 16 mg/ml Texas Red-conjugated 3000 MW Dextran. The Texas-Red-conjugated Dextran is taken up by the motor neuron termini, and undergoes retrograde transport to mark the motor neuron cell body (Nance and Burns, 1990). Spinal cords were removed 48 h post-injection. Tissues were fixed as described above and longitudinal sections were collected until Texas Red stained-motor neurons were detected by immunofluorescence. The next sequential section was then stained for β-gal activity and viewed using a Leica M80 microscope.

Chemiluminescent β-galactosidase assay

The liver samples were processed as previously described (Parks et al., 1999). Briefly, the entire liver was homogenised in 1 ml of PBS using a Power Gen 125 (Fisher Scientific) at a speed of 5.5 for approximately 10 s. The samples were sonicated twice for 15 s on ice, with a 10 s rest period in between. Samples were centrifuged at 375*g* for 5 min and the supernatant removed to a fresh tube. TA muscles where pulverised using a liquid nitrogen chilled-mortar and pestle. The ground muscle was transferred to a microfuge tube, and solubilized in 400 μl RIPA buffer (50 mM Tris pH 8.0, 100 mM NaCl, 1 mM EDTA, 1% glycerol, 1% NP40, and protease inhibitors). Both liver and TA muscle samples were heated in a 55 °C water bath for 15 min (to inactivate endogenous β-gal activity), followed by a final centrifugation at 16000*g* for 10 min. The supernatants were collected and assayed for β-gal activity using a commercial kit (Galacto-star, Applied Biosystems) and a 20/20n luminometer (Turner BioSystems). Data was normalised to the amount of protein in each sample, as determined by Bradford assay (BioRad).

Statistical analysis

SigmaStat 2.0 was used to determine statistical significance. All error bars represent standard deviation and the *p*-Value was set to 0.05.

Acknowledgments

We thank Kathy Poulin, Melissa Geoffroy, Kalisa Campbell, Natacha Provost, Kristin Willemsen and Benoit Goulet for technical assistance. We thank Dr. Justin Boyer and Chantal Mazerolle for advice on mouse surgery. Research in the Parks laboratory is supported by grants from the Canadian Institutes of Health Research (CIHR) (MOP102554, MOP136898), the Canadian Foundation for Innovation (29974), and the National Sciences and Engineering Research Council (NSERC) (238824-2012). E.R.M. was supported by an Ontario Graduate Scholarship from the Ontario Provincial Government and a scholarship from the CIHR. R.K. is a recipient of a University Health Research Chair from the University of Ottawa.

References

Addison, C.L., Hitt, M., Kunsken, D., Graham, F.L., 1997. Comparison of the human versus murine cytomegalovirus immediate early gene promoters for transgene expression by adenoviral vectors. J. Gen. Virol. 78, 1653–1661.

Ahn, J., Jee, Y., Seo, I., Yoon, S.Y., Kim, D., Kim, Y.K., Lee, H., 2008. Primary neurons become less susceptible to coxsackievirus B5 following maturation: the correlation with the decreased level of CAR expression on cell surface. J. Med. Virol. 80, 434–440.

Alba, R., Bradshaw, A.C., Coughlan, L., Denby, L., McDonald, R.A., Waddington, S.N., Buckley, S.M., Greig, J.A., Parker, A.L., Miller, A.M., Wang, H., Lieber, A., van Rooijen, N., McVey, J.H., Nicklin, S.A., Baker, A.H., 2010. Biodistribution and retargeting of FX-binding ablated adenovirus serotype 5 vectors. Blood 116, 2656–2664.

Alba, R., Bradshaw, A.C., Mestre-Frances, N., Verdier, J.M., Henaff, D., Baker, A.H., 2012. Coagulation factor X mediates adenovirus type 5 liver gene transfer in non-human primates (*Microcebus murinus*). Gene Ther. 19, 109–113.

Amalfitano, A., Parks, R.J., 2002. Separating fact from fiction: assessing the potential of modified adenovirus vectors for use in human gene therapy. Curr. Gene Ther. 2, 111–133.
Baumgartner, B.J., Shine, H.D., 1998. Neuroprotection of spinal motoneurons following targeted transduction with an adenoviral vector carrying the gene for glial cell line-derived neurotrophic factor. Exp. Neurol. 153, 102–112.
Bergelson, J.M., Cunningham, J.A., Droguett, G., Kurt-Jones, E.A., Krithivas, A., Hong, J.S., Horwitz, M.S., Crowell, R.L., Finberg, R.W., 1997. Isolation of a common receptor for Coxsackie B viruses and adenoviruses 2 and 5. Science 275, 1320–1323.
Bergelson, J.M., Krithivas, A., Celi, L., Droguett, G., Horwitz, M.S., Wickham, T., Crowell, R.L., Finberg, R.W., 1998. The murine CAR homolog is a receptor for coxsackie B viruses and adenoviruses. J. Virol. 72, 415–419.
Berk, A.J., 2007. Adenoviridae: the viruses and their replication. In: Knipe, D.M., Howley, P.M. (Eds.), Fields Virology, 5th ed. Lippincott Williams & Wilkins, Philadelphia, PA, pp. 2355–2394.
Bernt, K.M., Ni, S., Li, Z.Y., Shayakhmetov, D.M., Lieber, A., 2003. The effect of sequestration by nontarget tissues on anti-tumor efficacy of systemically applied, conditionally replicating adenovirus vectors. Mol. Ther. 8, 746–755.
Bett, A.J., Prevec, L., Graham, F.L., 1993. Packaging capacity and stability of human adenovirus type 5 vectors. J. Virol. 67, 5911–5921.
Blau, H.M., Pavlath, G.K., Hardeman, E.C., Chiu, C.P., Silberstein, L., Webster, S.G., Miller, S.C., Webster, C., 1985. Plasticity of the differentiated state. Science 230, 758–766.
Bockstael, O., Foust, K.D., Kaspar, B., Tenenbaum, L., 2011. Recombinant AAV delivery to the central nervous system. Methods Mol. Biol. 807, 159–177.
Bradshaw, A.C., Parker, A.L., Duffy, M.R., Coughlan, L., van Rooijen, N., Kahari, V.M., Nicklin, S.A., Baker, A.H., 2010. Requirements for receptor engagement during infection by adenovirus complexed with blood coagulation factor X. PLoS Pathog. 6, e1001142.
Bramson, J.L., Grinshtein, N., Meulenbroek, R.A., Lunde, J., Kottachchi, D., Lorimer, I.A., Jasmin, B.J., Parks, R.J., 2004. Helper-dependent adenoviral vectors containing modified fibre for improved transduction of developing and mature muscle cells. Hum. Gene Ther. 15, 179–188.
Brunetti-Pierri, N., Ng, P., 2011. Helper-dependent adenoviral vectors for liver-directed gene therapy. Hum. Mol. Genet. 20, R7–13.
Brunetti-Pierri, N., Ng, T., Iannitti, D., Cioffi, W., Stapleton, G., Law, M., Breinholt, J., Palmer, D., Grove, N., Rice, K., Bauer, C., Finegold, M., Beaudet, A., Mullins, C., Ng, P., 2013. Transgene expression up to 7 years in nonhuman primates following hepatic transduction with helper-dependent adenoviral vectors. Hum. Gene Ther. 24, 761–765.
Brunetti-Pierri, N., Palmer, D.J., Beaudet, A.L., Carey, K.D., Finegold, M., Ng, P., 2004. Acute toxicity after high-dose systemic injection of helper-dependent adenoviral vectors into nonhuman primates. Hum. Gene Ther. 15, 35–46.
Chartier, C., Degryse, E., Gantzer, M., Dieterle, A., Pavirani, A., Mehtali, M., 1996. Efficient generation of recombinant adenovirus vectors by homologous recombination in *Escherichia coli*. J. Virol. 70, 4805–4810.
Chiu, C.Y., Wu, E., Brown, S.L., Von Seggern, D.J., Nemerow, G.R., Stewart, P.L., 2001. Structural analysis of a fiber-pseudotyped adenovirus with ocular tropism suggests differential modes of cell receptor interactions. J. Virol. 75, 5375–5380.
Christou, C., Parks, R.J., 2011. Rational design of murine secreted alkaline phosphatase for enhanced performance as a reporter gene in mouse gene therapy preclinical studies. Hum. Gene Ther. 22, 499–506.
Crawford-Miksza, L., Schnurr, D.P., 1996. Analysis of 15 adenovirus hexon proteins reveals the location and structure of seven hypervariable regions containing serotype-specific residues. J. Virol. 70, 1836–1844.
Doronin, K., Flatt, J.W., Di Paolo, N.C., Khare, R., Kalyuzhniy, O., Acchione, M., Sumida, J.P., Ohto, U., Shimizu, T., Akashi-Takamura, S., Miyake, K., MacDonald, J.W., Bammler, T.K., Beyer, R.P., Farin, F.M., Stewart, P.L., Shayakhmetov, D.M., 2012. Coagulation factor X activates innate immunity to human species C adenovirus. Science 338, 795–798.
Gaggar, A., Shayakhmetov, D.M., Lieber, A., 2003. CD46 is a cellular receptor for group B adenoviruses. Nat. Med. 9, 1408–1412.
Ghadge, G.D., Roos, R.P., Kang, U.J., Wollmann, R., Fishman, P.S., Kalynych, A.M., Barr, E., Leiden, J.M., 1995. CNS gene delivery by retrograde transport of recombinant replication-defective adenoviruses. Gene Ther. 2, 132–137.
Ginn, S.L., Alexander, I.E., Edelstein, M.L., Abedi, M.R., Wixon, J., 2013. Gene therapy clinical trials worldwide to 2012—an update. J. Gene Med. 15, 65–77.
Goldman, M., Su, Q., Wilson, J.M., 1996. Gradient of RGD-dependent entry of adenoviral vector in nasal and intrapulmonary epithelia: implications for gene therapy of cystic fibrosis. Gene Ther. 3, 811–818.
Goulet, B.B., Kothary, R., Parks, R.J., 2013a. At the "junction" of spinal muscular atrophy pathogenesis: the role of neuromuscular junction dysfunction in SMA disease progression. Curr. Mol. Med. 13, 1160–1174.
Goulet, B.B., McFall, E.R., Wong, C.M., Kothary, R., Parks, R.J., 2013b. Supraphysiological expression of survival motor neuron protein from an adenovirus vector does not adversely affect cell function. Biochem. Cell Biol. 91, 252–264.
Graham, F.L., 1987. Growth of 293 cells in suspension culture. J. Gen. Virol. 68, 937–940.
Graham, F.L., Smiley, J., Russell, W.C., Nairn, R., 1977. Characteristics of a human cell line transformed by DNA from human adenovirus type 5. J. Gen. Virol. 36, 59–74.
Gregorevic, P., Blankinship, M.J., Allen, J.M., Crawford, R.W., Meuse, L., Miller, D.G., Russell, D.W., Chamberlain, J.S., 2004. Systemic delivery of genes to striated muscles using adeno-associated viral vectors. Nat. Med. 10, 828–834.
Guo, Z.S., Wang, L.H., Eisensmith, R.C., Woo, S.L., 1996. Evaluation of promoter strength for hepatic gene expression in vivo following adenovirus-mediated gene transfer. Gene Ther. 3, 802–810.
Harui, A., Suzuki, S., Kochanek, S., Mitani, K., 1999. Frequency and stability of chromosomal integration of adenovirus vectors. J. Virol. 73, 6141–6146.
Havenga, M.J., Lemckert, A.A., Ophorst, O.J., van Meijer, M., Germeraad, W.T., Grimbergen, J., van Den Doel, M.A., Vogels, R., van Deutekom, J., Janson, A.A., de Bruijn, J.D., Uytdehaag, F., Quax, P.H., Logtenberg, T., Mehtali, M., Bout, A., 2002. Exploiting the natural diversity in adenovirus tropism for therapy and prevention of disease. J. Virol. 76, 4612–4620.
Hidaka, C., Milano, E., Leopold, P.L., Bergelson, J.M., Hackett, N.R., Finberg, R.W., Wickham, T.J., Kovesdi, I., Roelvink, P., Crystal, R.G., 1999. CAR-dependent and CAR-independent pathways of adenovirus vector-mediated gene transfer and expression in human fibroblasts. J. Clin. Investig. 103, 579–587.
Hillgenberg, M., Tonnies, H., Strauss, M., 2001. Chromosomal integration pattern of a helper-dependent minimal adenovirus vector with a selectable marker inserted into a 27.4-kilobase genomic stuffer. J. Virol. 75, 9896–9908.
Hirano, M., Kato, S., Kobayashi, K., Okada, T., Yaginuma, H., 2013. Highly efficient retrograde gene transfer into motor neurons by a lentiviral vector pseudotyped with fusion glycoprotein. PloS One 8, e75896.
Hotta, Y., Honda, T., Naito, M., Kuwano, R., 2003. Developmental distribution of coxsackie virus and adenovirus receptor localized in the nervous system. Brain research. Dev. Brain Res. 143, 1–13.
Jager, L., Ehrhardt, A., 2009. Persistence of high-capacity adenoviral vectors as replication-defective monomeric genomes in vitro and in murine liver. Hum. Gene Ther. 20, 883–896.
Kalyuzhniy, O., Di Paolo, N.C., Silvestry, M., Hofherr, S.E., Barry, M.A., Stewart, P.L., Shayakhmetov, D.M., 2008. Adenovirus serotype 5 hexon is critical for virus infection of hepatocytes in vivo. Proc. Natl. Acad. Sci. USA 105, 5483–5488.
Lieber, A., He, C.Y., Meuse, L., Schowalter, D., Kirillova, I., Winther, B., Kay, M.A., 1997. The role of Kupffer cell activation and viral gene expression in early liver toxicity after infusion of recombinant adenovirus vectors. J. Virol. 71, 8798–8807.
Meulenbroek, R.A., Sargent, K.L., Lunde, J., Jasmin, B.J., Parks, R.J., 2004. Use of adenovirus protein IX to display large polypeptides on the virion—generation of fluorescent virus through incorporation of pIX-GFP. Mol. Ther. 9, 617–624.
Morral, N., O'Neal, W.K., Rice, K., Leland, M.M., Piedra, P.A., Aguilar-Cordova, E., Carey, K.D., Beaudet, A.L., Langston, C., 2002. Lethal toxicity, severe endothelial injury, and a threshold effect with high doses of an adenoviral vector in baboons. Hum. Gene Ther. 13, 143–154.
Muruve, D.A., Barnes, M.J., Stillman, I.E., Libermann, T.A., 1999. Adenoviral gene therapy leads to rapid induction of multiple chemokines and acute neutrophil-dependent hepatic injury in vivo. Hum. Gene Ther. 10, 965–976.
Nakajima, H., Uchida, K., Kobayashi, S., Inukai, T., Yayama, T., Sato, R., Mwaka, E., Baba, H., 2008. Target muscles for retrograde gene delivery to specific spinal cord segments. Neurosci. Lett. 435, 1–6.
Nalbantoglu, J., Pari, G., Karpati, G., Holland, P.C., 1999. Expression of the primary coxsackie and adenovirus receptor is downregulated during skeletal muscle maturation and limits the efficacy of adenovirus-mediated gene delivery to muscle cells. Hum. Gene Ther. 10, 1009–1019.
Nance, D.M., Burns, J., 1990. Fluorescent dextrans as sensitive anterograde neuroanatomical tracers: applications and pitfalls. Brain Res. Bull. 25, 139–145.
Nicol, C.G., Graham, D., Miller, W.H., White, S.J., Smith, T.A., Nicklin, S.A., Stevenson, S.C., Baker, A.H., 2004. Effect of adenovirus serotype 5 fiber and penton modifications on in vivo tropism in rats. Mol. Ther.: J. Am. Soc. Gene Ther. 10, 344–354.
Palmer, D.J., Ng, P., 2005. Helper-dependent adenoviral vectors for gene therapy. Hum. Gene Ther. 16, 1–16.
Parks, R.J., Bramson, J.L., Wan, Y., Addison, C.L., Graham, F.L., 1999. Effects of stuffer DNA on transgene expression from helper-dependent adenovirus vectors. J. Virol. 73, 8027–8034.
Parks, R.J., Chen, L., Anton, M., Sankar, U., Rudnicki, M.A., Graham, F.L., 1996. A helper-dependent adenovirus vector system: removal of helper virus by Cre-mediated excision of the viral packaging signal. Proc. Natl. Acad. Sci. USA 93, 13565–13570.
Parks, R.J., Graham, F.L., 1997. A helper-dependent system for adenovirus vector production helps define a lower limit for efficient DNA packaging. J. Virol. 71, 3293–3298.
Poulin, K.L., Lanthier, R.M., Smith, A.C., Christou, C., Risco Quiroz, M., Powell, K.L., O'Meara, R.W., Kothary, R., Lorimer, I.A., Parks, R.J., 2010. Retargeting of adenovirus vectors through genetic fusion of a single-chain or single-domain antibody to capsid protein IX. J. Virol. 84, 10074–10086.
Poulin, K.L., Tong, G., Vorobyova, O., Pool, M., Kothary, R., Parks, R.J., 2011. Use of Cre/loxP recombination to swap cell binding motifs on the adenoviral capsid protein IX. Virology 420, 146–155.
Quantin, B., Perricaudet, L.D., Tajbakhsh, S., Mandel, J.L., 1992. Adenovirus as an expression vector in muscle cells in vivo. Proc. Natl. Acad. Sci. USA 89, 2581–2584.
Raper, S.E., Chirmule, N., Lee, F.S., Wivel, N.A., Bagg, A., Gao, G.P., Wilson, J.M., Batshaw, M.L., 2003. Fatal systemic inflammatory response syndrome in a ornithine transcarbamylase deficient patient following adenoviral gene transfer. Mol. Genet. Metab. 80, 148–158.
Ross, P.J., Parks, R.J., 2003. Oncolytic adenovirus: getting there is half the battle. Mol. Ther. 8, 705–706.
Ross PJ, Parks RJ. Construction and characterization of adenovirus vectors. Cold Spring Harb Protoc. 2009 May;2009(5):pdb.prot5011. http://dx.doi.org/10.1101/pdb.prot5011. PMID: 20147151.
Ruigrok, R.W., Barge, A., Albiges-Rizo, C., Dayan, S., 1990. Structure of adenovirus fibre. II. Morphology of single fibres. J. Mol. Biol. 215, 589–596.
Saban, S.D., Nepomuceno, R.R., Gritton, L.D., Nemerow, G.R., Stewart, P.L., 2005. CryoEM structure at 9A resolution of an adenovirus vector targeted to hematopoietic cells. J. Mol. Biol. 349, 526–537.

Salazar-Grueso, E.F., Kim, S., Kim, H., 1991. Embryonic mouse spinal cord motor neuron hybrid cells. Neuroreport 2, 505–508.
San Martin, C., 2012. Latest insights on adenovirus structure and assembly. Viruses 4, 847–877.
San Sebastian, W., Samaranch, L., Kells, A.P., Forsayeth, J., Bankiewicz, K.S., 2013. Gene therapy for misfolding protein diseases of the central nervous system. Neurother.: J. Am. Soc. Exp. Neurother. 10, 498–510.
Shayakhmetov, D.M., Lieber, A., 2000. Dependence of adenovirus infectivity on length of the fiber shaft domain. J. Virol. 74, 10274–10286.
Soudais, C., Laplace-Builhe, C., Kissa, K., Kremer, E.J., 2001. Preferential transduction of neurons by canine adenovirus vectors and their efficient retrograde transport in vivo. FASEB J.: Off. Publ. Fed. Am. Soc. Exp. Biol. 15, 2283–2285.
Stephen, S.L., Montini, E., Sivanandam, V.G., Al-Dhalimy, M., Kestler, H.A., Finegold, M., Grompe, M., Kochanek, S., 2010. Chromosomal integration of adenoviral vector DNA in vivo. J. Virol. 84, 9987–9994.
Stewart, P.L., Chiu, C.Y., Huang, S., Muir, T., Zhao, Y., Chait, B., Mathias, P., Nemerow, G.R., 1997. Cryo-EM visualization of an exposed RGD epitope on adenovirus that escapes antibody neutralization. EMBO J. 16, 1189–1198.
Su, L.T., Gopal, K., Wang, Z., Yin, X., Nelson, A., Kozyak, B.W., Burkman, J.M., Mitchell, M.A., Low, D.W., Bridges, C.R., Stedman, H.H., 2005. Uniform scale-independent gene transfer to striated muscle after transvenular extravasation of vector. Circulation 112, 1780–1788.
Terashima, T., Oka, K., Kritz, A.B., Kojima, H., Baker, A.H., Chan, L., 2009. DRG-targeted helper-dependent adenoviruses mediate selective gene delivery for therapeutic rescue of sensory neuronopathies in mice. J. Clin. Investig. 119, 2100–2112.
van Raaij, M.J., Mitraki, A., Lavigne, G., Cusack, S., 1999. A triple beta-spiral in the adenovirus fibre shaft reveals a new structural motif for a fibrous protein. Nature 401, 935–938.
Waddington, S.N., McVey, J.H., Bhella, D., Parker, A.L., Barker, K., Atoda, H., Pink, R., Buckley, S.M.K., Greig, J.A., Denby, L., Custers, J., Morita, T., Francischetti, I.M.B., Monteiro, R.Q., Barouch, D.H., van Rooijen, N., Napoli, C., Havenga, M.J.E., Nicklin, S.A., Baker, A.H., 2008. Adenovirus serotype 5 hexon mediates liver gene transfer. Cell 132, 397–409.
Wickham, T.J., Tzeng, E., Shears, L.L., Roelvink, P.W., Li, Y., Lee, G.M., Brough, D.E., Lizonova, A., Kovesdi, I., 1997. Increased in vitro and in vivo gene transfer by adenovirus vectors containing chimeric fiber proteins. J. Virol. 71, 8221–8229.
Willemsen, K., 2009. Improving Adenoviral Vectors for Muscle-Directed Gene Therapy. Biochemistry, Microbiology and Immunology. University of Ottawa, Ottawa, p. 145.
Wolff, G., Worgall, S., van, R.N., Song, W.R., Harvey, B.G., Crystal, R.G., 1997. Enhancement of in vivo adenovirus-mediated gene transfer and expression by prior depletion of tissue macrophages in the target organ. J. Virol. 71, 624–629.
Wong, C.M., McFall, E.R., Burns, J.K., Parks, R.J., 2013. The role of chromatin in adenoviral vector function. Viruses 5, 1500–1515.
Worgall, S., Wolff, G., Falck-Pedersen, E., Crystal, R.G., 1997. Innate immune mechanisms dominate elimination of adenoviral vectors following in vivo administration. Hum. Gene Ther. 8, 37–44.
Wu, E., Pache, L., Von Seggern, D.J., Mullen, T.M., Mikyas, Y., Stewart, P.L., Nemerow, G.R., 2003. Flexibility of the adenovirus fiber is required for efficient receptor interaction. J. Virol. 77, 7225–7235.

Title: A reduction in the human adenovirus virion size through use of a shortened fibre protein does not enhance muscle transduction following systemic or localised delivery in mice

Author: Emily R. McFall,Lyndsay M. Murray,John A. Lunde,Bernard J. Jasmin,Rashmi Kothary,Robin J. Parks

Publication: Virology

Publisher: Elsevier

Date: November 2014

Curriculum vitae EMILY MCFALL

SUMMARY OF QUALIFICATIONS

- Masters in Microbiology and Immunology
- Experienced in different laboratory environments
- Excellent time management, organization and multitasking skills honed through research experience
- Knowledgeable in Microsoft Office and literature searches

EDUCATION

Masters of Science, Microbiology and Immunology 2012 - 2014
University of Ottawa, Ontario

- Thesis title: "Exploring novel methods to achieve systemic delivery of SMN for treatment of spinal muscular atrophy"
- University of Ottawa Dean's and Admission scholarships

Bachelor of Science, Honours in Biopharmaceutical Sciences - Genomics Option with CO-OP
University of Ottawa, Ontario 2007 - 2012

- Thesis title: "Glycosylation, *cis* interactions and light chain species origin regulate Ly49 NK receptor binding with class I MHC molecules"
- Graduated with honors: Summa Cum Laude
- University of Ottawa Dean's honors and Admission scholarships

SKILLS

Research

- Practiced in animal care, breeding, injections, dissections, homogeneous of tissues, RNA purification, tissue sectioning and staining
- Experienced in RT, PCR, q-PCR, RT-PCR, melt curves and electrophoresis
- Proficient at tissue culture, sterile conditions, transformation, digestion, cloning and transfection
- Studied viral and exosome purifications
- Skillful in co-immunoprecipitations, western blot, flow cytometry, immunohistochemistry and ELISA
- Able to operate autoclave, luminometer, nanosight, nano-drop and pH meters
- Examined both human and murine serum samples and collected human DNA
- Capable of following lab procedures and writing formal scientific lab reports for subjects such as cell biology, molecular biochemistry, genetics, general chemistry and organic chemistry

Academic Training

- Educated in biochemistry, cell biology, genetics, microbiology, molecular biology, organic chemistry, plant biology, virology, metabolism, pharmacology and cellular physiology
- Studied immune cells and their function, various pathogens and their replication, protein formation, cellular organelles, organic mechanisms, muscle development, pharmokinetics, energy potentials, drug development and bioinformatics

Transferable

- Practiced both oral and written communication through various presentation methods
- Strong organization, time management, multi-tasking and problem-solving skills
- Knowledge of experimental design and project development
- Motivated learner
- Proven ability to work individually and as a team member
- Computer skills include Microsoft Office, Access and literature searches

PROFESSIONAL EXPERIENCE

Ottawa Hospital Research Institute – Dr. Rashmi Kothary July 2014 - present
Laboratory Research Assistant

- Perform murine dissections at various ages and harvested diverse tissues
- Set-up breeding pairs and maintained several murine lines
- Conducted both RNA and protein extractions
- Practiced in Q-PCR

Ottawa Hospital Research Institute – Dr. Robin Parks May 2012 – July 2014
Masters Student

- Conducted *in vivo* studies involving several injection methods of purified virus followed by collection of diverse tissues
- Examined both human and murine serum samples
- Collected and purified viruses and exosomes
- Operated a nanosight to determine sizes of nanoparticles
- Gained time management and organization skills while managing multiple research projects
- Expanded knowledge of experimental design and project development
- Involved with the training of new laboratory members

Ottawa Hospital, General Campus – Dr. Andrew Makrigiannis September 2011 – April 2012
Honors Student

- Performed staining and flow cytometry experiments using various fluorophores
- Initiated cloning experiments to development new cell lines for future testing

Viral Vaccine Division, BGTD, Health Canada May 2011 – August 2011
Laboratory Assistant - Co-op Student

- Performed ELISA optimizations on three different Hepatitis protocols
- Updated inventory and created records of calibrated scientific equipment

Drug GMP Inspection Unit, HPFB, Health Canada September 2010 – December 2010
Co-op student

- Created tracking sheets for foreign drug manufacturing, packaging or testing sites and organized documents as per the pre-screening process
- Participated in meetings with the Drug GMP and other units

Spartan Bioscience May 2010 – August 2010
Laboratory Research Assistant - Co-op Student

- Collected human DNA samples from co-workers ensuring no contamination to performed PRC reactions and melt curves using a DX12 real-time PCR machine

University of Ottawa January 2010 – April 2010
Laboratory Assistant – Co-op Student

- Followed and developed experimental protocols involving bioreports and mer-lux while working under sterile conditions

MDS Nordion, Kanata, Ontario May 2009 – August 2009
Safety and Environment – Summer Student

- Recorded radioactive and chemical inventory, located in radioactive and non-radioactive areas in the form of weekly updates and final audit reports
- Nuclear worker training – Radiation safety

Best Theratronics, Kanata, Ontario June 2008 – August 2008
Dosimetry Lab Technician – Summer Student

- Responsible for preparing dosimetry kits which included light sensitive film, Fricke, a mild acid used for radiation, and analyzing irradiated film and preparing reports for customers

SCHOLARSHIPS AND AWARDS

- Dean's scholarship, University of Ottawa 2014
- BMI MSc Microbiology and Immunology Seminar Day, University of Ottawa 2014
- Syed Sattar Master Student Award, University of Ottawa 2014
- Sir Frederick Banting and Charles Best Canada Graduate Scholarship, CIHR 2013 - 2014
- Microbiology and Immunology Award of Excellence, University of Ottawa 2013
- BMI MSc Microbiology and Immunology Poster Day, University of Ottawa 2013
- Queen Elizabeth II graduate scholarships in science and technology, Ontario government (Declined) 2012 - 2013
- Ontario Graduate scholarship, Ontario government 2012 - 2013
- Outstanding Research Project by an Biopharmaceutical Sciences student, University of Ottawa 2012
- Industrial Undergraduate Student Research Award, NSERC 2010
- Dean's Honours list, University of Ottawa 2007 - 2012

PUBLICATIONS

1. Daguen, V., McFall, E., Yumvihoze, E., Xiang, S., Amyot, M., & Poulain, A. J. (2012). Divalent base cations hamper Hg(II) uptake. *Environ Sci Technol, 46*(12), 6645-6653.
2. McFall, E., Tu, M. M., Al-Khattabi, N., Tai, L. H., St-Laurent, A. S., Tzankova, V., Makrigiannis, A. P. (2013). Optimized tetramer analysis reveals Ly49 promiscuity for MHC ligands. *J Immunol, 191*(11), 5722-5729.
3. Goulet, B. B., McFall, E. R., Wong, C. M., Kothary, R., & Parks, R. J. (2013). Supraphysiological expression of survival motor neuron protein from an adenovirus vector does not adversely affect cell function. *Biochem Cell Biol, 91*(4), 252-264.
4. Wong, C. M., McFall, E. R., Burns, J. K., & Parks, R. J. (2013). The role of chromatin in adenoviral vector function. *Viruses, 5*(6), 1500-1515.
5. McFall, E. R., Murray, L. M., Lunde, J. A., Jasmin, B. J., Kothary, R., Parks, R. J. (2014). A reduction in the human adenovirus virion size through use of a shortened fibre protein does not enhance muscle transduction following systemic or localized delivery in mice. V*irology*, 468, 444–453.

TRAINING

- National Institutional Animal User Training
- Laboratory and Bio-Safety Training
- Autoclave Operation and Safety Training
- Reliability Status security clearance
- WHIMS
- Health Canada Division 5 – Drugs for Clinical Trials Involving Human Subjects
- Ontario G Driver's licence

ACTIVITIES AND ASSOCIATIONS

- Educational: French as a second language (Beginner level) 2013 - 2014
- Academic: BMI Graduate Student Association, OHRI Institution Rep 2012 - 2014
- Fundraising: Relay for Life – Canadian Cancer Society 2012 – Present
  Ottawa Walk for Muscular Dystrophy 2012 – Present